Electronic Supplementary Material (ESI) for Chemical Science

Self-assembly of New Fluorescent Pd(II) and Pt(II) 2,7-Diazapyrenium-based Metallocycles. Study of its inclusion complexes and [3]catenanes.

Victor Blanco, Marcos D. García, Carlos Peinador* and José M. Quintela*

Departamento de Química Fundamental, Universidade da Coruña,
Facultad de Ciencias, A Zapateira, s/n, 15008, La Coruña, Spain .
Fax: +34 981167065;
E-mail: carlos.peinador@udc.es

–Supporting Information –

TABLE OF CONTENTS

General Methods

2,7-diazapyrene,[1] ligand **1**·2PF_6,[2] Pd and Pt complexes,[3] 4-(4'-cloromethylphenyl)pyridine,[4] metallocycle **3**·2PF_6,[2] cyclophanes BPPC34C10 (**8**)[5] and DN38C10 (**9**)[6] and guests **11**,[7]**13**,[8]**15**,[5]**17**,[9]**19**[10] and **21**[11] were prepared according to literature procedures. All other reagents used were commercial grade chemicals from freshly opened containers. Milli-Q water was purified with a Millipore Gradient A10 apparatus. Merck 60 F_{254} foils were used for thin layer chromatography, and Merck 60 (230-400 mesh) silica gel was used for flash chromatography. Proton and carbon nuclear magnetic resonance spectra were recorded on a Bruker Avance 300 or a Bruker Avance 500 spectrometer equipped with a dual cryoprobe for ^{1}H and ^{13}C, using the deuterated solvent as lock and the residual protiated solvent as internal standard. DOSY experiments were referenced using the value 1.92×10^{-9} m^2 s^{-1} for the DHO signal in D_2O at 298 K[12] and the value 1.97×10^{-9} m^2 s^{-1} for the CHD_2NO_2 signal in CD_3NO_2 at 298 K.[13] Mass spectrometry experiments were carried out in a LCQ-q-TOF Applied Biosystems QSTAR Elite spectrometer for low- and high-resolution ESI. UV-Vis spectra were recorded on a Perkin Elmer Lambda 900 spectrometer. Fluorescence spectra were recorded at room temperature on a Perkin Elmer LS 50B fluorescence spectrometer using a 1% T filter and a slit width of 8 nm. Melting points were measured using Stuart Scientific SMP3 apparatus. Microanalyses for C, H and N were performed by the elemental analyses general service of the University of A Coruña.

Crystal structure analysis

The structure was solved by direct methods and refined with the full-matrix least-squares procedure (SHELX-97)[14] against F^2. The X-ray diffraction data were collected on a Bruker X8 ApexII. Non-Solvent hydrogen atoms were placed in idealized positions with U_{eg}(H) = 1.2U_{eg}(C) and were allowed to ride on their parent atoms. Solvent hydrogen atoms were placed in idealized positions with U_{eg}(H) = 1.5U_{eg}(C) and were allowed to ride on their parent atoms.

Ligand 4·PF_6

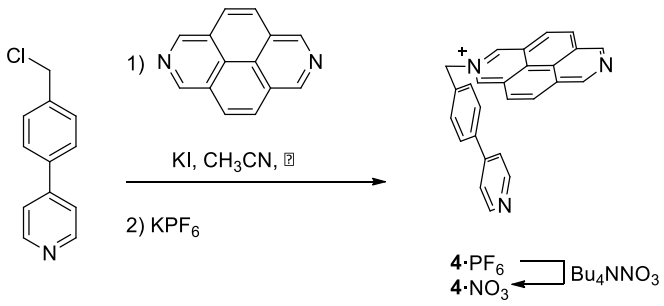

To a solution of 2,7-diazapyrene (1.44 g, 7.00 mmol) and a catalytic amount of KI in refluxing CH_3CN (90 mL) was slowly added a solution of 4-(4'-cloromethylphenyl)pyridine

(0.95 g, 4.66 mmol) cooled to 0 °C in CH_3CN (70 mL). The reaction was refluxed for 72 h; after cooling, the solvent was evaporated in vacuo to give a crude product which was purified by column chromatography (SiO_2, acetone/NH_4Cl 1.5M/MeOH 5:4:1). The product-containing fractions were combined and the solvents were removed in vacuo. The residue was dissolved in H_2O/CH_3OH (50/30, 800 mL) and an excess of KPF_6 was added until no further precipitation was observed. The solid was filtered and washed with water to give **4**·PF_6 (0.76 g, 31%) as a yellow solid. Mp: 189-191 ºC (dec.). ^{1}H NMR *(500 MHz, CD_3NO_2)* δ: 6.45 (2H, s); 7.84 (2H, d, J = 8.5 Hz); 8.00 (2H, d, J = 6.4 Hz); 8.03 (2H, d, J = 6.4 Hz); 8.61 (2H, d, J = 9.1 Hz); 8.77 (4H, m); 9.83 (2H, s); 9.88 (2H, s); ^{13}C NMR *(125 MHz, CD_3NO_2)* δ: 67.1 (CH_2); 124.6 (CH); 125.5 (C); 127.2 (CH); 127.5 (C); 130.0 (CH); 130.4 (C); 130.9 (C); 131.5 (CH); 132.8 (CH); 137.2 (C); 139.2 (C); 139.5 (CH); 147.4 (CH); 149.8 (CH); 153.7 (C). MS-ESI *(m/z)*: 372.2 [M – PF_6^-]$^+$. Anal. Calcd. C, 53.90; H, 3.13; N, 9.67. Found. C, 53.67; H, 3.22; N, 9.60.

Ligand 4·NO_3

To a solution of **4**·PF_6 (197.0 mg, 0.38 mmol) in CH_3CN (90 mL) Bu_4NNO_3 was added until no further precipitation is observed. The mixture was stirred at rt for 6h and the precipitate was filtered and washed with CH_3CN to yield **4**·NO_3 (130.1 mg, 79 %) as a yellow solid. Mp: 161-163 ºC. ^{1}H NMR (*500 MHz, D_2O*) δ: 6.20 (2H, s); 7.69 (4H, m); 7.80 (2H, d, J = 8.3 Hz); 8.31 (2H, d, J = 9.1 Hz); 8.44 (4H, m); 9.51 (2H, s); 9.75 (2H, s); ^{13}C NMR (*125 MHz, D_2O*) δ: 65.9 (CH2); 123.2 (CH); 124.6 (C); 126.5 (CH); 126.7 (C); 128.6 (C); 129.0 (CH); 129.7 (C); 130.6 (CH); 131.7 (CH); 135.9 (C); 138.5 (C); 138.8 (CH); 147.3 (CH); 147.6 (CH); 150.9 (C). MS-ESI (*m/z*): 372.2 [M – NO_3^-]+. Anal. Calcd. C, 71.88; H, 4.18; N, 12.90. Found. C, 71.99; H, 4.10; N, 12.72.

Metallocycles 6a,b·6NO_3

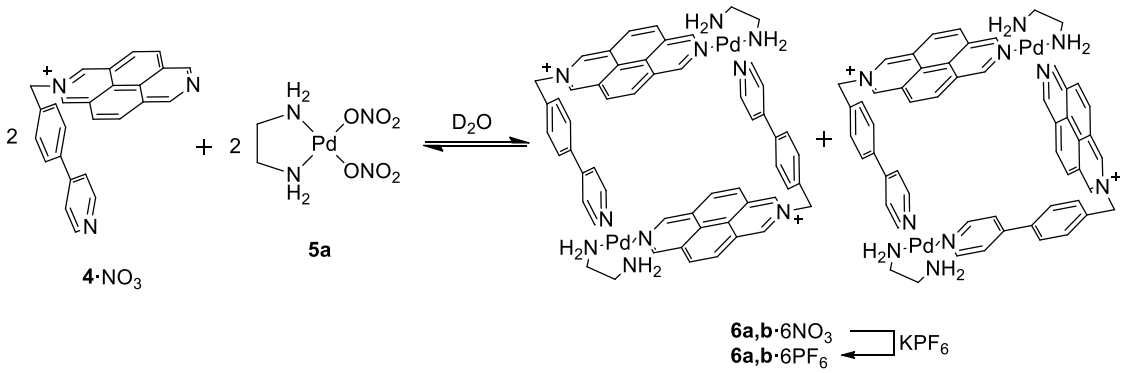

A solution of **4**·NO_3 (8.7 mg; 0.020 mmol) and (en)Pd(NO_3)$_2$ (**5a**) (5.8 mg, 0.020 mmol) in D_2O (4.0 mL) was stirred at 60 ºC for 1 h. ^{1}H NMR *(500 MHz, D_2O)* δ: 3.00 (8H, m); 6.28 (4H, s); 7.59-7.69 (12H, m); 8.50 (4H, m); 8.55-8.61 (6H, m); 8.77 (2H, d, J = 6.8 Hz); 9.95 (4H, s); 9.98 (2H, s); 10.15 (2H, s); ^{13}C NMR *(125 MHz, D_2O)* δ: 46.8 (CH_2); 46.9 (CH_2);

47.1 (CH_2); 47.2 (CH_2); 65.9 (CH_2); 124.1 (CH); 124.2 (CH); 125.0 (C); 125.1 (C); 127.4 (C); 127.4 (C); 127.9 (CH); 128.0 (CH); 128.1 (CH); 128.4 (C); 128.5 (C); 129.5 (C); 129.5 (C); 129.7 (CH); 129.7 (CH); 129.9 (CH); 129.9 (CH); 136.1 (C); 136.1 (C); 136.4 (C); 136.6 (C); 139.4 (CH); 139.5 (CH); 148.1 (CH); 148.1 (CH); 150.6 (C); 150.7 (C); 151.0 (CH); 151.0 (CH).

Metallocycles 6a,b·6PF_6

A solution of **4**·NO_3 (21.7 mg; 0.050 mmol) and **5a** (14.5 mg, 0.050 mmol) in H_2O (10.0 mL) was stirred at 60 ºC for 1h. An excess of KPF_6 was added until no further precipitation was observed. The solid was filtered and washed with water to obtain **6a,b**·6PF_6 (32.0 mg, 66%) as a pale brown solid. Mp: 195-197 ºC. ^{1}H NMR *(500 MHz, CD_3NO_2)* δ: 3.22 (8H, m); 4.59 (2H, m); 4.76 (2H, m); 6.34 (4H, s); 7.66 (12H, m); 8.58 (4H, m); 8.63 (4H, m); 8.69 (2H, d, J = 6.4 Hz); 8.83 (2H, d, J = 6.5 Hz); 9.84 (4H, m); 10.00 (2H, s); 10.18 (2H, s); ^{13}C NMR *(125 MHz, CD_3NO_2)* δ: 48.5 (CH_2); 48.6 (CH_2); 48.7 (CH_2); 48.9 (CH_2); 67.6 (CH_2); 125.4 (CH); 125.5 (CH); 126.5 (C); 129.0 (C); 129.1 (C); 129.5 (CH); 129.5 (CH); 129.6 (CH); 129.9 (C); 130.0 (C); 131.0 (CH); 131.0 (C); 131.1 (C); 131.1 (CH); 131.6 (CH); 131.6 (CH); 137.7 (C); 137.8 (C); 137.9 (C); 141.0 (CH); 141.0 (CH); 150.1 (CH); 150.2 (CH); 152.0 (C); 152.0 (C); 152.9 (CH); 153.0 (CH).

Metallocycles 7a,b·6PF_6

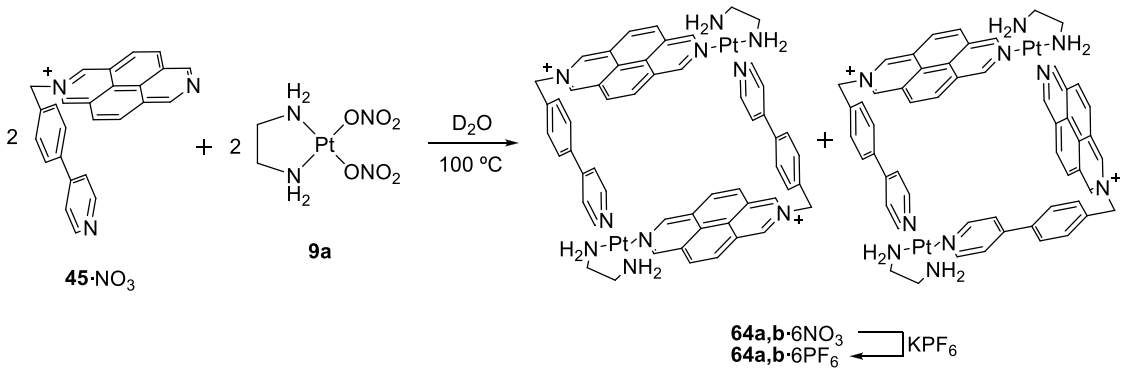

A solution of ligand **4**·NO_3 (39.0 mg, 0.090 mmol) and (en)Pt(NO_3)$_2$ (**5b**) (34.0 mg, 0.090 mmol) in H_2O (24.0 mL) was stirred at 100 ºC for 8d. Upon cooling to room temperature, an excess of KPF_6 was added until no further precipitation was observed. The solid was filtered to yield **7a,b**·6PF_6 (88.1 mg, 92 %) as a pale brown solid. Mp: 243-245 ºC (dec.). ^{1}H NMR *(500 MHz, CD_3NO_2)* δ: 3.17 (8H, m); 4.93 (2H, m); 5.13 (4H, m); 5.33 (2H, m); 6.34 (4H, s); 7.67 (12H, m); 8.62 (8H, m); 8.71 (2H, d, J = 5,6 Hz); 8.86 (2H, d, J = 5,7 Hz); 9.85 (4H, m); 10.01 (2H, s); 10.19 (2H, s). ^{13}C NMR *(125 MHz, CD_3NO_2)* δ: 49.6 (CH_2); 49.7 (CH_2); 49.8 (CH_2); 49.9 (CH_2); 67.6 (CH_2); 67.6 (CH_2); 125.7 (CH); 125.8 (CH); 126.4 (C); 126.4 (C); 128.9 (C); 129.0 (C); 129.2 (CH); 129.3 (CH); 129.5 (CH); 130.4 (C); 130.4 (C); 131.0 (CH); 131.1 (C); 131.1 (C); 131.1 (CH); 131.5 (CH); 131.6

(CH); 137.5 (C); 137.7 (C); 137.8 (C); 137.9 (C); 141.0 (CH); 151.1 (CH); 151.1 (CH); 151.9 (C); 153.6 (CH); 153.7 (CH). HRMS-ESI (*m/z*): Calcd para $[M - 2PF_6^-]^{2+}$ 917-1114, found 917.1085; calcd. for $[M - 3PF_6^-]^{3+}$ 563.0860, found 563.0843; calcd. for $[M - 4PF_6^-]^{4+}$ 386.0733, found. 386.0726; calcd. for $[M - 5PF_6^-]^{5+}$ 289.8657, found 279.8645.

Metallocycles 7a,b·6NO$_3$

To a solution of **7a,b**·6PF$_6$ (55.0 mg, 0.026 mmol) in CH_3CN (4 mL) Bu_4NNO_3 was added until no further precipitation is observed. The precipitate was filtered and washed with CH_3CN to yield **7a,b**·6NO$_3$ (31.1 mg, 74 %) as a pale brown solid. ^{1}H NMR *(500 MHz, D_2O)* δ: 2.92 (8H, m); 6.28 (4H, s); 7.61-7.69 (12H, m); 8.50-8.58 (8H, m); 8.63 (2H, d, J = 6.9 Hz); 8.80 (2H, d, J = 6.9 Hz); 9.96 (4H, s); 9.99 (2H, s); 10.17 (2H, s); ^{13}C NMR *(125 MHz, D_2O)* δ: 47.4 (CH_2); 47.6 (CH_2); 47.6 (CH_2); 47.8 (CH_2); 65.8 (CH_2); 65.9 (CH_2); 124.4 (CH); 124.4 (CH); 124.8 (C); 124.9 (C); 127.2 (C); 127.3 (C); 128.0 (CH); 128.0 (CH); 128.1 (CH); 128.9 (C); 128.9 (C); 129.5 (C); 129.5 (C); 129.7 (CH); 129.7 (CH); 136.1 (C); 136.1 (C); 136.2 (C); 136.3 (C); 139.4 (CH); 139.4 (CH); 149.0 (CH); 149.0 (CH); 150.3 (C); 150.5 (C); 151.6 (CH); 151.7 (CH).

Pseudorotaxane 1·2PF$_6$⊂8

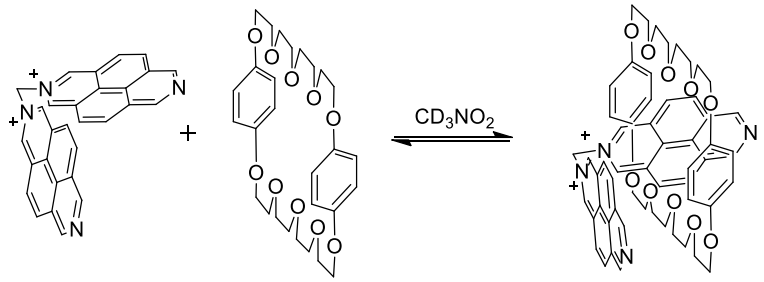

1·2PF$_6$ **8** **1**·2PF$_6$⊂**8**

To a solution of **1**·2PF$_6$ (2.1 mg; 3.0×10^{-3} mmol) in CD_3NO_2 (0.6 mL) **8** (1.6 mg, 3.0×10^{-3} mmol) was added. ^{1}H NMR (*500 MHz, CD_3NO_2*) δ: 10.14 (4H, s), 9.98 (4H, s), 8.80 (4H, d, J = 9.1 Hz), 8.58 (4H, d, J = 9.1 Hz), 8.41 (2H, s), 5.90 (8H, s), 3.93–3.72 (24H, m), 3.64 (8H, m). ^{13}C NMR (*125 MHz*, *CD_3NO_2*) δ*:* 153.0 (C), 150.8 (CH), 139.0 (CH), 134.3 (CH), 131.2 (C), 131.1 (C), 127.3 (C), 126.9 (CH), 125.1 (C), 115.1 (CH), 82.0 (CH_2), 71.8 (CH_2), 71.6 (CH_2), 71.0 (CH_2), 68.9 (CH_2).

Pseudorotaxane 1·2PF$_6$⊂9

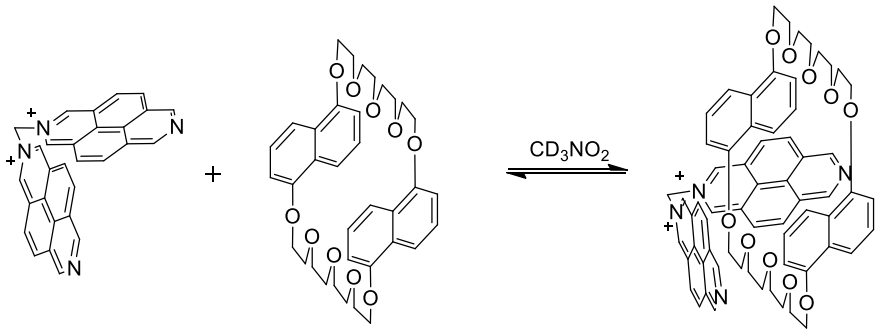

1·2PF$_6$ 9 1·2PF$_6$⊂9

To a solution of **1**·2PF$_6$ (2.1 mg; 3.0 × 10^{-3} mmol) in CD_3NO_2 (0.6 mL) **9** (1.9 mg, 3.0 × 10^{-3} mmol) was added. ^{1}H NMR (*500 MHz, CD_3NO_2*) δ: 10.10 (4H, s), 9.88 (4H, s), 8.70 (4H, d, J = 9.1 Hz), 8.42 (4H, d, J = 9.1 Hz), 8.26 (2H, s), 6.43 (8H, m), 6.15 (4H, d, J = 7.1 Hz), 4.06 (8H, m), 4.02 (8H, m), 3.95 (16H, m). ^{13}C NMR (*125 MHz, CD_3NO_2*) δ: 154.3 (C) 150.5 (CH), 138.4 (CH), 134.1 (CH), 130.7 (C), 130.3 (C), 127.3 (C), 126.7 (C), 125.9 (C), 125.9 (CH), 124.3 (C), 113.9 (CH), 106.0 (CH), 82.2 (CH_2), 72.3 (CH_2), 72.2 (CH_2), 71.2 (CH_2), 69.2 (CH_2).

Catenane 3(8)$_2$·4OTf·4PF$_6$

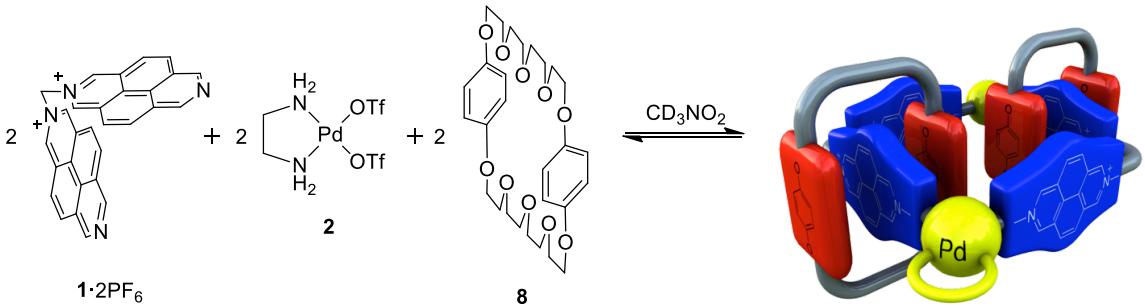

1·2PF$_6$ 2 8 3(8)$_2$·4OTf·4PF$_6$

To a solution of **1**·2PF$_6$ (7.1 mg; 0.010 mmol) and **2** (5.6 mg, 0.024 mmol) in CD_3NO_2 (4.0 mL) **8** (5.4 mg, 0.010 mmol) was added. ^{1}H NMR *(500 MHz, CD_3NO_2)* δ: 3.11 (4H, m); 3.32 (8H, br s); 3.83 (58H, m); 4.09 (4H, m); 4.64 (2H, m); 5.00 (4H, br s); 5.30 (4H, br s); 5.50 (8H, s); 8.26 (4H, s); 8.33 (4H, d, *J* = 9.2 Hz); 8.48 (4H, d, *J* = 9.3 Hz); 8.82 (4H, d, *J* = 9.4 Hz); 8.89 (4H, d, *J* = 9.4 Hz); 10.11 (4H, s); 10.36 (4H, s); 10.53 (4H, s); 10.61 (4H, s); ^{13}C NMR *(125 MHz, CD_3NO_2)* δ: 49.1 (CH_2); 49.4 (CH_2); 66.9 (CH_2); 69.2 (CH_2); 70.5 (CH_2); 71.0 (CH_2); 71.2 (CH_2); 71.7 (CH_2); 72.1 (CH_2); 82.6 (CH_2); 115.0 (CH); 119.1 (C); 121.0 (C); 123.5 (C); 124.7 (C); 125.6 (C); 128.6 (C); 128.8 (CH); 129.2 (C); 129.7 (C); 129.9 (CH); 130.1 (C); 130.4 (C); 131.4 (C); 132.6 (CH); 133.0 (CH); 140.4 (C); 141.6 (C); 151.4 (CH); 152.3 (C).

Catenane $3(9)_2 \cdot 4OTf \cdot 4PF_6$

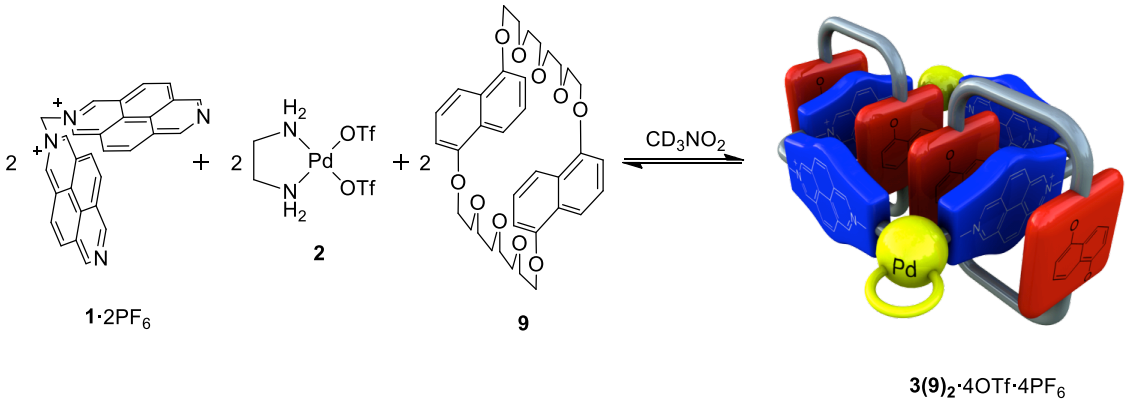

1·$2PF_6$ **2** **9** $3(9)_2 \cdot 4OTf \cdot 4PF_6$

To a solution of **1**·$2PF_6$ (7.1 mg; .010 mmol) and (en)Pd$(OTf)_2$ (**2**) (5.6 mg, 0.024 mmol) in CD_3NO_2 (4.0 mL) DNP34C10 (9) (6,4 mg, 0,010 mmol) was added. ^{1}H NMR *(500 MHz, CD_3NO_2)*: The complexity of the spectrum precluded its analysis (Figure S46).

X-ray diffraction quality single crystals of the catenane were grown by slow diffusion of diethyl ether into a solution of **1**·$2PF_6$, (en)Pd$(OTf)_2$ (**2**) and **9** in acetonitrile.

Regioselective catenation

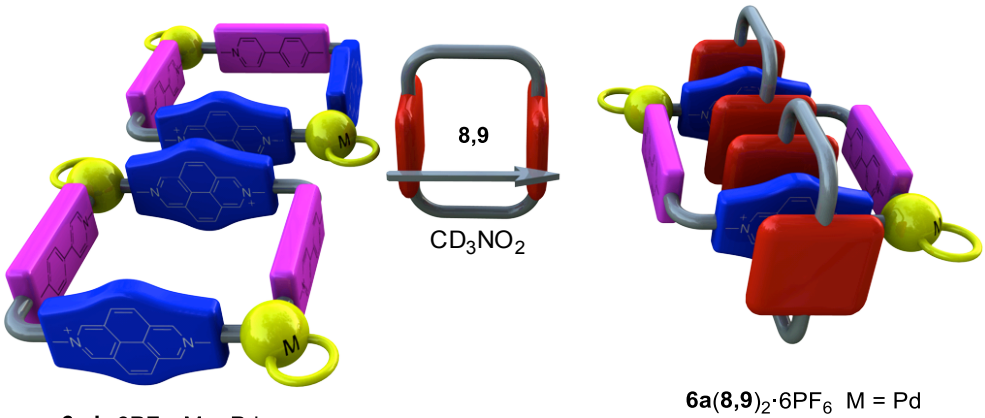

6a,b·$6PF_6$ M = Pd
7a,b·$6PF_6$ M = Pt

6a$(8,9)_2 \cdot 6PF_6$ M = Pd
7a$(8,9)_2 \cdot 6PF_6$ M = Pt

Catenane $6a(8)_2 \cdot 6PF_6$

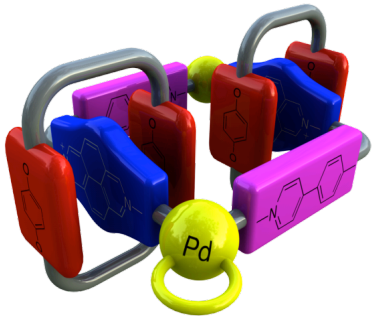

6a$(8)_2 \cdot 6PF_6$

To a solution of **6a,b**·$6PF_6$ (5.8 mg, 3.0×10^{-3} mmol) in CD_3NO_2 (0.6 mL) **8** (3,2 mg, 6.0×10^{-3} mmol) was added. ^{1}H NMR *(500 MHz, CD_3NO_2)* δ: 3.23 (16H, m); 3.44 (12H, m); 3.59-4.19

(52H, m); 4.60 (4H, m); 4.85 (4H, m); 5.11 (4H, s); 5.39 (8H, s); 6.24 (4H, s); 7.73 (4H, d, J = 8.4 Hz); 7.83 (4H, d, J = 6.7 Hz); 7.92 (4H, d, J = 8.4 Hz); 8.27 (8H, m); 9.19 (4H, d, J = 6.6 Hz); 9.77 (4H, s); 9.87 (4H, s); ^{13}C NMR *(500 MHz, CD_3NO_2)* δ: 48.6 (CH_2); 49.2 (CH_2); 66.7 (CH_2); 67.2 (CH_2); 68.8 (CH_2); 69.2 (CH_2); 70.7 (CH_2); 70.8 (CH_2); 71.0 (CH_2); 71.4 (CH_2); 71.6 (CH_2); 71.7 (CH_2); 71.8 (CH_2); 112.1 (CH); 114.4 (CH); 125.1 (C); 126.2 (CH); 127.9 (C); 129.2 (CH); 129.3 (CH); 129.5 (C); 129.9 (C); 131.0 (CH); 132.0 (CH); 137.8 (C); 138.1 (C); 141.0 (CH); 149.6 (CH); 152.1 (C); 153.6 (CH).

Single crystals suitable for X-ray diffraction analysis were grown by slow diffusion of diethyl ether into a soluiton of **1**·PF_6, (en)Pd$(OTf)_2$ (**2**) and **8** in nitromethane.

Catenane 6a(9)$_2$·6PF$_6$

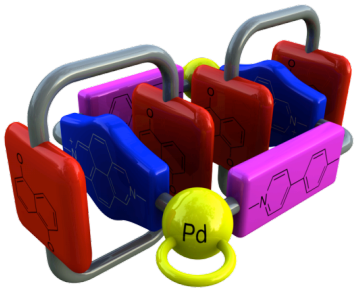

6a(**9**)$_2$·6PF$_6$

To a solution of **6a,b**·6PF_6 (5.8 mg, 3.0×10^{-3} mmol) in CD_3NO_2 (0.6 mL) **9** (3.8 mg, 6.0×10^{-3} mmol) was added. ^{1}H NMR *(500 MHz, CD_3NO_2)*. The complexity of the spectrum precluded it analysis (Figure S55).

Catenane 7a(8)$_2$·6PF$_6$

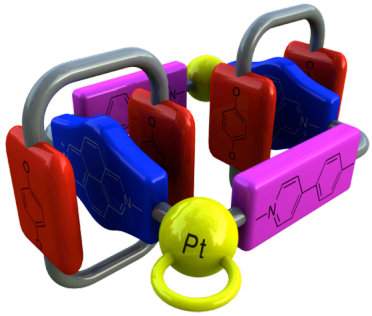

7a(**8**)$_2$·6PF$_6$

A solution of **7a,b**·6PF_6 (25.0 mg, 0.012 mmol) and BPP34C10 (**8**) (25.2 mg, 0.047 mmol) in CH_3NO_2 (2.4 mL) was stirred at 100 °C for 7d. After cooling to rt, the solvent was removed under reduced pressure without heating. The resulting residue was suspended in water (12 mL) and Amberlite^{TM} IRA-402 (0,50 g) was added. The mixture was stirred at rt for 24h. The resin was removed by filtration and the filtrate was concentrated under reduce pressure. The resulting crude was purified by flash chromatography (SiO_2, acetone/NH_4Cl_{aq} 1.5M/MeOH 5:4:1). The

product containing fractions were combined and the solvent removed under reduced pressure to afford a residue that was dissolved in H_2O (15 mL). An excess of KPF_6 was added until no further precipitation is observed. The solid was filtered and washed with water to yield catenane **7a**(**8**)$_2$·6PF_6 (24.0 mg, 64 %) as a yellow solid. ^{1}H NMR *(500 MHz, CD_3NO_2)* δ: 3.16 (16H, m); 3.45 (12H, m); 3.59-4.19 (52H, m); 4.88 (4H, m); 5.16 (4H, s); 5.41 (8H, s); 6.25 (4H, s); 7.75 (4H, d, J = 8.6 Hz); 7.81 (4H, d, J = 7.0 Hz); 7.93 (4H, d, J = 8.6 Hz); 8.27 (8H, m); 9.21 (4H, d, J = 6.9 Hz); 9.78 (4H, s); 9.90 (4H, s); ^{13}C NMR *(125 MHz, CD_3NO_2)* δ: 49.4 (CH_2); 50.2 (CH_2); 66.7 (CH_2); 67.2 (CH_2); 68.8 (CH_2); 70.7 (CH_2); 70.9 (CH_2); 71. 0 (CH_2); 71,5 (CH_2); 71.7 (CH_2); 71.8 (CH_2); 112.1 (CH); 114.5 (CH); 125.0 (C); 126.4 (CH); 127.7 (C); 129.4 (CH); 129.5 (CH); 129.6 (C); 130.0 (C); 131.0 (CH); 132.0 (CH); 137.9 (C); 137.9 (C); 141.1 (CH); 149.8 (CH); 152.1 (C); 153.8 (CH). *HRMS-ES (m/z):* calc. for [M – 3PF_6^-]$^{3+}$ 920.5941, found 920.5905; calc. for [M – 4PF_6^-]$^{4+}$ 654.2044, found. 654.2035; calc. for [M – 5PF_6^-]$^{5+}$ 494.3705, found 494,3700.

Catenane 7a(9)$_2$·6PF_6

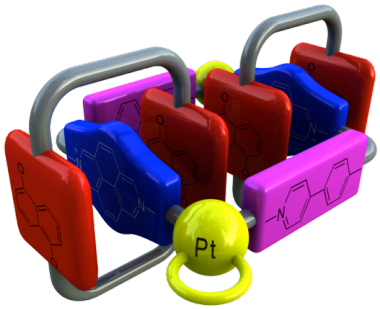

64a(43)$_2$·6PF_6

A solution of **7a,b**·6PF_6 (25.0 mg, 0.012 mmol) and **9** (30.0 mg, 0.047 mmol) in CH_3NO_2 (2.4 mL) was stirred at 100 °C for 7d. After cooling to rt, the solvent was removed under reduced pressure without heating. The resulting residue was suspended in water (12 mL) and Amberlite™ IRA-402 (0,50 g) was added. The mixture was stirred at rt for 24h. The resin was removed by filtration and the filtrate was concentrated under reduce pressure. The resulting crude was purified by flash chromatography (SiO_2, acetone/NH_4Cl_{aq} 1.5M/MeOH 5:4:1). The product containing fractions were combined and the solvent removed under reduced pressure to afford a residue that was dissolved in H_2O (15 mL). An excess of KPF_6 was added until no further precipitation is observed. The solid was filtered and washed with water to yield catenane **7a**(**9**)$_2$·6PF_6 (25.3 mg, 63 %) as a yellow solid.^{1}H NMR *(500 MHz, CD_3NO_2)* The complexity of the spectrum precluded its analysis (Figure S58).

HRMS-ES (m/z): calc. for [M – 3PF_6^-]$^{3+}$ 987.2816, found 987.2800; calc. for [M – 4PF_6^-]$^{4+}$ 704.2200, found 704.2212; calc. for [M – 5PF_6^-]$^{5+}$ 534.3831, found 534.3828; calc. for [M – 6PF_6^-]$^{6+}$ 421.1585, found 421.1593.

General procedure for the regioselective formation of inclusion complexes

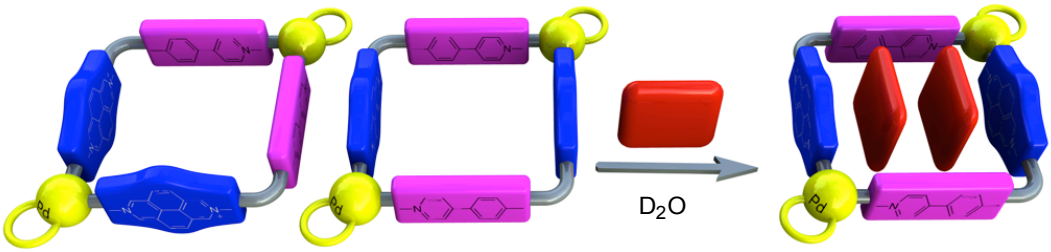

6a,b·6NO_3 (guest)$_2$⊂ **6a**·6NO_3

To a solution of **4**·NO_3 (4.3 mg; 0.010 mmol) and (en)Pd(NO_3)$_2$ (**5a**) (2.9 mg; 0.010 mmol) in D_2O (2.0 mL) guests **15**, **17**, **19**, **20**, **21** (0.010 mmol), **11**, **13**, **16**, **18** (0.020 mmol) or **10** (0.070 mmol) were added and the mixture was stirred at 60ºC for 1h.

Inclusion complex (10)$_2$⊂6a·6NO_3

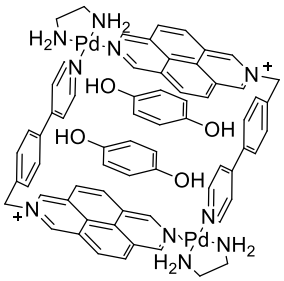

(**10**)$_2$⊂ **6a**·6NO_3

^{1}H NMR (500 MHz, D_2O) δ: 3.01 (8H, s); 6.13 (4H, s); 6.24 (56H, s); 7.74 (4H, d, J = 8.5 Hz); 7.84 (8H, m); 8.31 (4H, d, J = 9.2 Hz); 8.44 (4H, d, J = 9.2 Hz); 9.01 (4H, d, J = 6.8 Hz); 9.80 (4H, s); 10.01 (4H, s); ^{13}C NMR *(125 MHz, D_2O)* δ: 46.4 (CH_2); 46.5 (CH_2); 65.4 (CH_2); 115.3 (CH); 123.8 (CH); 124.2 (C); 125.7 (C); 127.5 (CH); 127.7 (C); 127.9 (CH); 128.8 (C); 129.1 (CH); 129.6 (CH); 135.8 (C); 135.9 (C); 138.0 (CH); 147.3 (CH); 148.0 (C); 150.2 (C); 150.8 (CH).

Inclusion complex (11)$_2$⊂6a·6NO_3

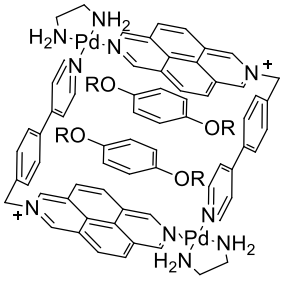

R=$CH_2CH_2OCH_2CH_2OH$

(**11**)$_2$⊂ **6a**·6NO_3

^{1}H NMR *(500 MHz, D_2O)* δ: 3.00 (8H, s); 3.72-3.83 (64H, m); 6.18 (4H, s); 7.81 (4H, d, J = 8.5 Hz); 7.90 (8H, m); 8.36 (4H, d, J = 9.2 Hz); 8,48 (4H, d, J = 9.2 Hz); 9.11 (4H, d, J = 6.8 Hz); 9.90 (4H, s); 10.08 (4H, s); ^{13}C NMR *(125 MHz, D_2O)* δ: 46.8 (CH_2); 46.9 (CH_2); 60.5 (CH_2); 65.8 (CH_2); 67.2 (CH_2); 68.9 (CH_2); 71.9 (CH_2); 114.4 (CH); 124.3 (CH); 126.1 (C); 127.8 (CH); 128.1 (C); 128.3 (CH); 129.1 (C); 129.8 (CH); 130.2 (CH); 136.4 (C); 136.6 (C); 138.7 (CH); 147.9 (CH); 150.4 (C); 151.3 (C); 151.5 (CH).

Inclusion complex $(13)_2\subset$6a·6NO_3

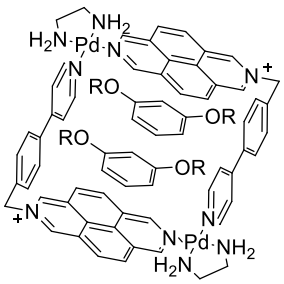

R = $CH_2CH_2OCH_2CH_2OH$

$(13)_2\supset$ **6a**·6NO_3

^{1}H NMR *(500 MHz, D_2O)* δ: 3.00 (8H, s); 3.72-3.81 (64H, m); 5.93 (6H, br); 6.18 (4H, s); 7.80 (4H, d, J = 8.5 Hz); 7.89 (8H, m); 8.35 (4H, d, J = 9.2 Hz); 8,46 (4H, d, J = 9.2 Hz); 9.07 (4H, d, J = 6.8 Hz); 9.90 (4H, s); 10.05 (4H, s); ^{13}C NMR *(125 MHz, D_2O)* δ: 46.8 (CH_2); 46.9 (CH_2); 60.5 (CH_2); 65,8 (CH_2); 66.8 (CH_2); 68.9 (CH_2); 71.9 (CH_2); 100.5 (CH); 106.5 (CH); 124.3 (CH); 126.3 (C); 127.9 (CH); 128.1 (C); 128.3 (CH); 129.0 (C); 129.3 (CH); 129.7 (CH); 130.4 (CH); 136.3 (C); 136.5 (C); 138.8 (CH); 147.9 (CH); 150.5 (C); 151.5 (CH); 158.3 (C).

Inclusion complex $(14)_2\subset$6a·6NO_3

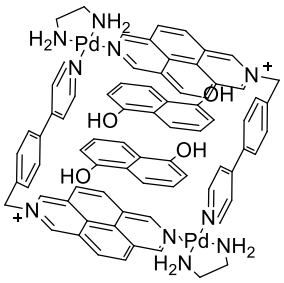

$(14)_2\supset$ **6a**·6NO_3

^{1}H NMR *(500 MHz, D_2O)* δ: 2.99 (8H, m); 5.60 (8H, m); 6.01 (4H, s); 7.77 (4H, d, J = 9.1 Hz); 7.92 (8H, m); 7.97 (4H, d, J = 8.6 Hz); 8.08 (4H, d, J = 6.8 Hz); 9.13 (4H, d, J = 6.9 Hz); 9.47 (4H, s); 9.72 (4H, s); ^{13}C NMR *(125 MHz, D_2O)* δ: 46.7 (CH_2); 46.8 (CH_2); 65.8 (CH_2); 107.1 (CH); 111.4 (CH); 123.1 (C); 124.5 (CH); 124.9 (C); 126.7 (CH); 127.5 (C); 128.2 (C); 128.4 (CH); 128.8 (CH); 130.5 (CH); 135.4 (C); 136.6 (C); 137.7 (CH); 147.3 (CH); 149.5 (C); 150.7 (C); 151.4 (CH).

Inclusion complex $(15)_2 \subset 6a \cdot 6NO_3$

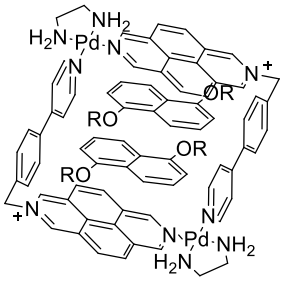

R = $CH_2CH_2OCH_2CH_2OH$

$(15)_2 \supset 6a \cdot 6NO_3$

^{1}H NMR *(500 MHz, D_2O, 353 K)* δ: 3.40-3.49 (8H, m); 4.06 (8H, m); 4.33 (8H, m); 4.41 (8H, m); 4.50 (8H, m); 5.90-6.07 (6H, m); 6.55 (4H, s); 8.38 (4H, d, J = 9.1 Hz); 8.48-8.59 (12H, m); 8.68 (4H, d, J = 5.7 Hz); 9.71 (4H, d, J = 6.7 Hz); 10.02 (4H, s); 10.21 (4H, s).

Inclusion complex $(16)_2 \subset 6a \cdot 6NO_3$

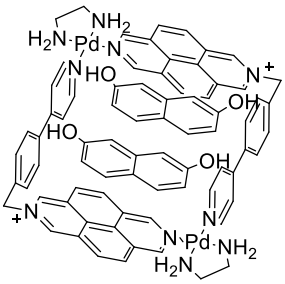

$(16)_2 \supset 6a \cdot 6NO_3$

^{1}H NMR *(500 MHz, D_2O)* δ: 3.01 (8H, s); 6.03 (4H, s); 7.81 (4H, d, J = 9.2 Hz); 7.94 (4H, d, J = 8.7 Hz); 8.00 (4H, d, J = 8.7 Hz); 8.05 (4H, d, J = 9.2 Hz); 8.12 (4H, d, J = 7.0 Hz); 9.19 (4H, d, J = 7.0 Hz); 9.50 (4H, s); 9.87 (4H, s); ^{13}C NMR *(125 MHz, D_2O)* δ: 46.8 (CH_2); 46.9 (CH_2); 65.7 (CH_2); 105.9 (CH); 113.3 (CH); 121.1 (C); 123.5 (C); 124.5 (CH); 124.9 (C); 126.8 (CH); 127.2 (C); 127.8 (C); 128.5 (CH); 128.6 (C); 128.9 (CH); 130.4 (CH); 133.1 (C); 136.4 (C); 136.6 (C); 137.8 (CH); 147.4 (CH); 150.5 (C); 151.6 (CH); 152.0 (C).

Inclusion complex $(17)_2 \subset 6a \cdot 6NO_3$

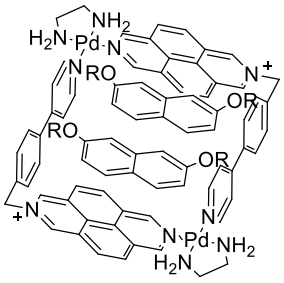

R = $CH_2CH_2OCH_2CH_2OH$

$(17)_2 \supset 6a \cdot 6NO_3$

^{1}H NMR *(500 MHz, D_2O)* δ: 3.00 (8H, s); 3.29 (4H, m); 3.88-4.00 (32H, m); 4.51 (4H, m); 5.46 (m); 6.11 (4H, s); 7.89 (4H, d, J = 9.2 Hz); 8.00 (8H, m); 8.11 (4H, d, J = 9.1 Hz); 8.16 (4H, d, J

= 5.4 Hz); 9.33 (4H, m); 9.69 (4H, s); 9.96 (4H, s); ^{13}C NMR *(125 MHz, D_2O)* δ: 46.8 (CH_2); 46.9 (CH_2); 60.7 (CH_2); 65.7 (CH_2); 68.8 (CH_2); 72.3 (CH_2); 102.8 (CH); 114.2 (CH); 123.3 (C); 124.3 (CH); 125.2 (C); 126.9 (CH); 127.9 (C); 128.3 (CH); 128.7 (C); 129.4 (CH); 130.4 (CH); 136.3 (C); 137.1 (C); 138.1 (CH); 147.6 (CH); 150.4 (C); 152.0 (CH); 154.1 (C).

Inclusion complex $(18)_2$⊂6a·6NO_3

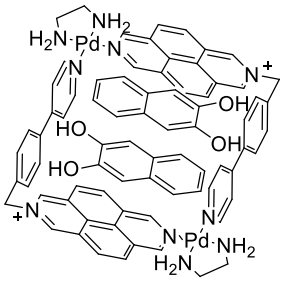

$(\mathbf{56})_2$⊂ **63a**·6NO_3

^{1}H NMR *(500 MHz, D_2O)* δ: 3.00 (8H, m); 4.26 (8H, m); 5.51 (4H, m); 6.05 (4H, s); 7.86 (4H, d, J = 9,1 Hz); 7.95 (4H, d, J = 8.5 Hz); 7.99 (4H, d, J = 8.2 Hz); 8.10 (8H, m); 9.18 (4H, d, J = 6.3 Hz); 9.53 (4H, s); 9.87 (4H, s); ^{13}C NMR *(125 MHz, D_2O)* δ: 46.8 (CH_2); 46.9 (CH_2); 65.7 (CH_2); 108.2 (CH); 121.5 (CH); 122.9 (CH); 123.7 (C); 124.5 (CH); 125.1 (C); 125.9 (C); 126.9 (CH); 127.9 (C); 128.5 (CH); 128.7 (C); 129.0 (CH); 130.5 (CH); 136.5 (C); 136.5 (C); 138.0 (CH); 142.8 (C); 147.4 (CH); 150.6 (C); 151,6 (CH).

Inclusion complex $(19)_2$⊂6a·6NO_3

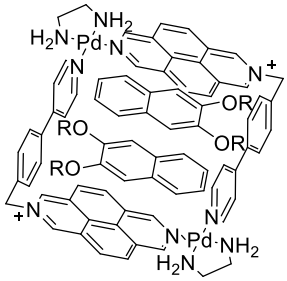

R = $CH_2CH_2OCH_2CH_2OH$

$(\mathbf{57})_2$⊂ **63a**·6NO_3

^{1}H NMR *(500 MHz, D_2O)* δ: 2.98 (8H, m); 3.90-3.98 (32H, m); 5.99 (4H, m); 6.14 (4H, s); 7.89 (4H, m); 8.05 (4H, d, J = 8.6 Hz); 8.10 (4H, d, J = 8.5 Hz); 8.22 (4H, d, J = 6.5 Hz); 9,32 (4H, d, J = 6.7 Hz); 9.68 (4H, s); 9.94 (4H, s); ^{13}C NMR *(125 MHz, D_2O)* δ: 46.9 (CH_2); 47.0 (CH_2); 60.6 (CH_2); 65.7 (CH_2); 68.4 (CH_2); 72.3 (CH_2); 104.4 (CH); 123.0 (CH); 123.4 (C); 124.2 (CH); 125.1 (C); 127.0 (CH); 128.0 (C); 128.4 (CH); 128.8 (C); 129.2 (CH); 130.7 (CH); 136.1 (C); 137.3 (C); 138.2 (CH); 145.2 (CH); 147.6 (CH); 150.4 (C); 151.1 (CH).

Inclusion complex $(20)_2 \subset 6a \cdot 6NO_3$

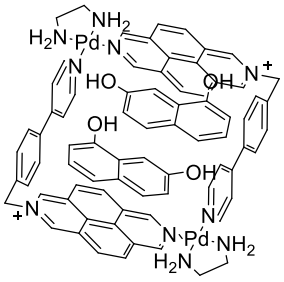

$(\mathbf{20})_2 \supset \mathbf{6a} \cdot 6NO_3$

^{1}H NMR *(500 MHz, D_2O)* δ: 2.98 (8H, m); 5.28 (4H, br m); 5.52 (4H, br m); 6.01 (4H, s); 7.75 (4H, d, J = 9.1 Hz); 7.99 (16H, m); 9.06 (4H, d, J = 7.0 Hz); 9.45 (4H, s); 9.82 (4H, s); ^{13}C NMR *(125 MHz, D_2O)* δ: 46.7 (CH_2); 46.8 (CH_2); 65.8 (CH_2); 101.7 (CH); 106.3 (CH); 115.8 (CH); 117.0 (C); 121.6 (CH); 122.5 (C); 123.6 (C); 124.6 (CH); 125.0 (C); 126.5 (CH); 127.0 (C); 127.6 (C); 128.5 (CH); 128.8 (CH); 130.4 (CH); 135.9 (C); 137.0 (C); 137.8 (CH); 147.5 (CH); 148.5 (C); 150.5 (C); 151.2 (CH).

Inclusion complex $(21)_2 \subset 6a \cdot 6NO_3$

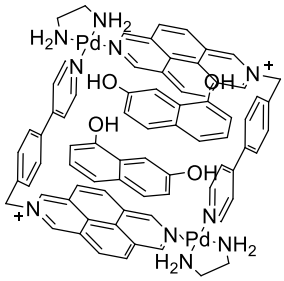

R=$CH_2CH_2OCH_2CH_2OH$

$(\mathbf{21})_2 \supset \mathbf{6a} \cdot 6NO_3$

^{1}H NMR *(500 MHz, D_2O, 338 K)* δ: 3.35-3.42 (8H, m); 4.11-4.29 (24H, m); 4.46 (8H, m); 6.50 (4H, s); 6.78 (8H, m); 7.10 (8H, m); 8.23 (4H, d, J = 9.5 Hz); 8.33 (4H, d, J = 8.3 Hz); 8.41 (8H, m); 8.49 (4H, d, J = 6.6 Hz); 9.60 (4H, d, J = 6.2 Hz); 9.95 (4H, s); 10.25 (4H, s).

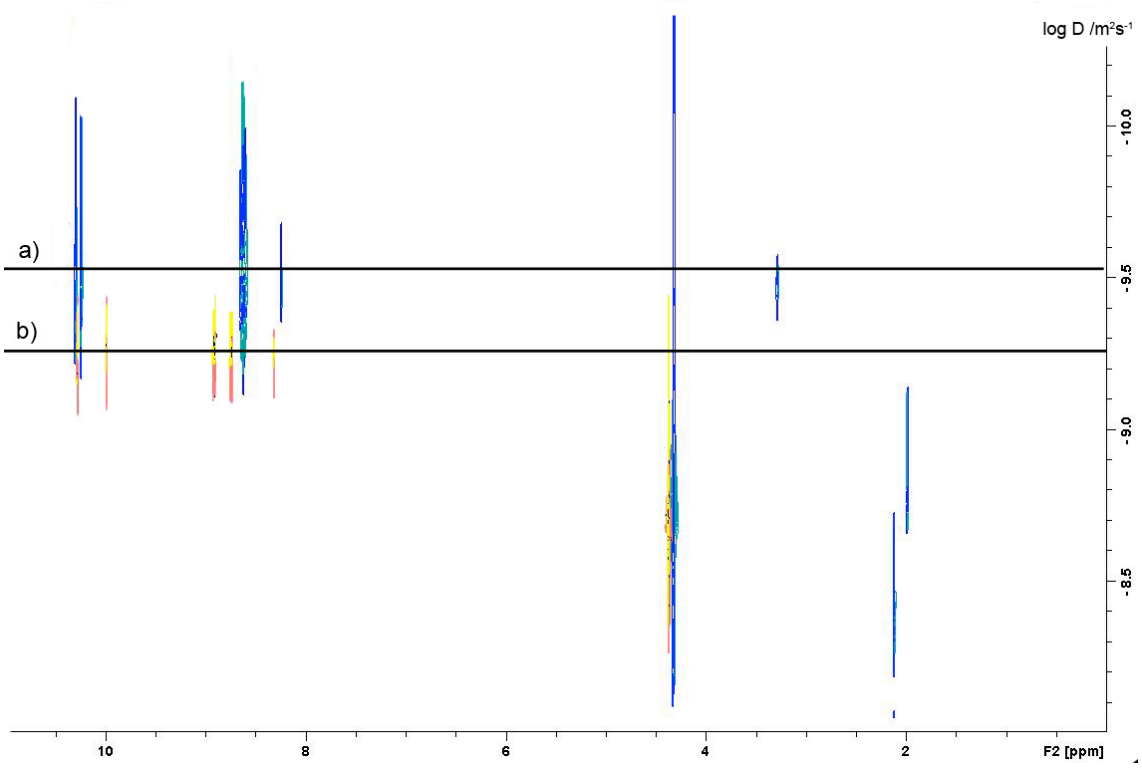

Figure S1: Superposed DOSY (CD_3NO_2, 500 MHz, 298 K) experiment of: a) 1.25 mM solution of **3**·4OTf·4PF_6 (blue). b) 2.5 mM solution of ligand **1**·2PF_6 (yellow).

1-(4-(pyridin-4-yl)benzyl)-2,7-diazapyren-1-ium hexafluorophosphate (4·PF_6)

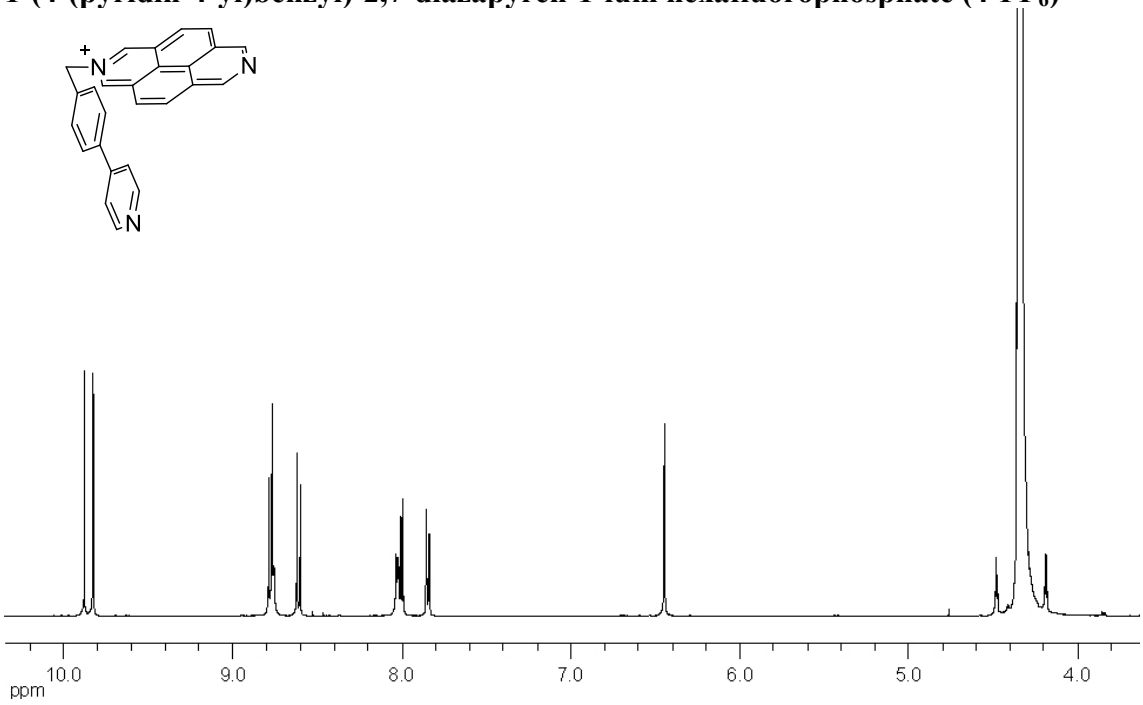

Figure S2: ^{1}H NMR (CD_3NO_2, 500 MHz) spectrum of **4**·PF_6

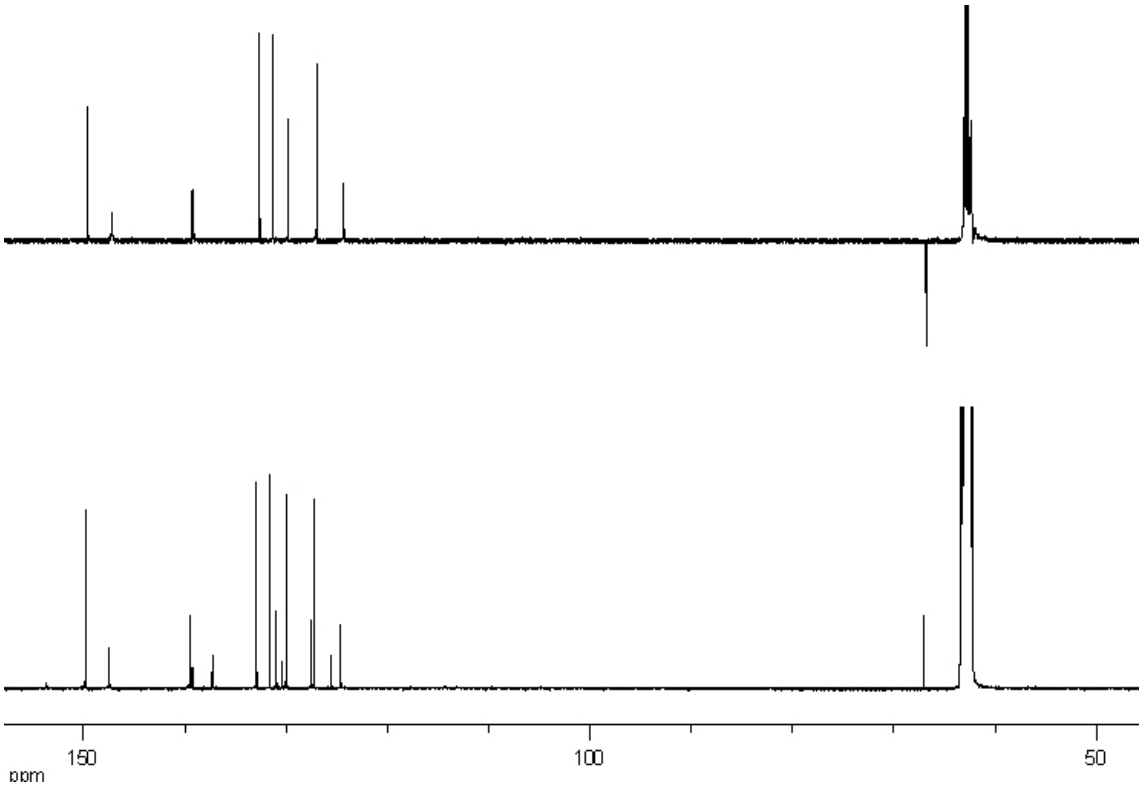

Figure S3: ^{13}C NMR (CD_3NO_2, 125 MHz) spectrum of **4**·PF_6.

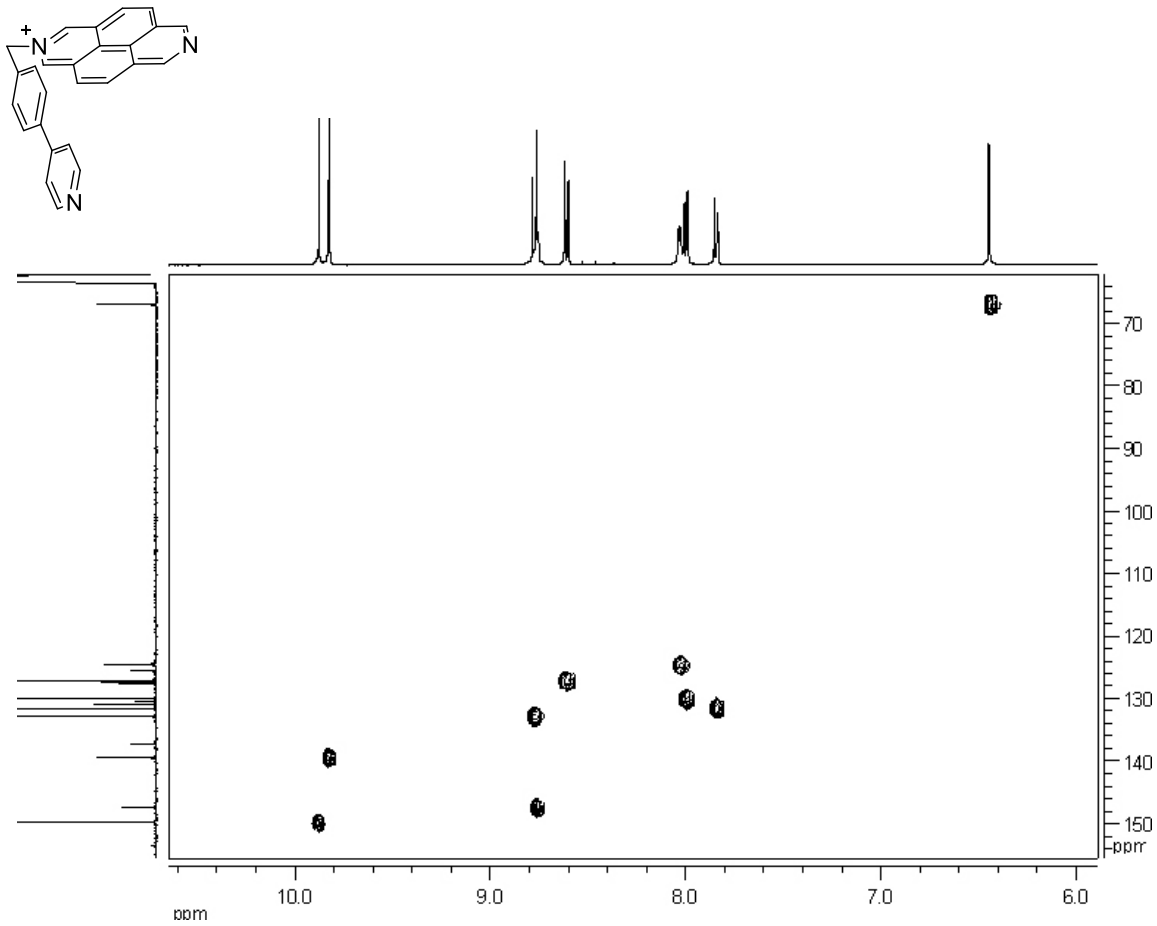

Figure S4: HSQC (CD_3NO_2, 500 and 125 MHz) spectrum of **4**·PF_6.

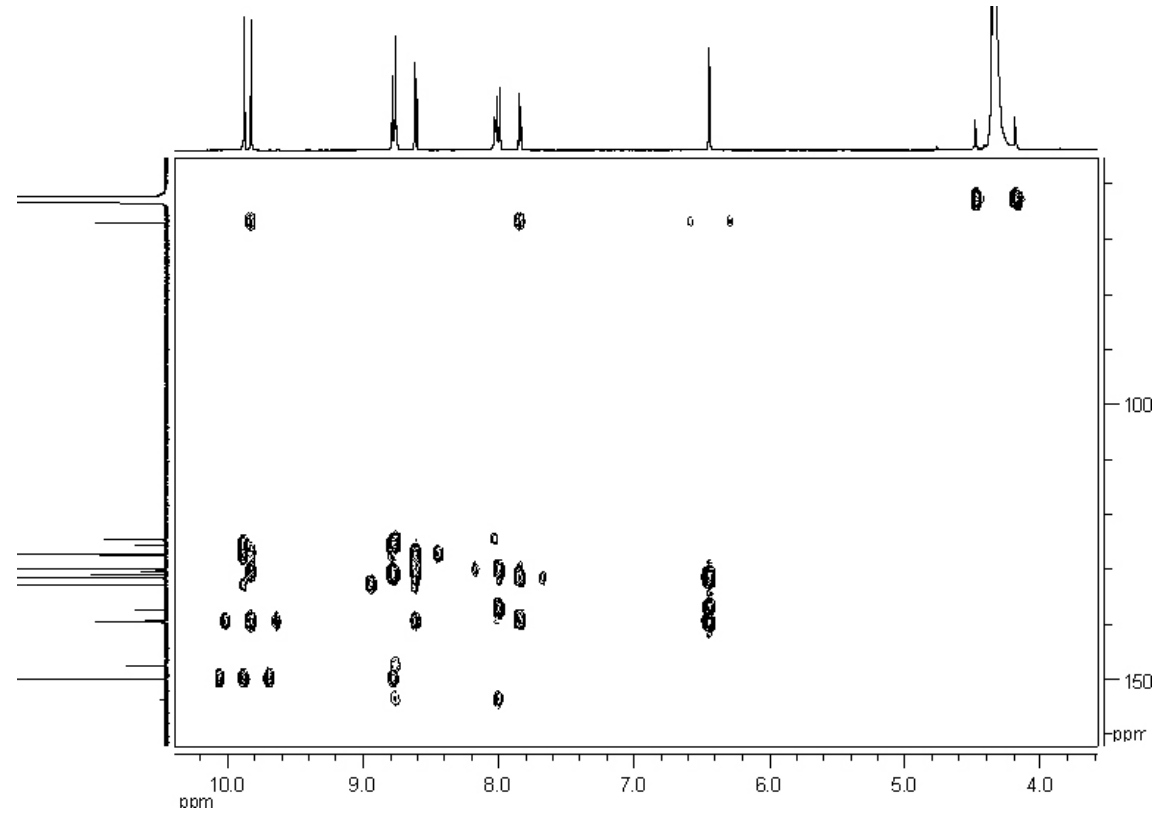

Figure S5: HMBC (CD_3NO_2, 500 and 125 MHz) spectrum of **4**·PF_6

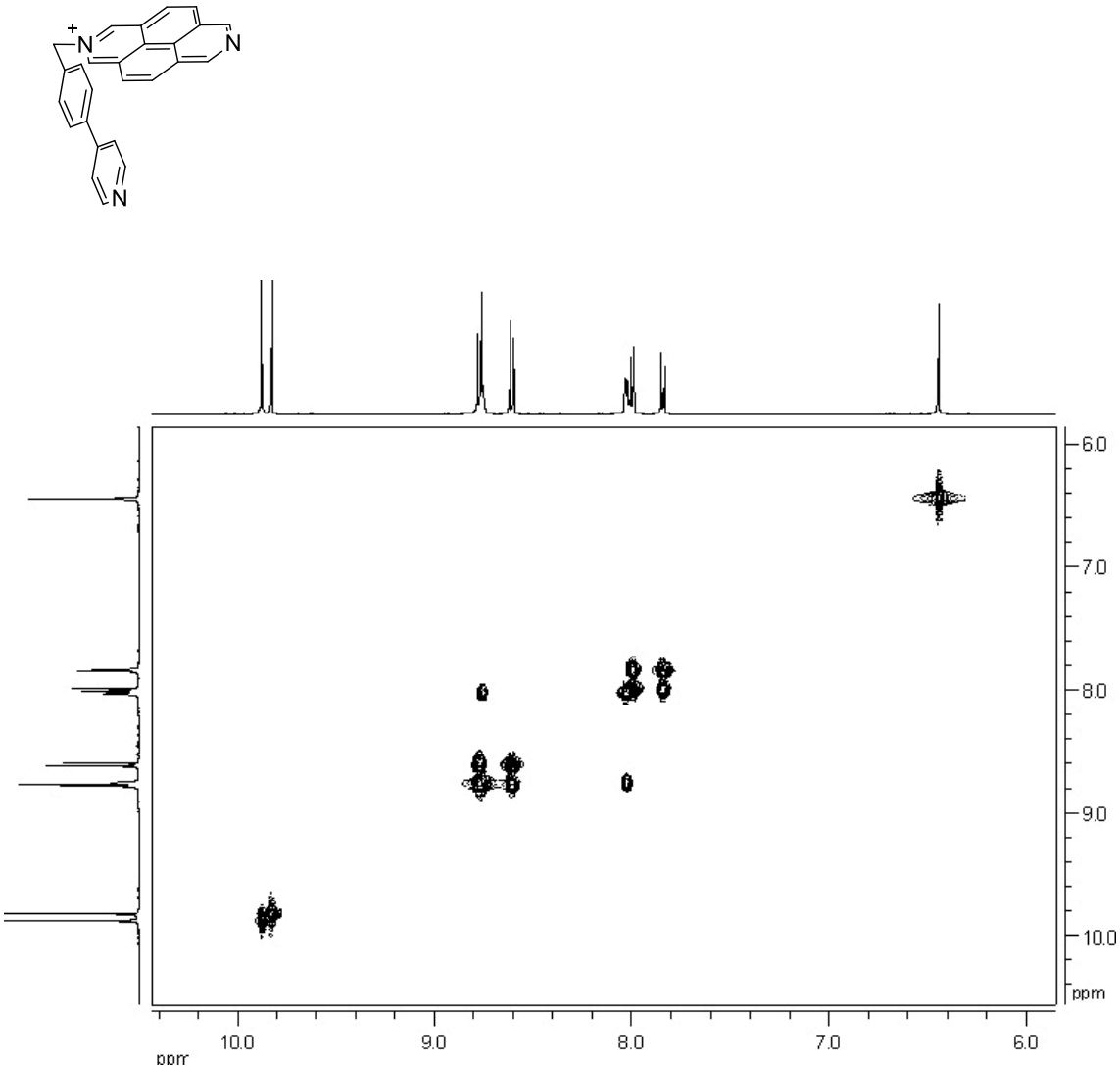

Figure S6: COSY (CD_3NO_2, 500 MHz) spectrum of **4**·PF_6.

1-(4-(pyridin-4-yl)benzyl)-2,7-diazapyren-1-ium nitrate (4·NO_3)

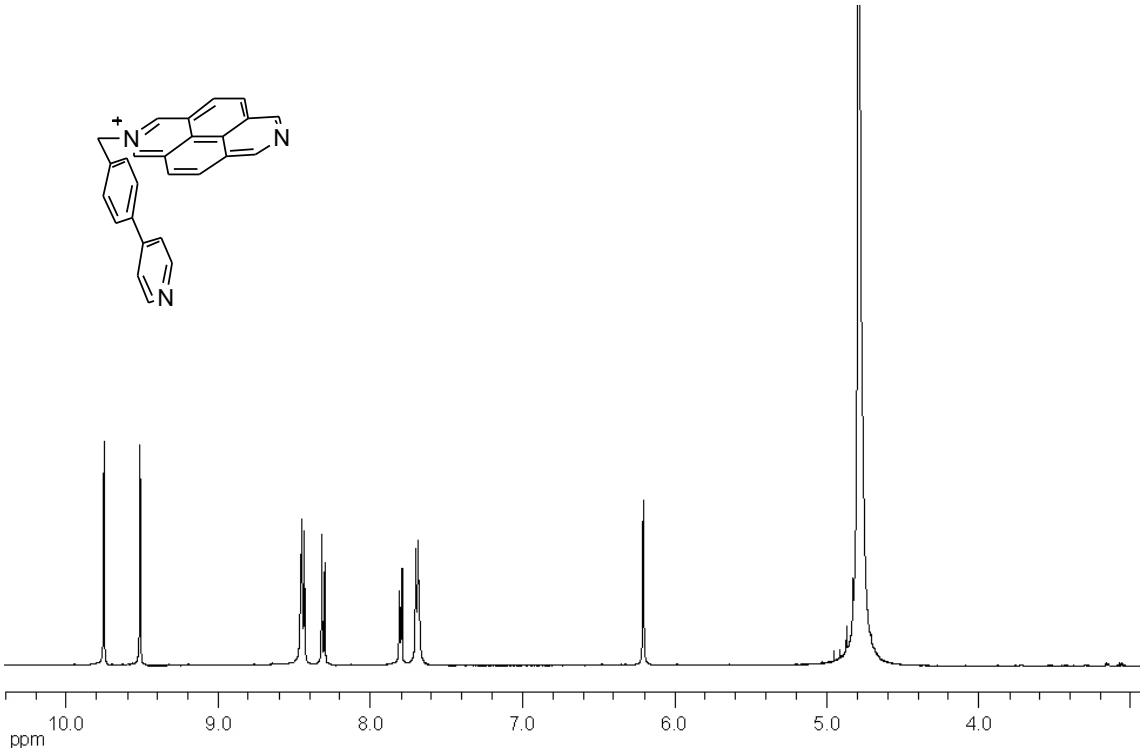

Figure S7: ^{1}H NMR (D_2O, 500 MHz) spectrum of **4**·NO_3

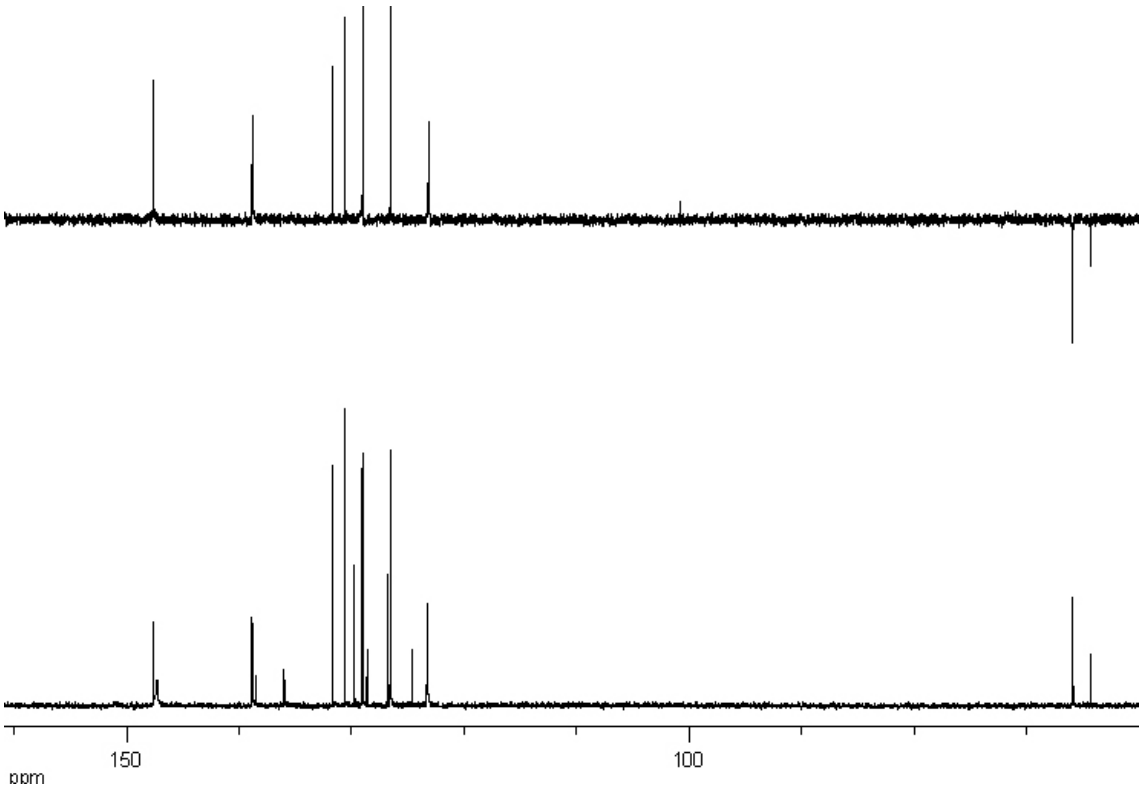

Figure S8: ^{13}C NMR (D_2O, 125 MHz) spectrum of **4**·NO_3**.**

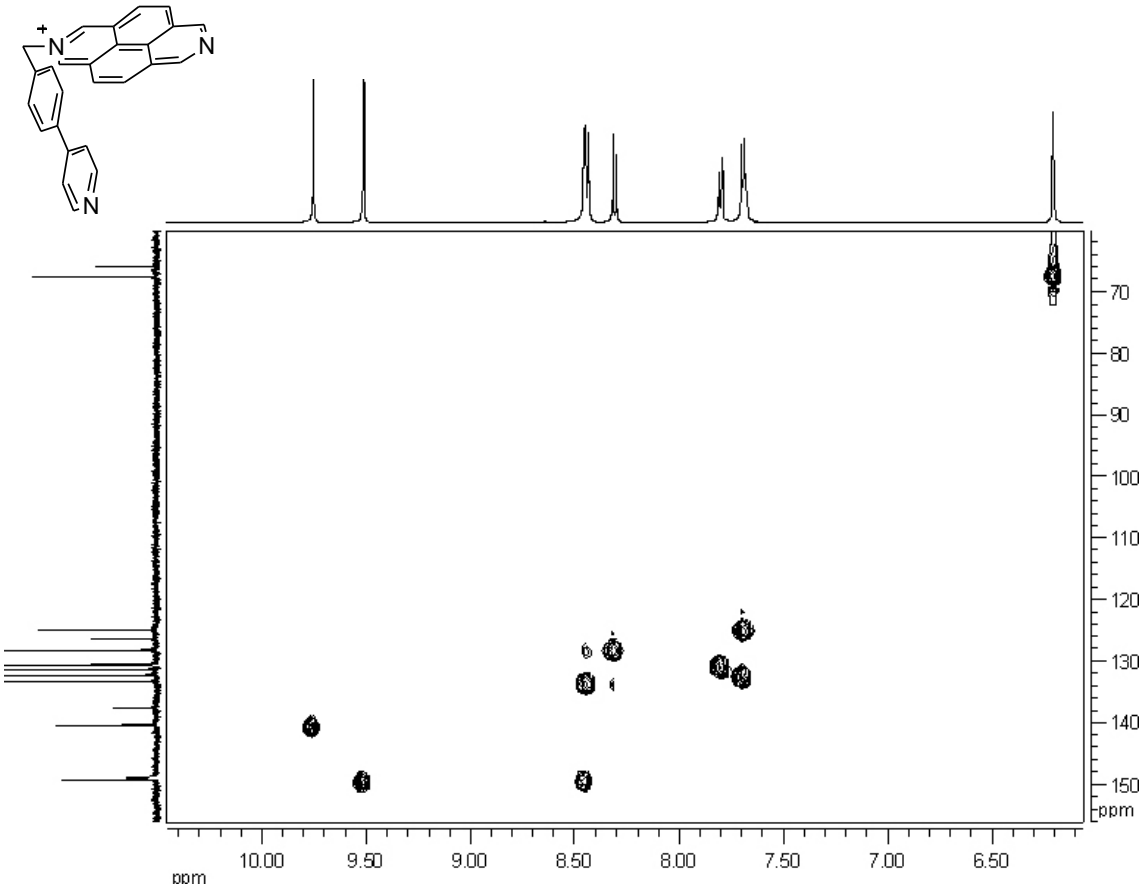

Figure S9: HSQC (D_2O, 500 and 125 MHz) spectrum of **4**·NO_3

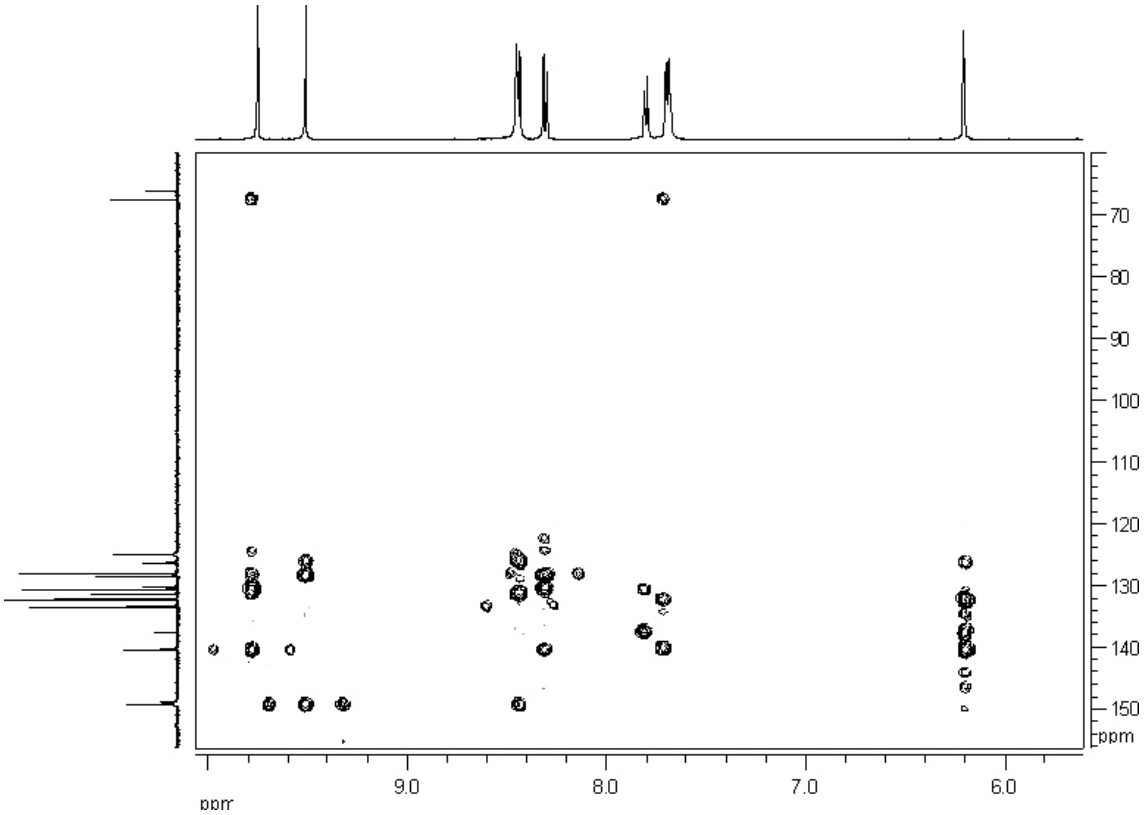

Figure S10: HMBC (D_2O, 500 and 125 MHz) spectrum of **4**·NO_3.

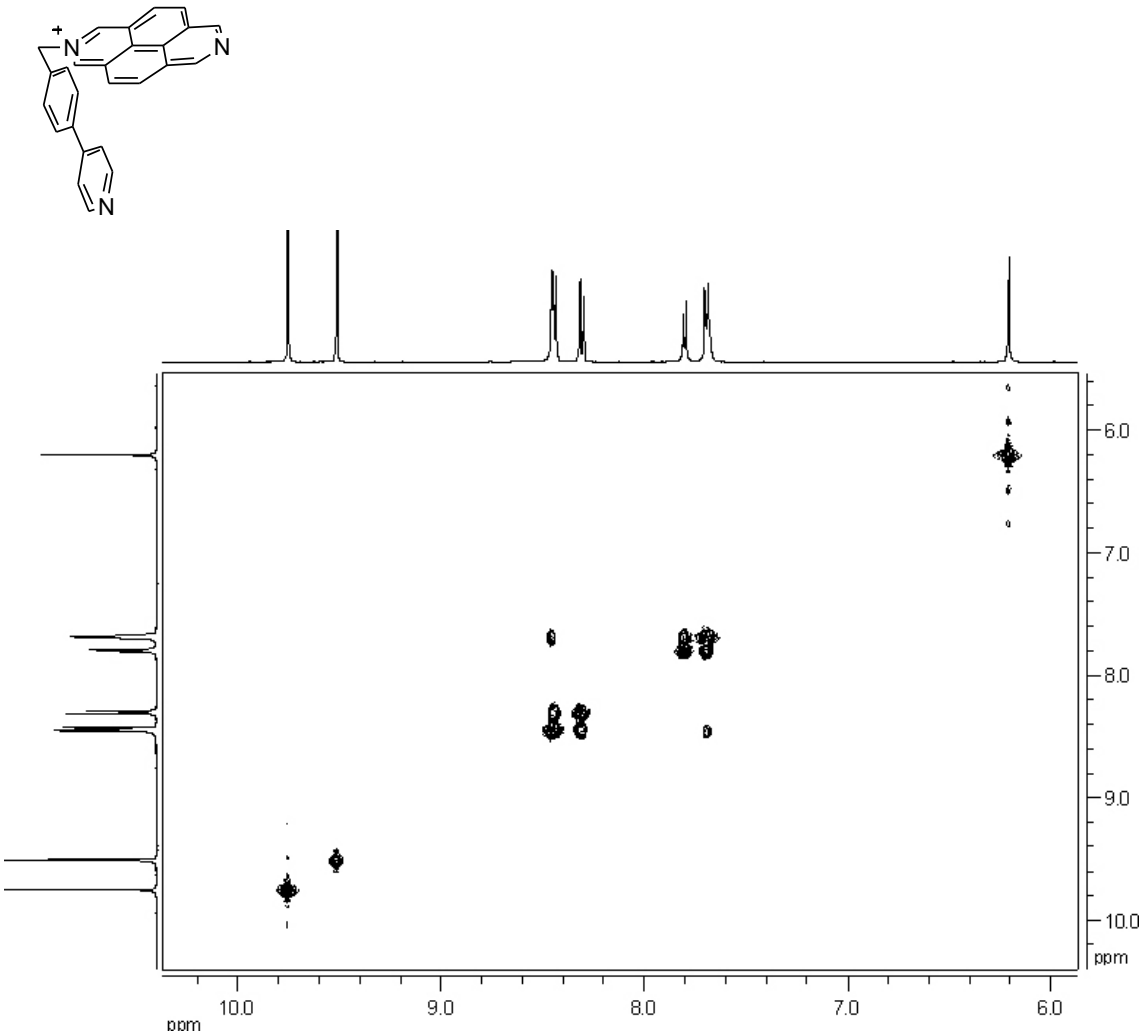

Figure S11: COSY (D_2O, 500 MHz) spectrum of **4**·NO_3**.**

Metallocycles 6a,b·6NO_3

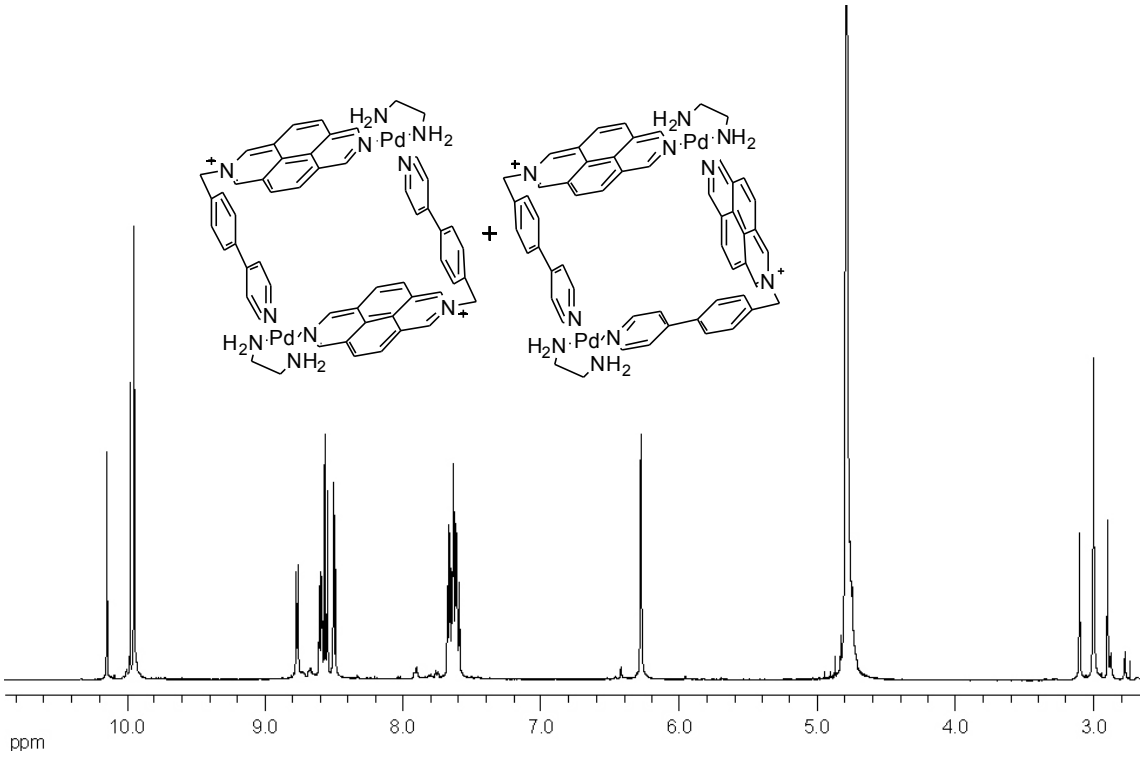

Figure S12: ^{1}H NMR (D_2O, 500 MHz) spectrum of **6a,b**·6NO_3

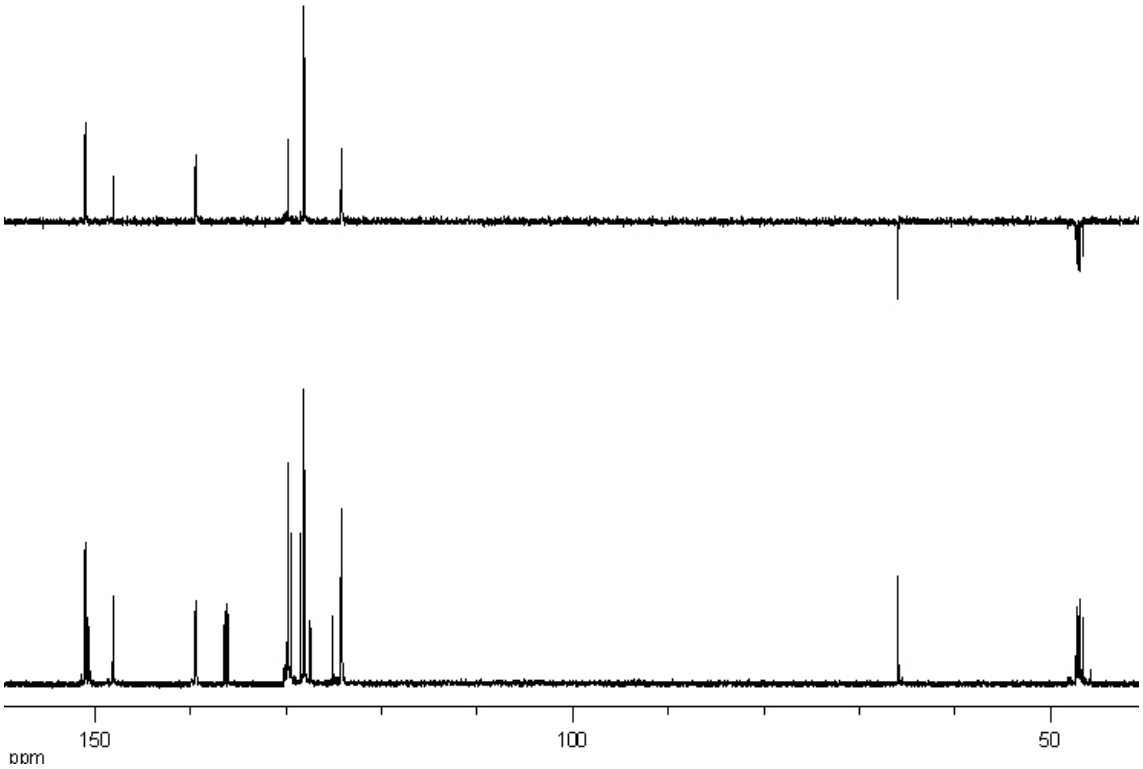

Figure S13: ^{13}C NMR (D_2O, 125 MHz) spectrum of **6a,b**·6NO_3.

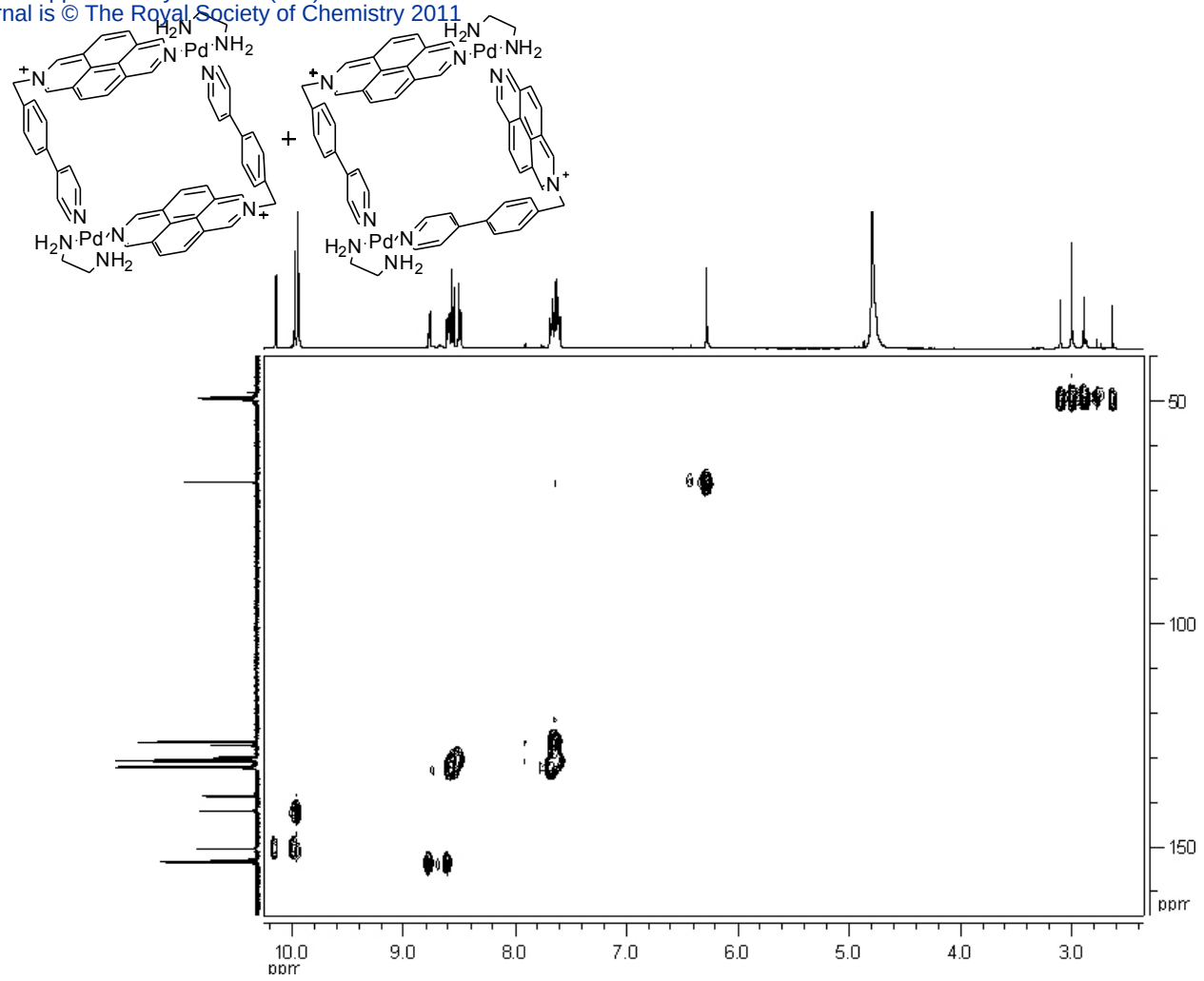

Figure S14: HSQC (D_2O, 500 and 125 MHz) spectrum of **6a,b**·$6NO_3$.

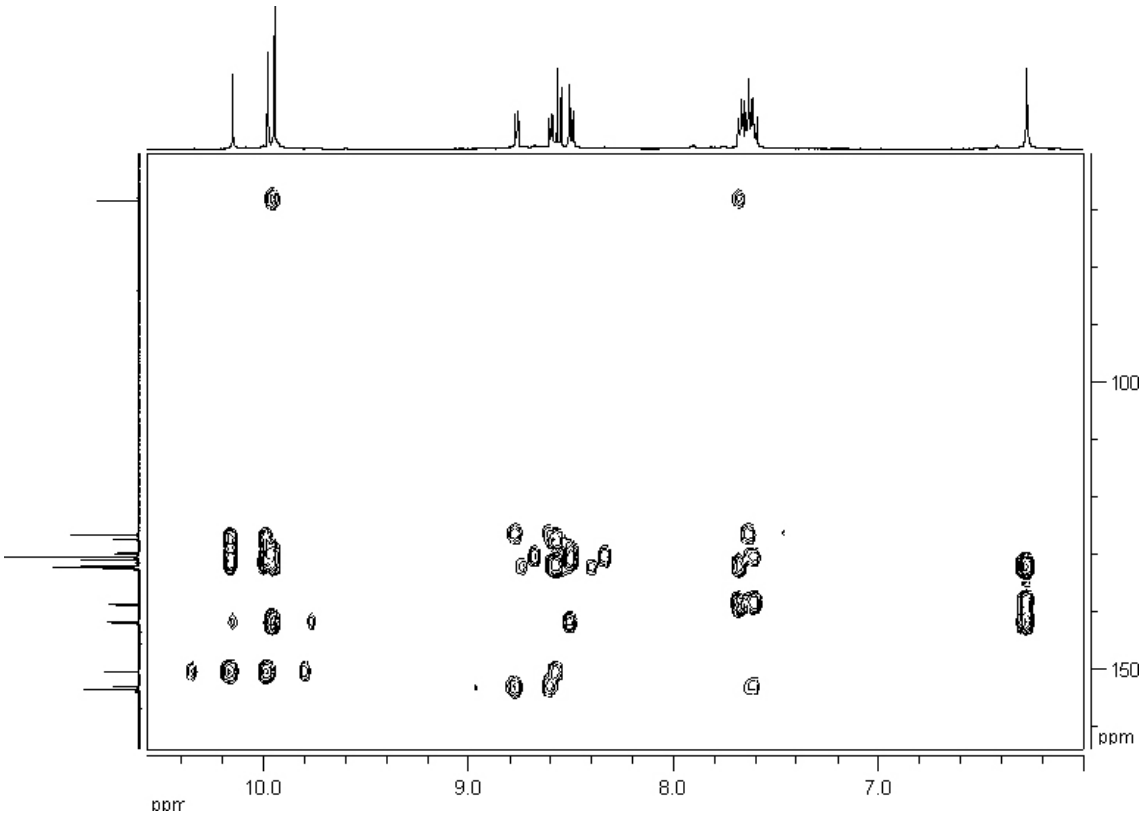

Figure S15: HMBC (D_2O, 500 and 125 MHz) spectrum of **6a,b**·$6NO_3$.

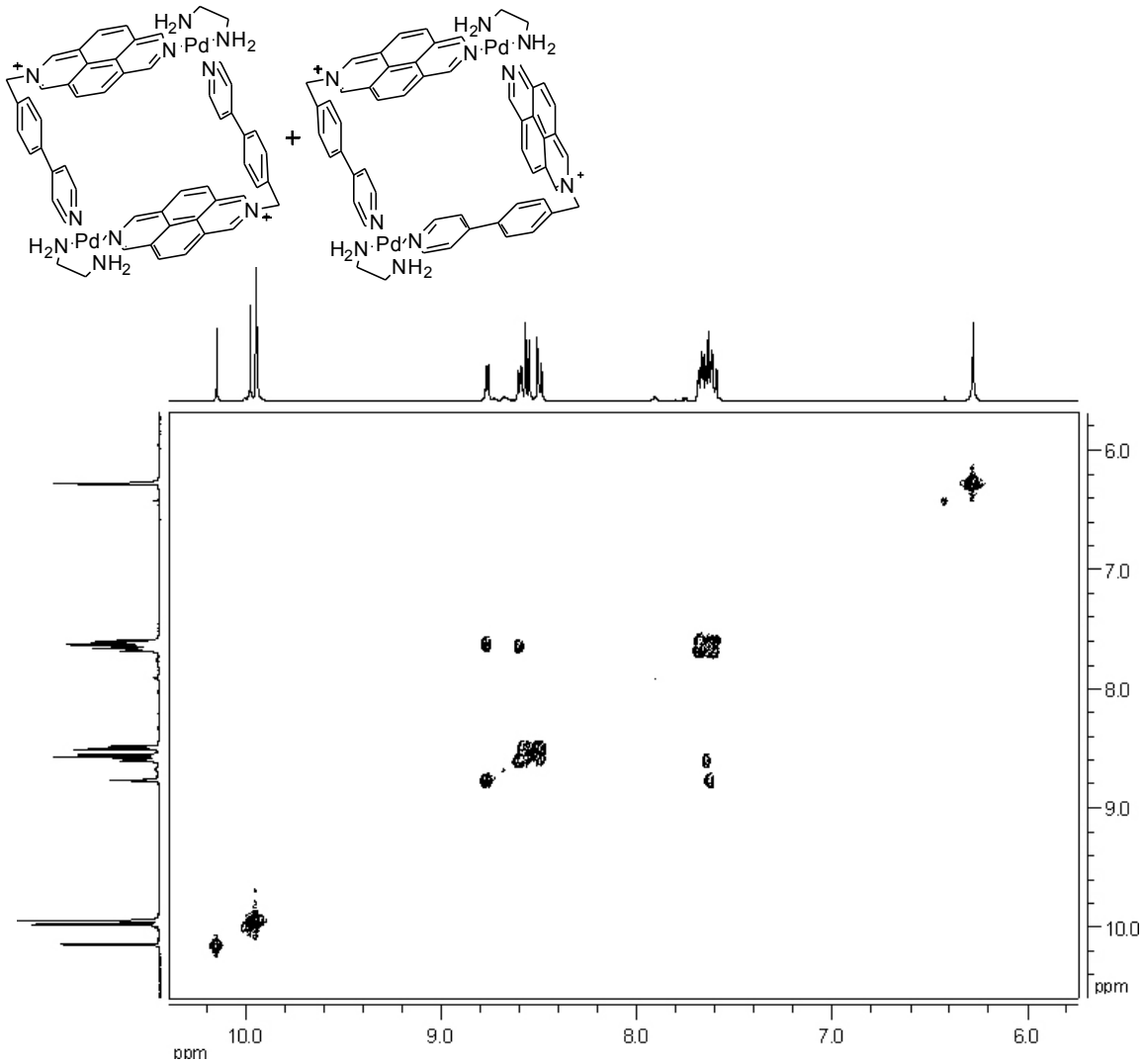

Figure S16: COSY (D_2O, 500 MHz) spectrum of **6a,b**·$6NO_3$**.**

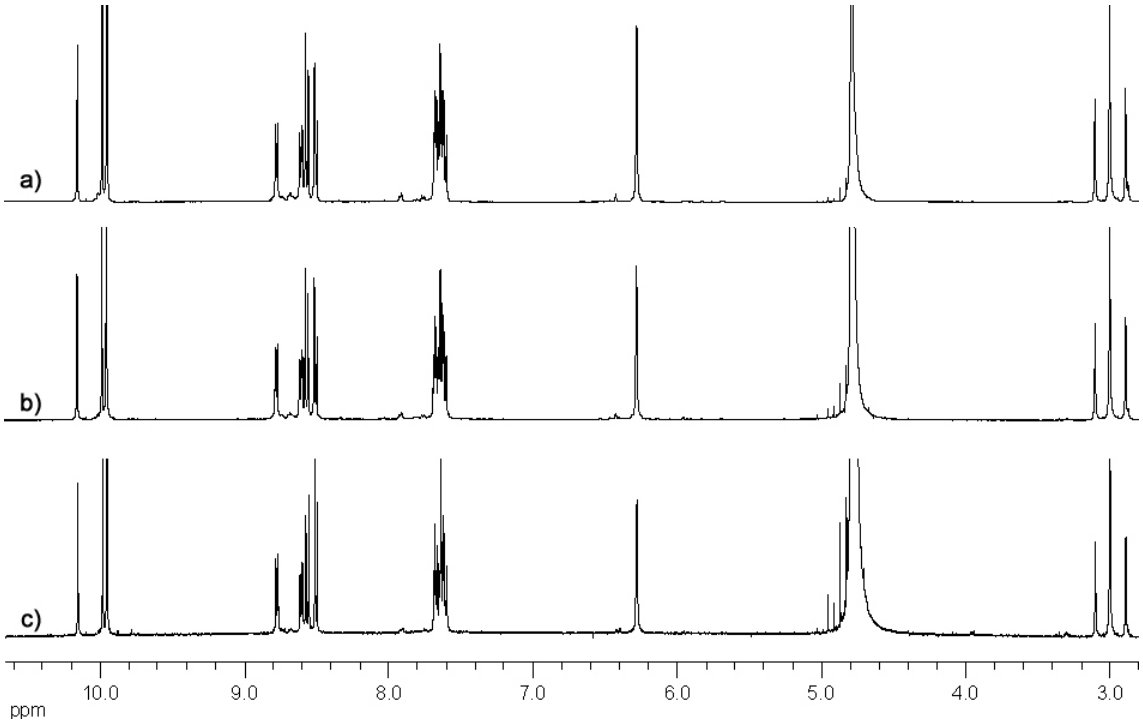

Figure S17: ^{1}H NMR (D_2O, 300 MHz) spectra of **6a,b**·$6NO_3$ at different concentrations: a) 2.5 mM. b) 1 mM. c) 0.25 mM.

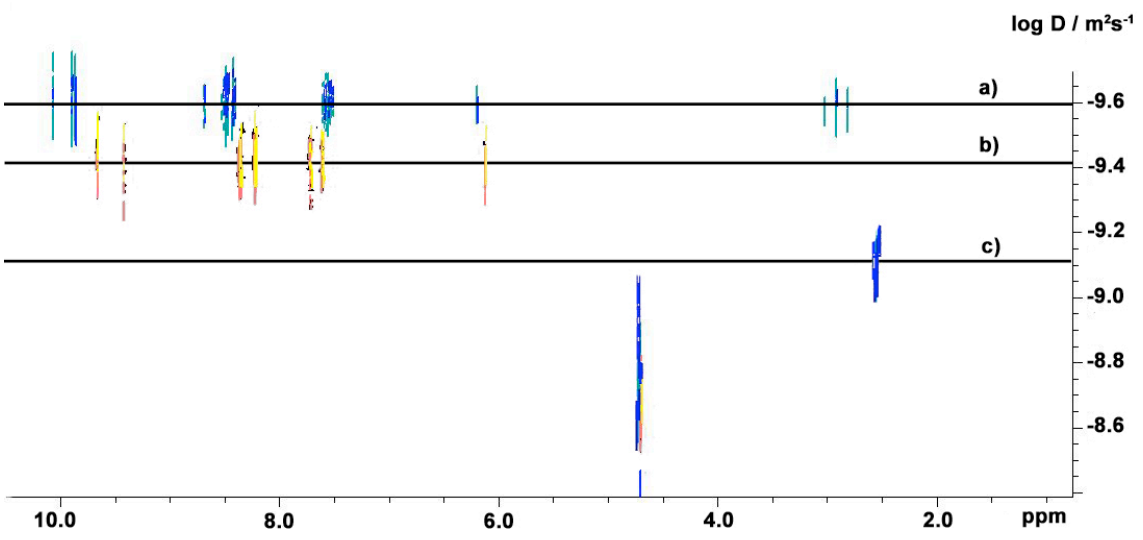

Figure S18: Superposed DOSY (D_2O, 500 MHz, 298 K) experiments of: a) 10 mM solution of **4**·NO_3 and **5a**. b) 10 mM solution of **4**·NO_3. c) **5a**.

Metalocycles 6a,b·6PF$_6$

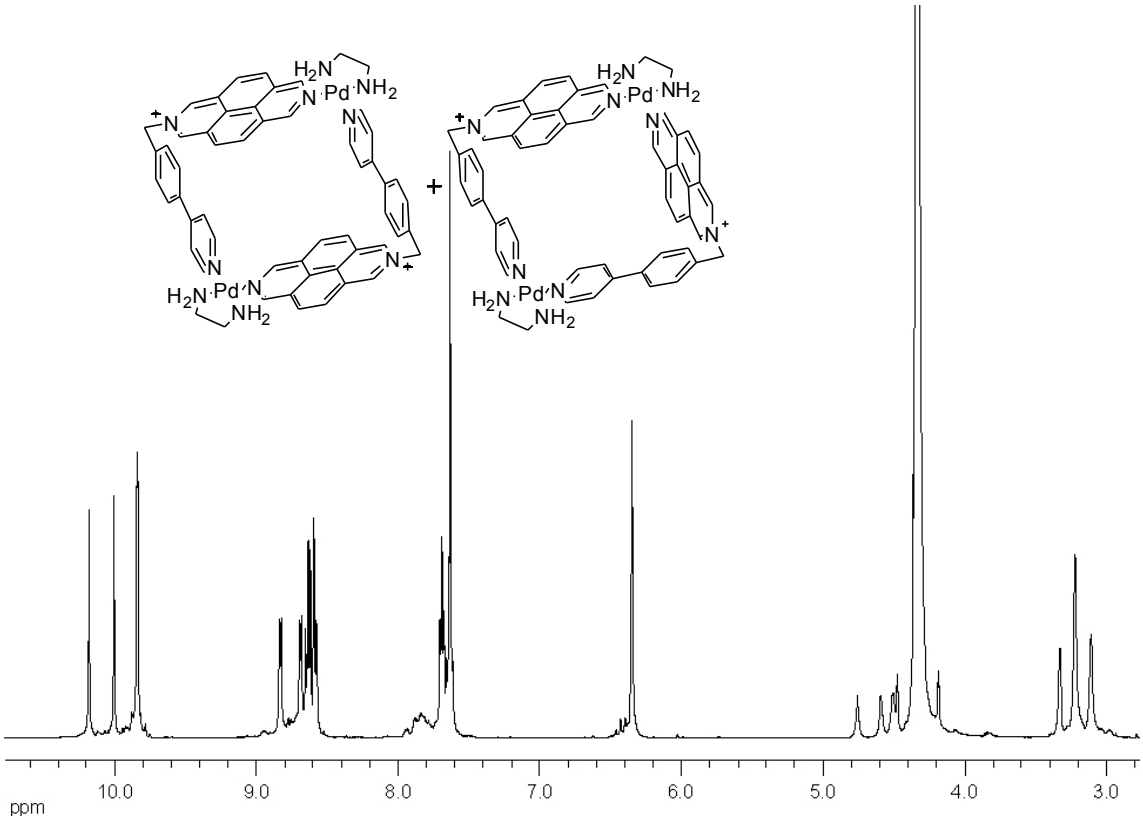

Figure S19: ^{1}H NMR (CD_3NO_2, 500 MHz) spectrum of **6a,b**·6PF$_6$

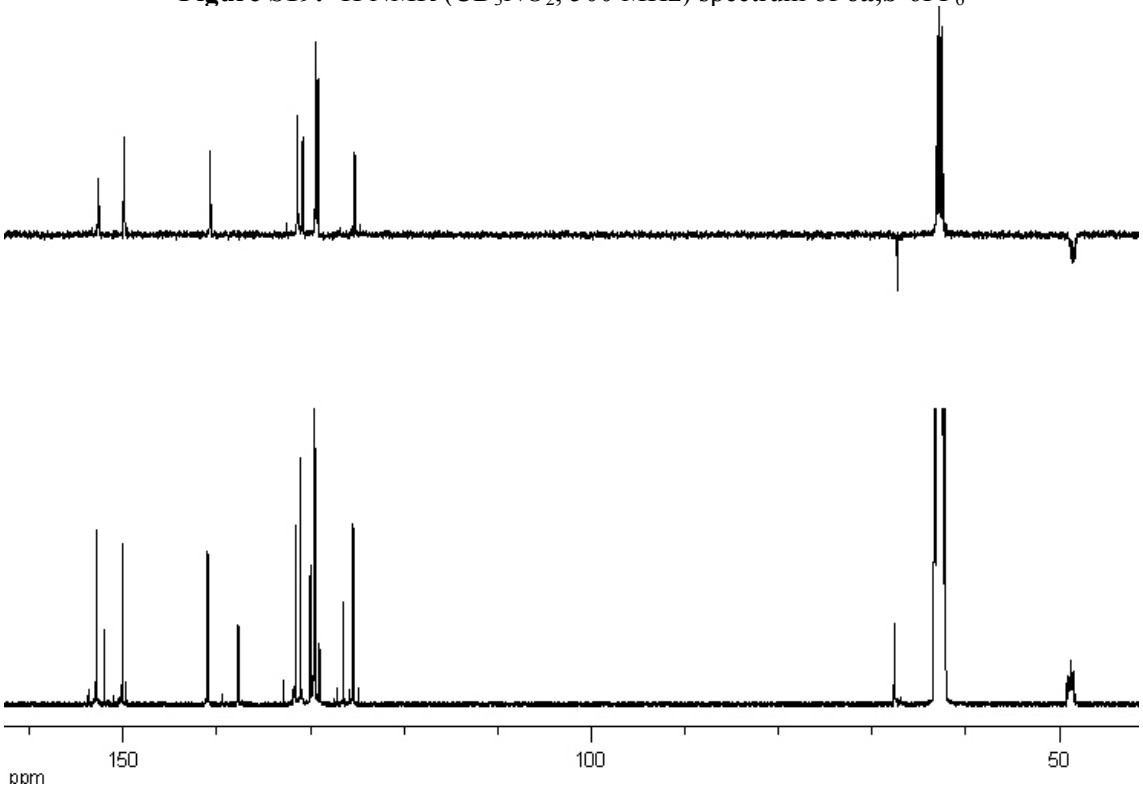

Figure S20: ^{13}C NMR (CD_3NO_2, 125 MHz) spectrum of **6a,b**·6PF$_6$.

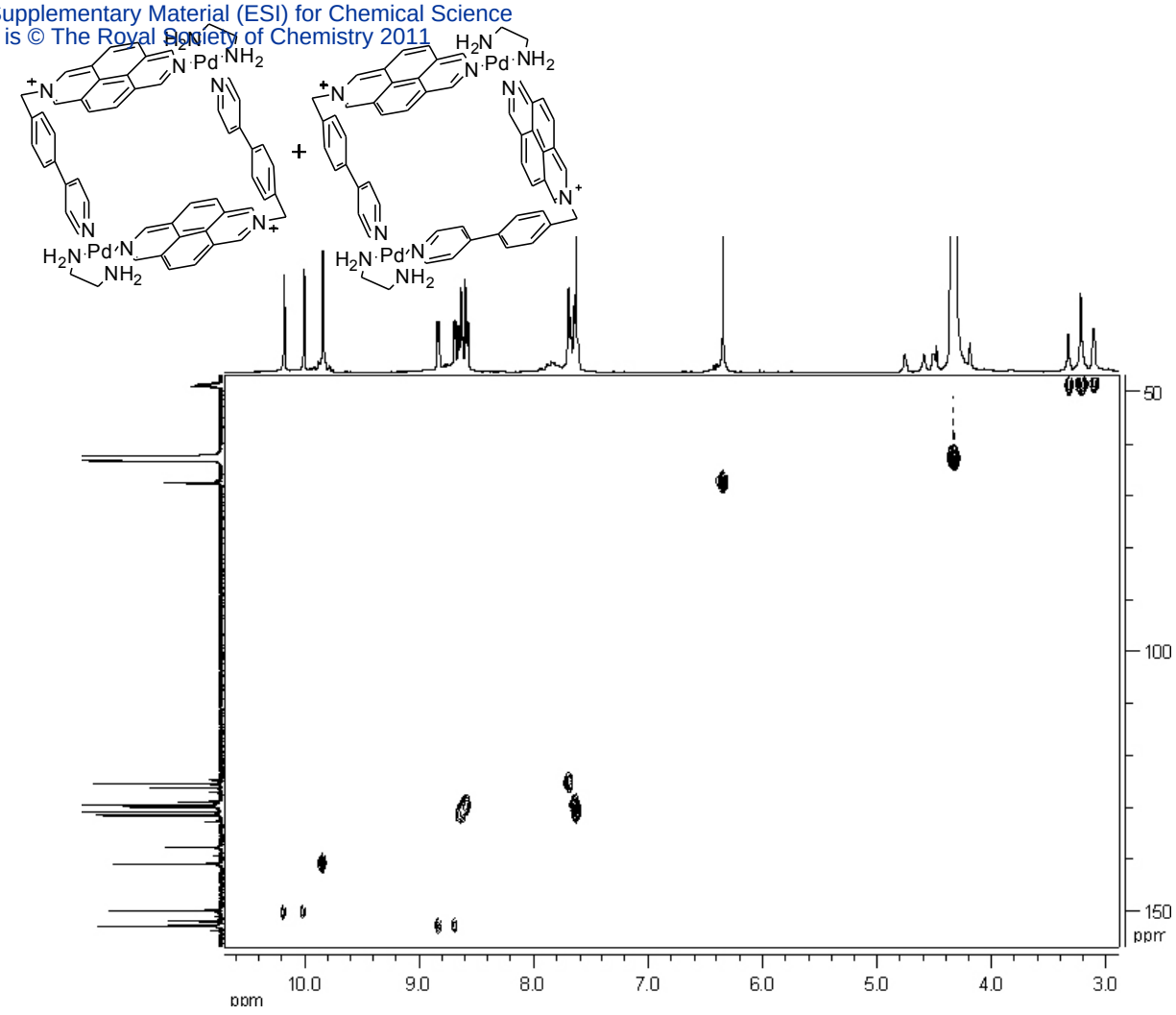

Figure S21: HSQC (CD_3NO_2, 500 and 125 MHz) spectrum of **6a,b**·$6PF_6$

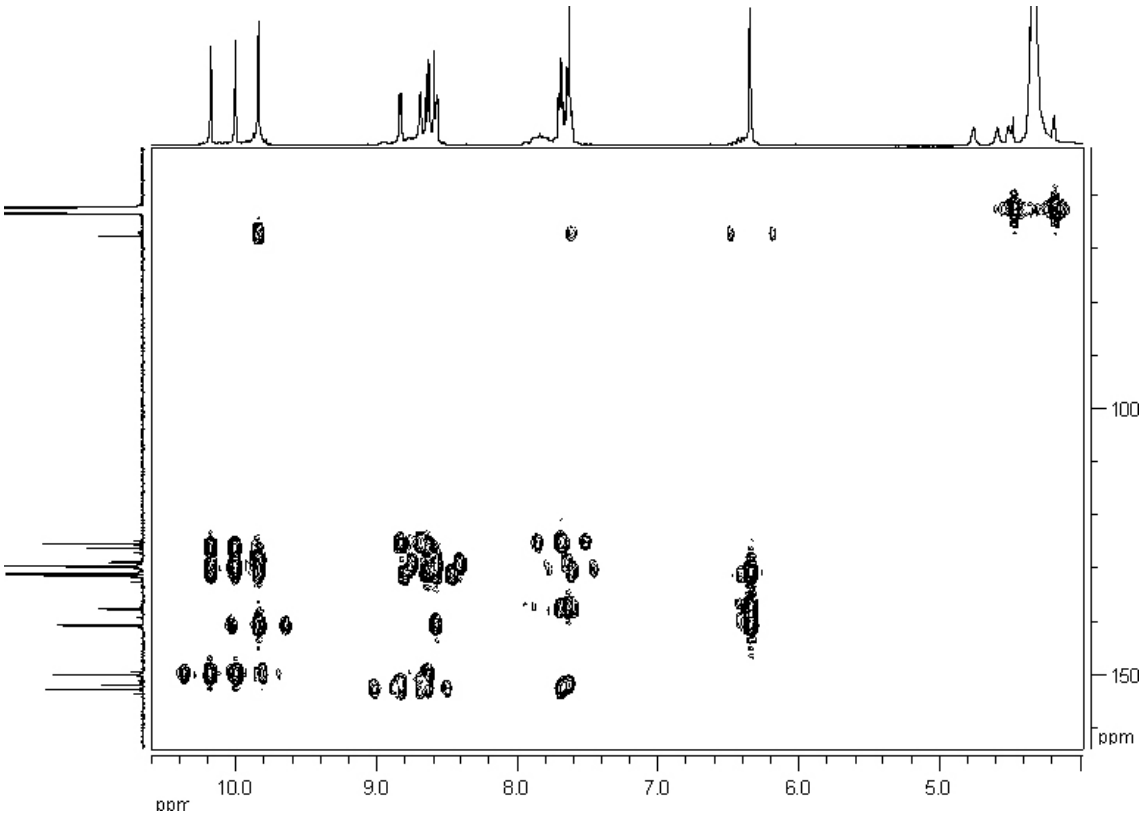

Figure 22: HMBC (CD_3NO_2, 500 and 125 MHz) spectrum of **6a,b**·$6PF_6$

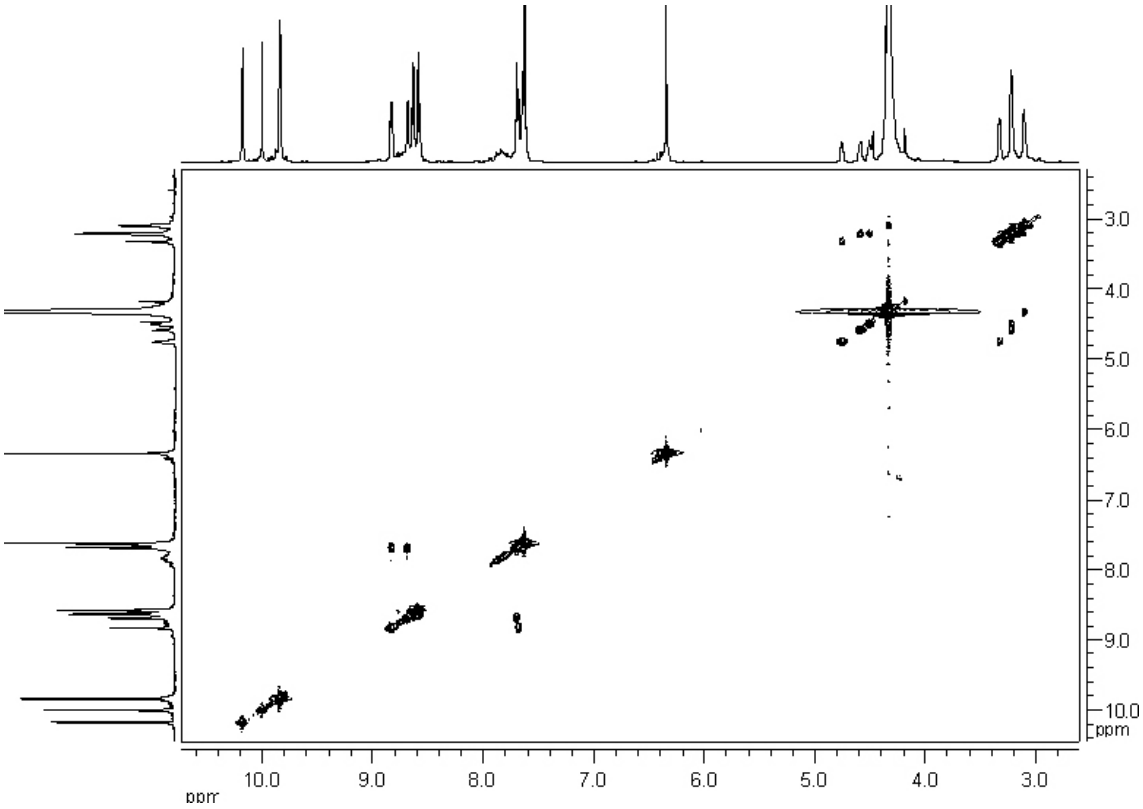

Figure S23: COSY (CD_3NO_2, 500 MHz) spectrum of **6a,b**·$6PF_6$.

Metalocycles 7a,b·6PF$_6$

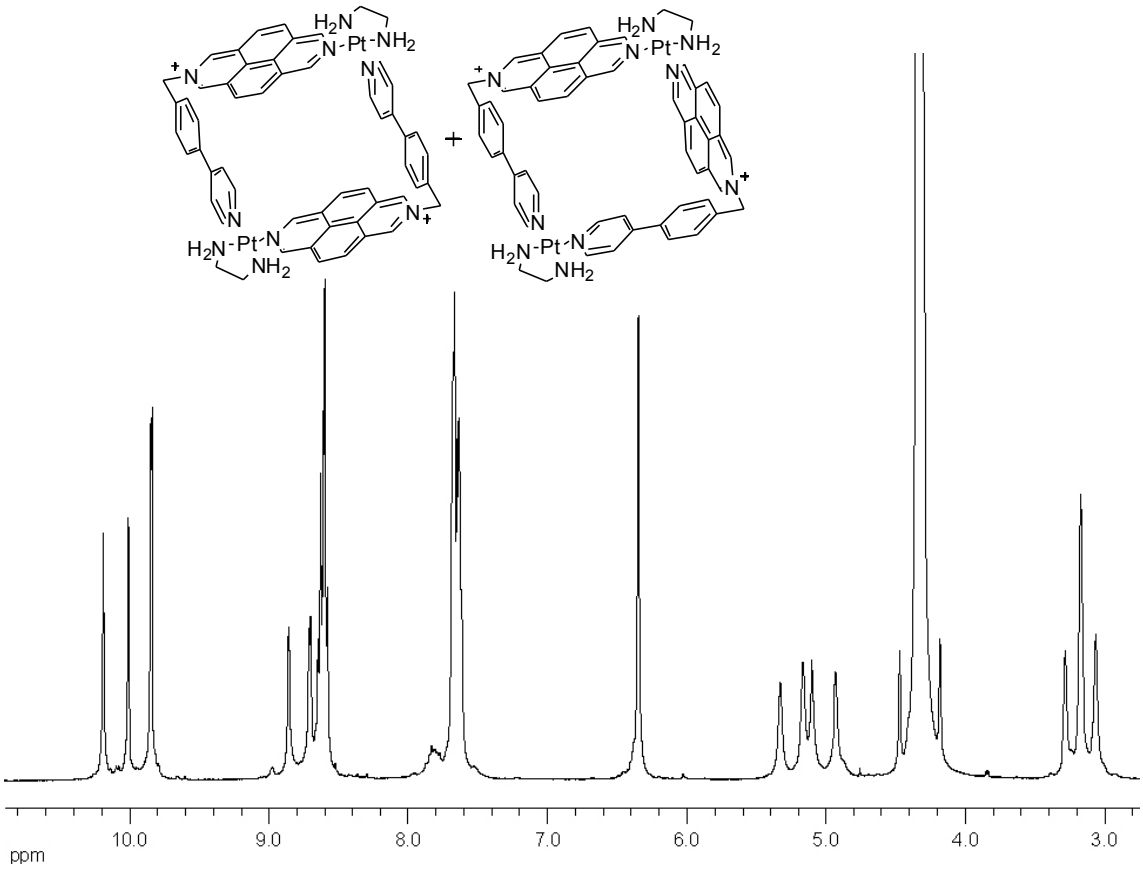

Figure S24: ^{1}H NMR (CD_3NO_2, 500 MHz) spectrum of **7a,b**·6PF$_6$.

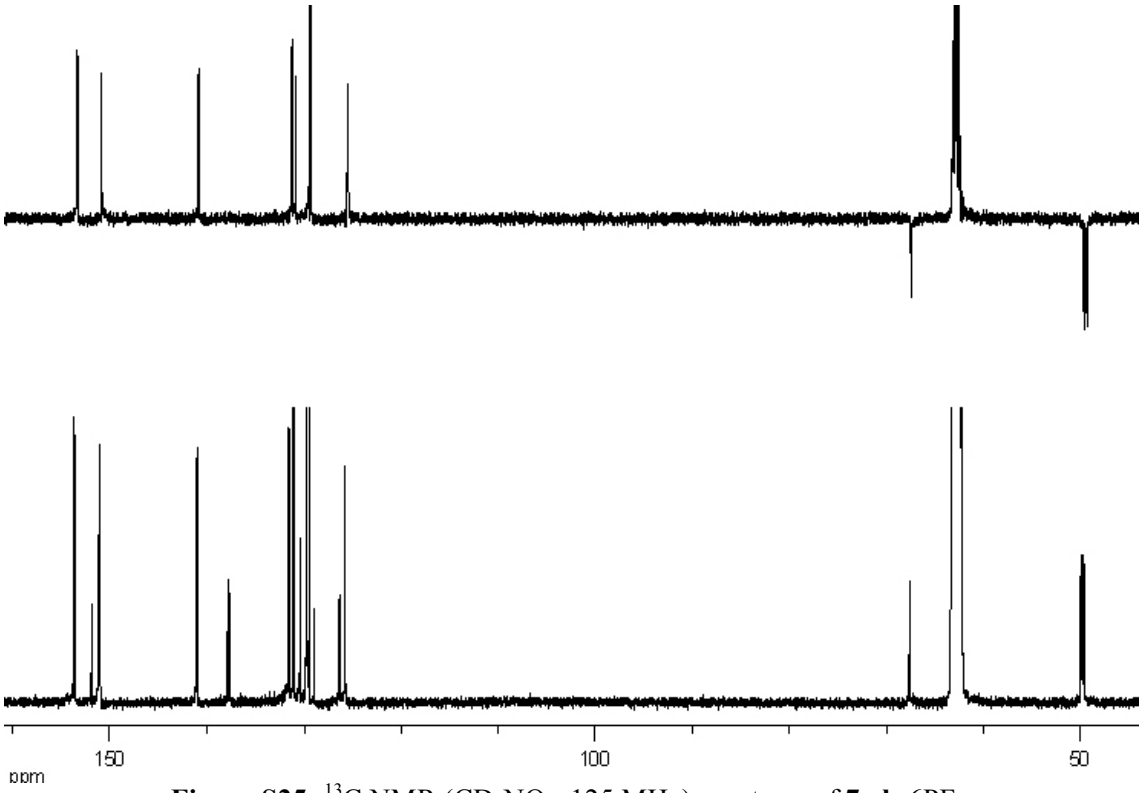

Figure S25: ^{13}C NMR (CD_3NO_2, 125 MHz) spectrum of **7a,b**·6PF$_6$.

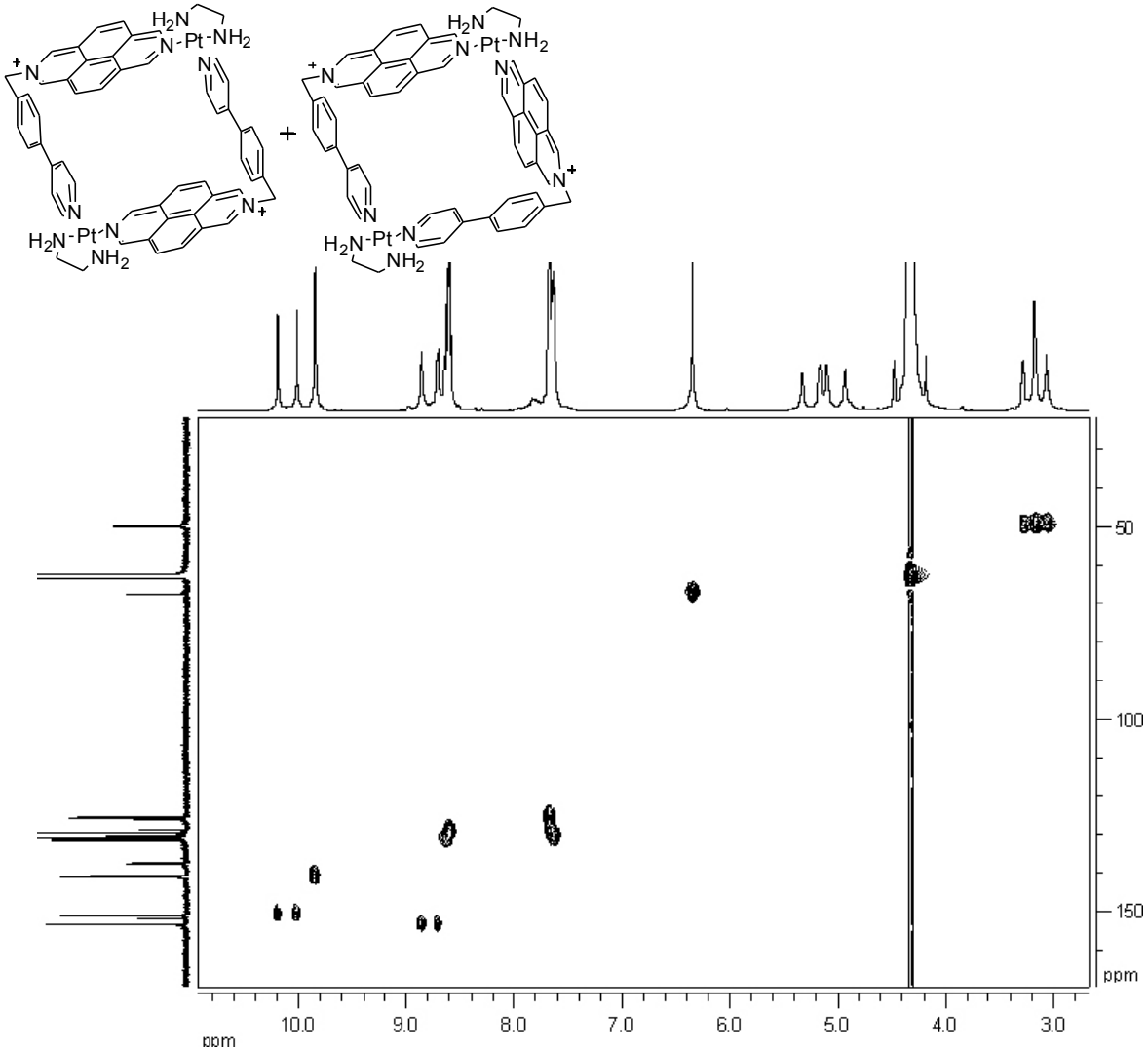

Figure S26: HSQC (CD_3NO_2, 500 and 125 MHz) spectrum of **7a,b**·$6PF_6$.

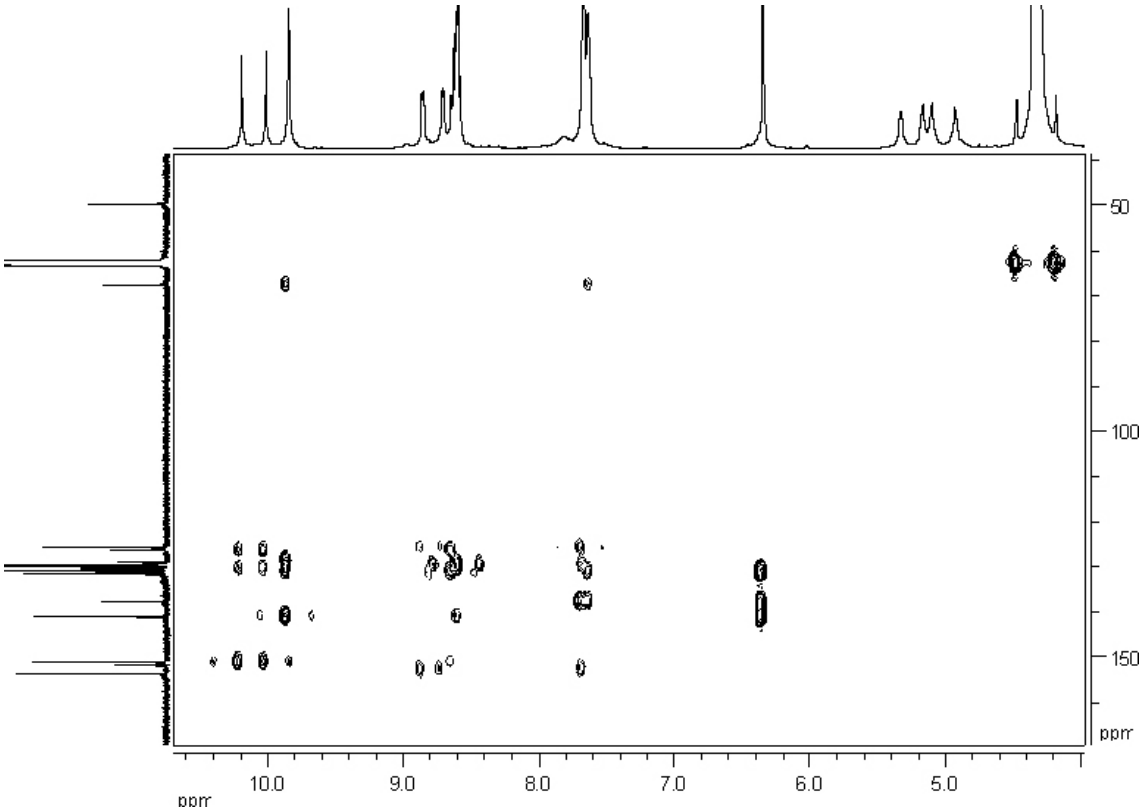

Figure S27: HMBC (CD_3NO_2, 500 and 125 MHz) spectrum of **7a,b**·$6PF_6$.

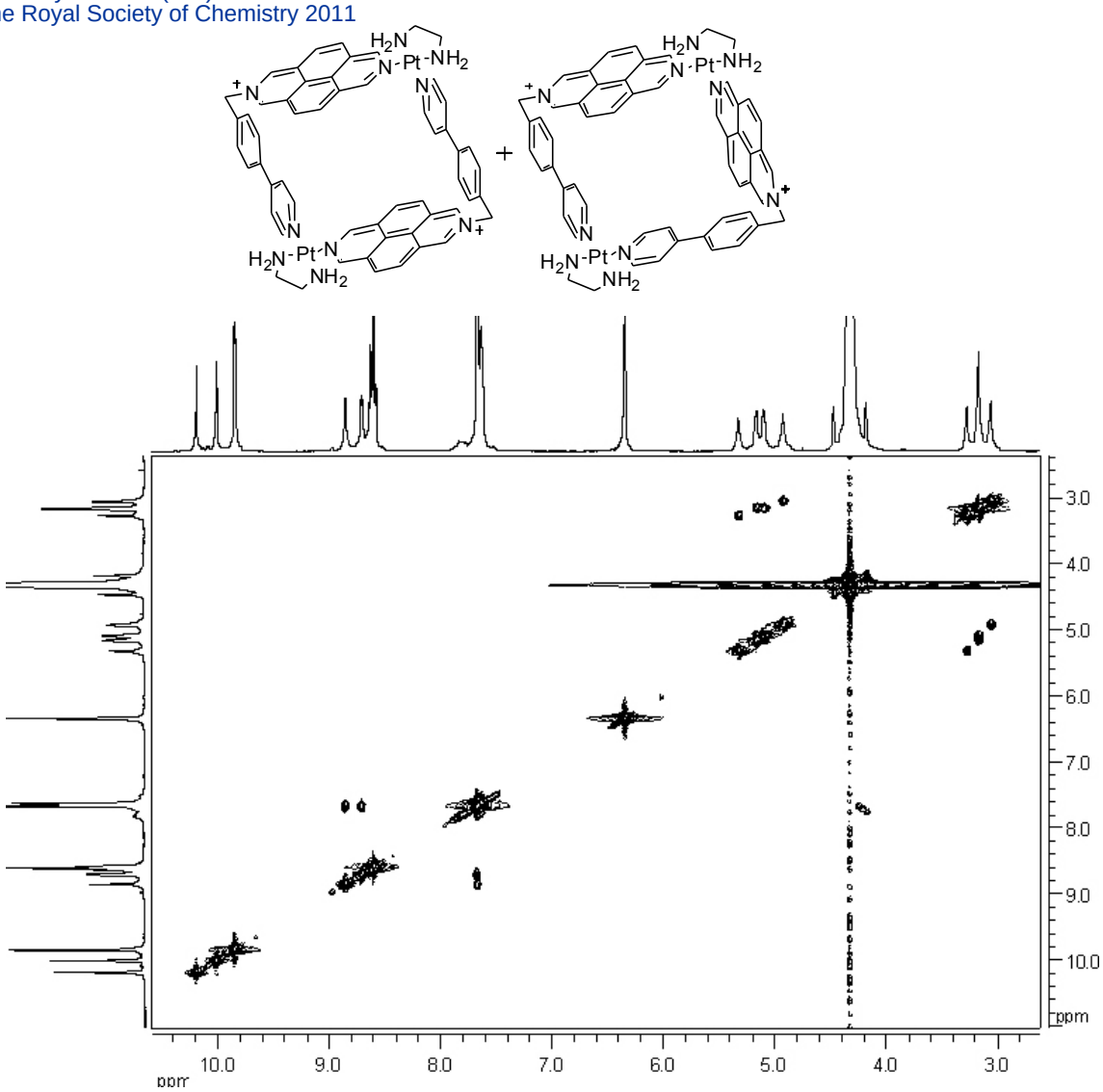

Figure S28: COSY (CD_3NO_2, 500 MHz) spectrum of **7a,b**·$6PF_6$

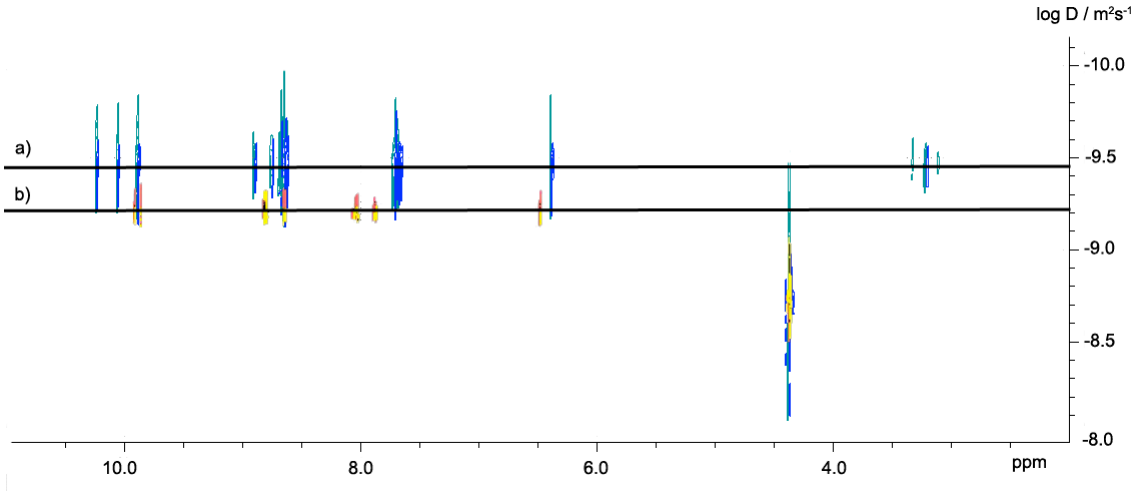

Figure S29: Superposed DOSY (CD_2NO_2, 500 MHz, 298 K) experiments of: a) metallocycles **7a,b**·$6PF_6$ (blue). b) ligand **4**·PF_6 (yellow).

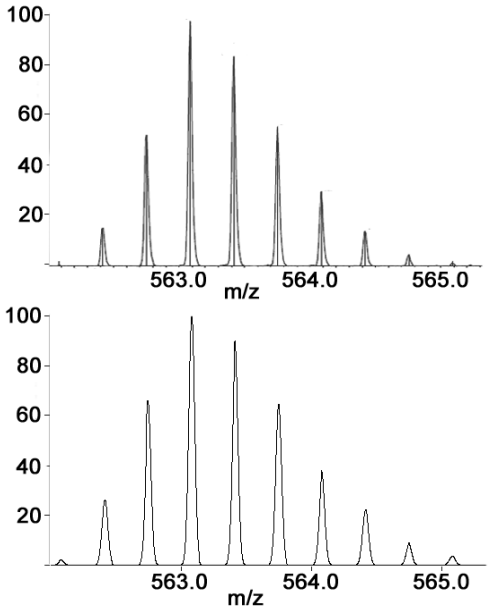

Figure S30: Observed (top) and theoretical (bottom) isotopic distribution for fragment [**7a,b** – $3PF_6^-$]$^{3+}$ (exp. m/z = 563.0843, theoretical m/z = 563.0860).

Metalocycles 7a,b·6NO$_3$

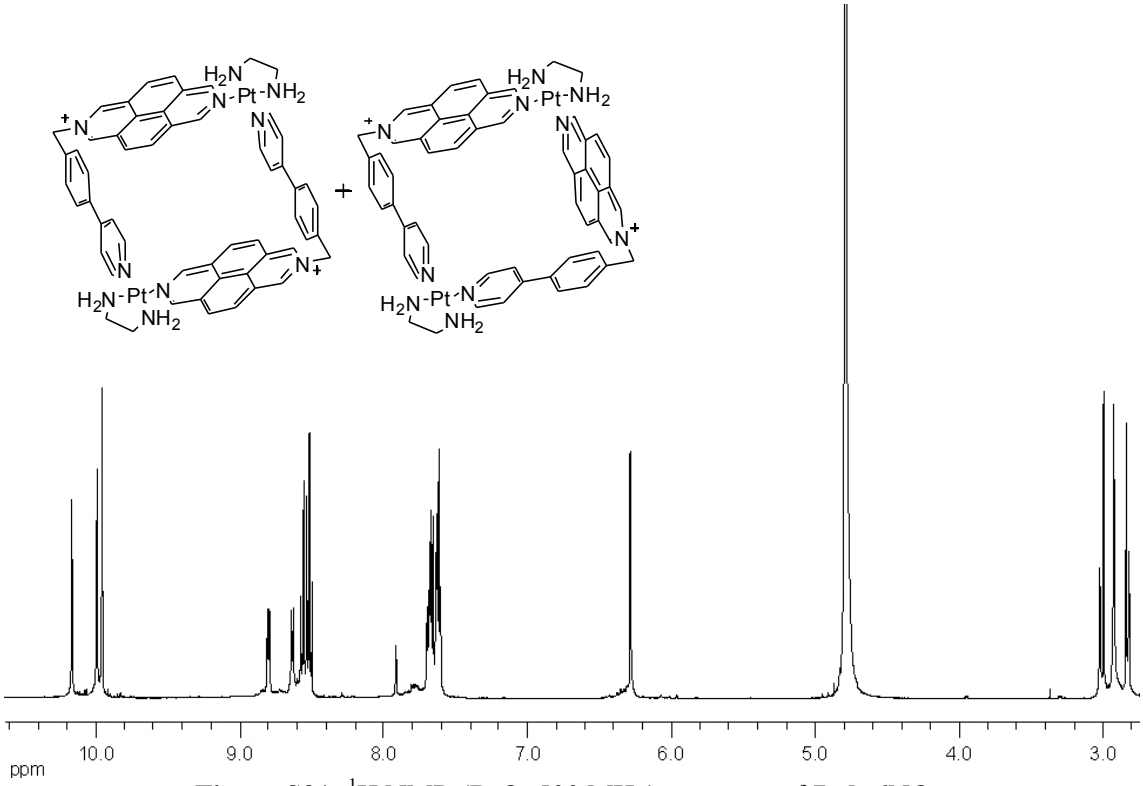

Figure S31: ^{1}H NMR (D_2O, 500 MHz) spectrum of **7a,b**·6NO_3.

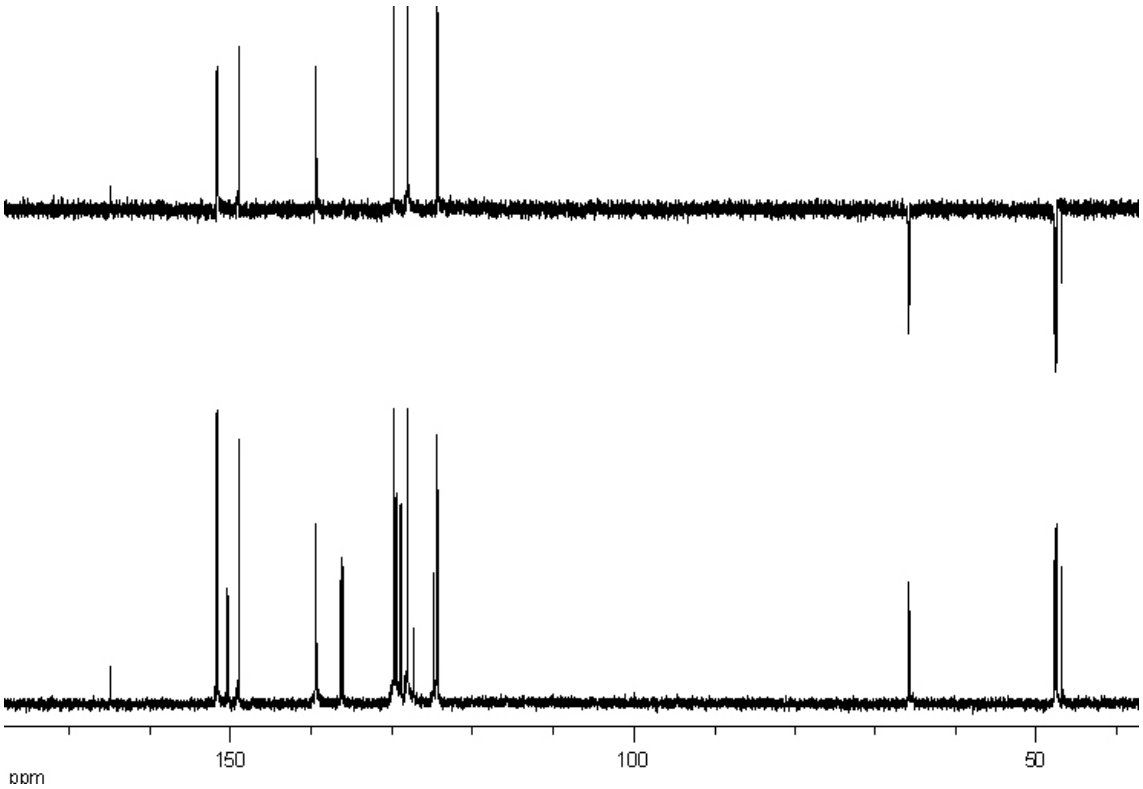

Figure S32: ^{13}C NMR (D_2O, 125 MHz) spectrum of **7a,b**·6NO_3.

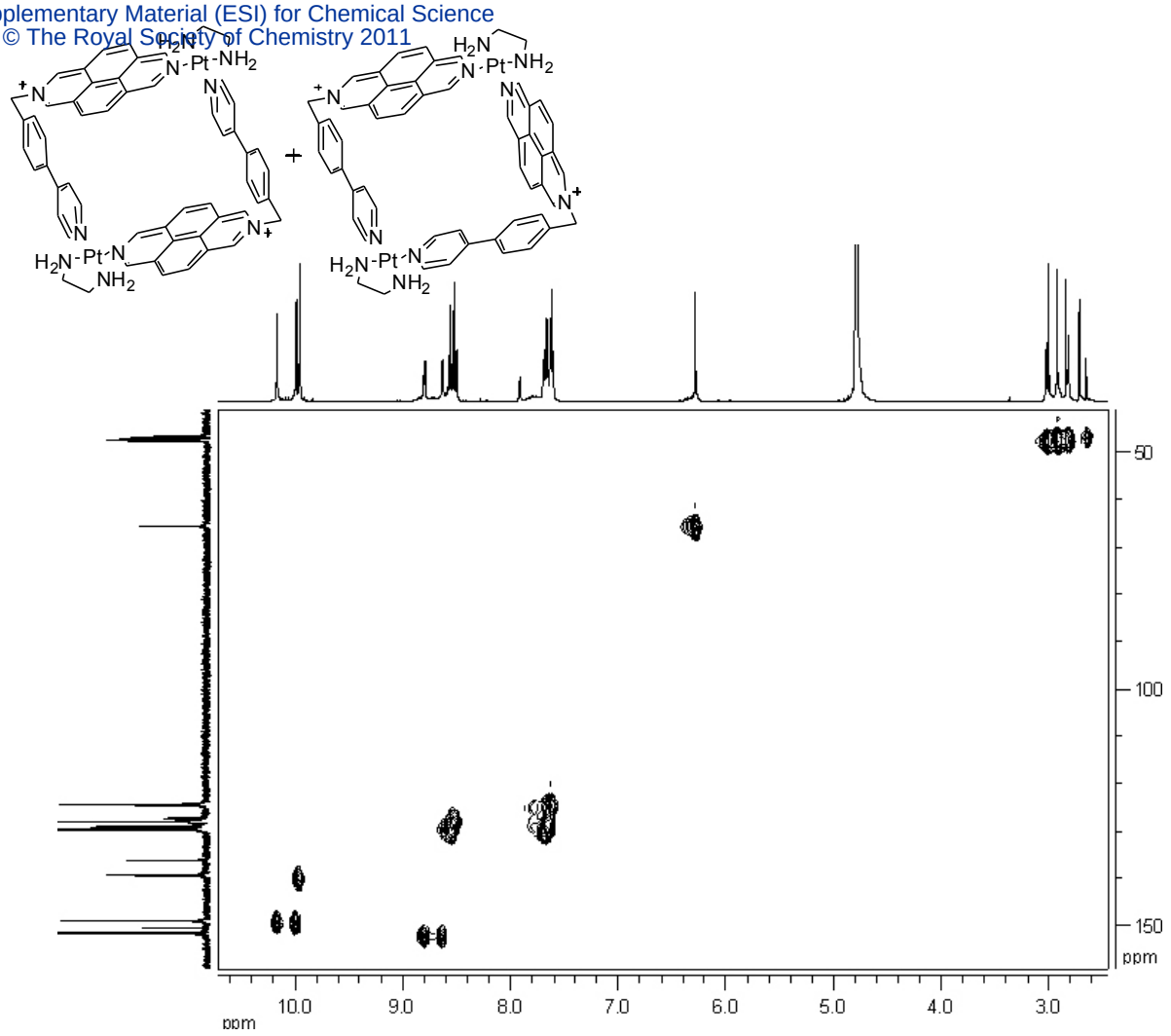

Figure S33: HSQC (D_2O, 500 and 125 MHz) spectrum of **7a,b**·$6NO_3$.

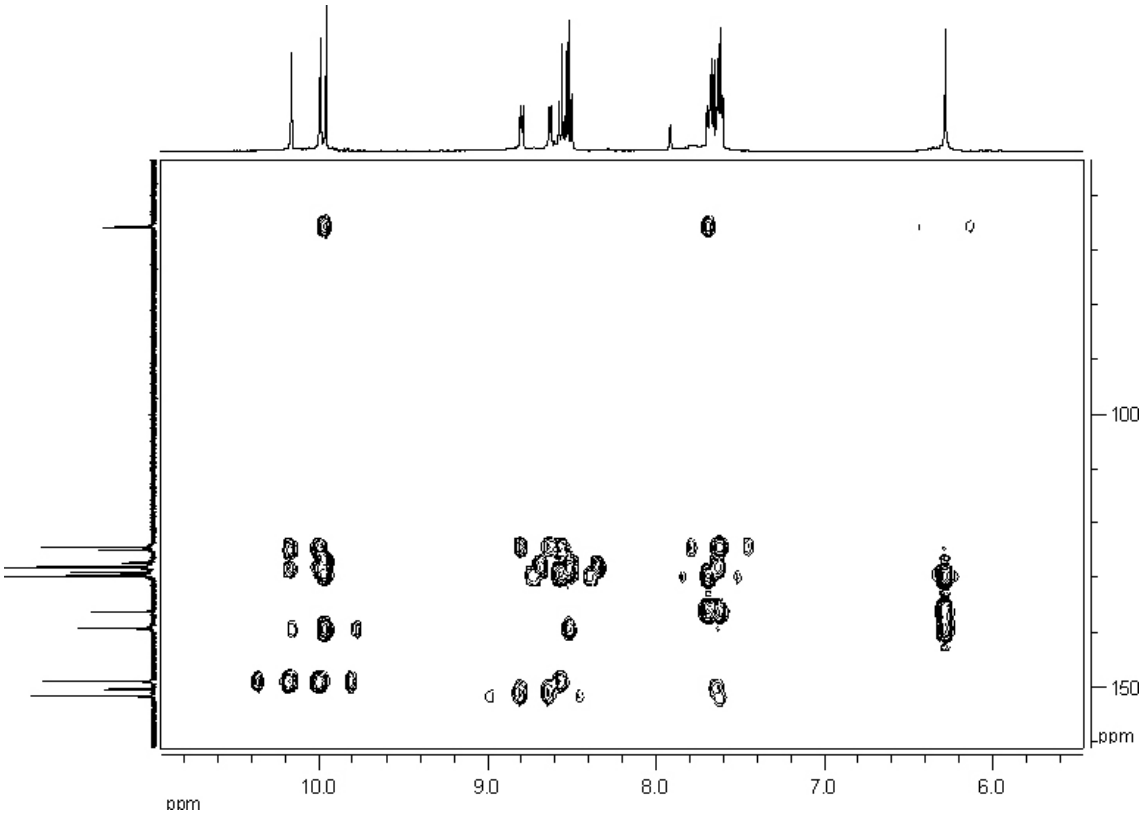

Figure S34: HMBC (D_2O, 500 and 125 MHz) spectrum of **7a,b**·$6NO_3$.

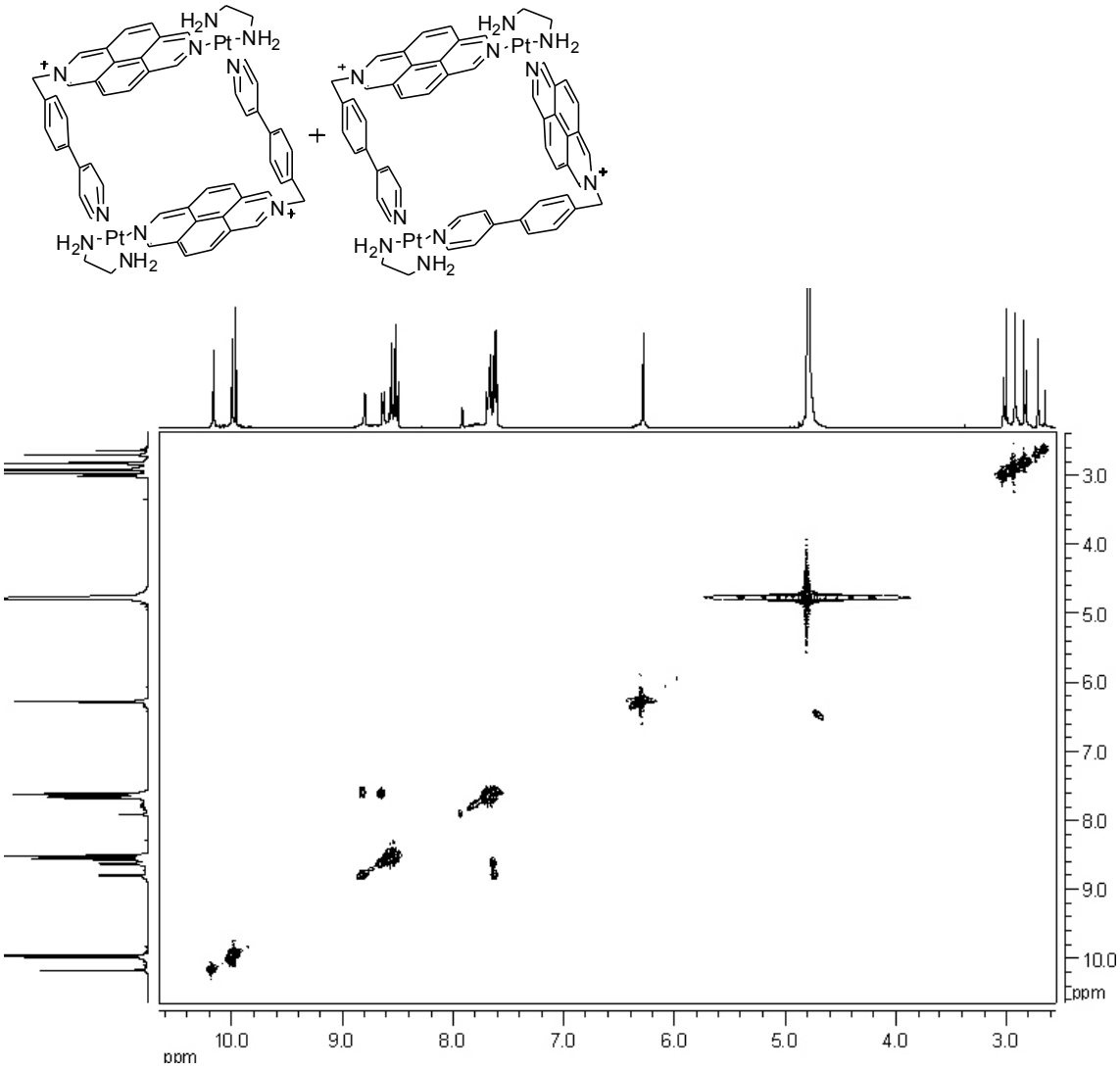

Figure S35: COSY (D_2O, 500 MHz) spectrum of **7a,b**·$6NO_3$.

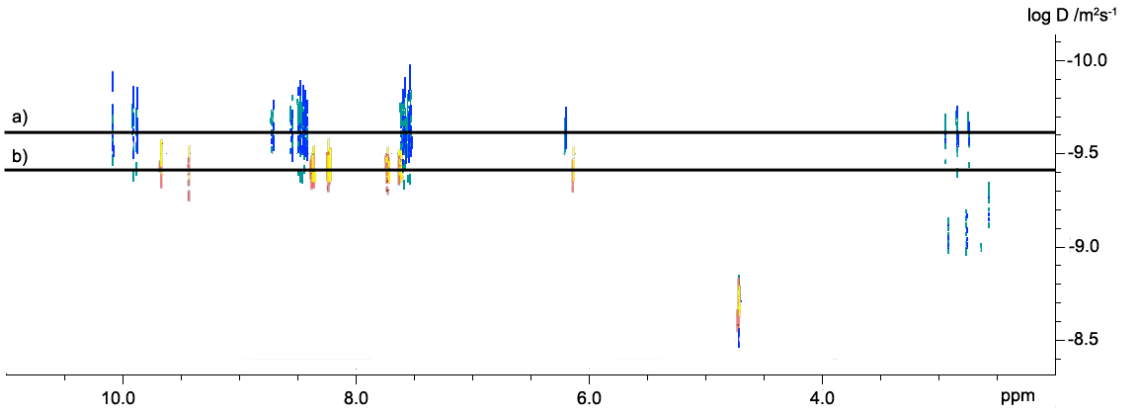

Figure S36: Superposed DOSY (D_2O, 500 MHz, 298 K) experiments of: a) metallocycles **7a,b**·$6NO_3$ (blue). b) ligand **4**·NO_3 (yellow).

Pseudorotaxane $1 \cdot 2PF_6 \subset 8$

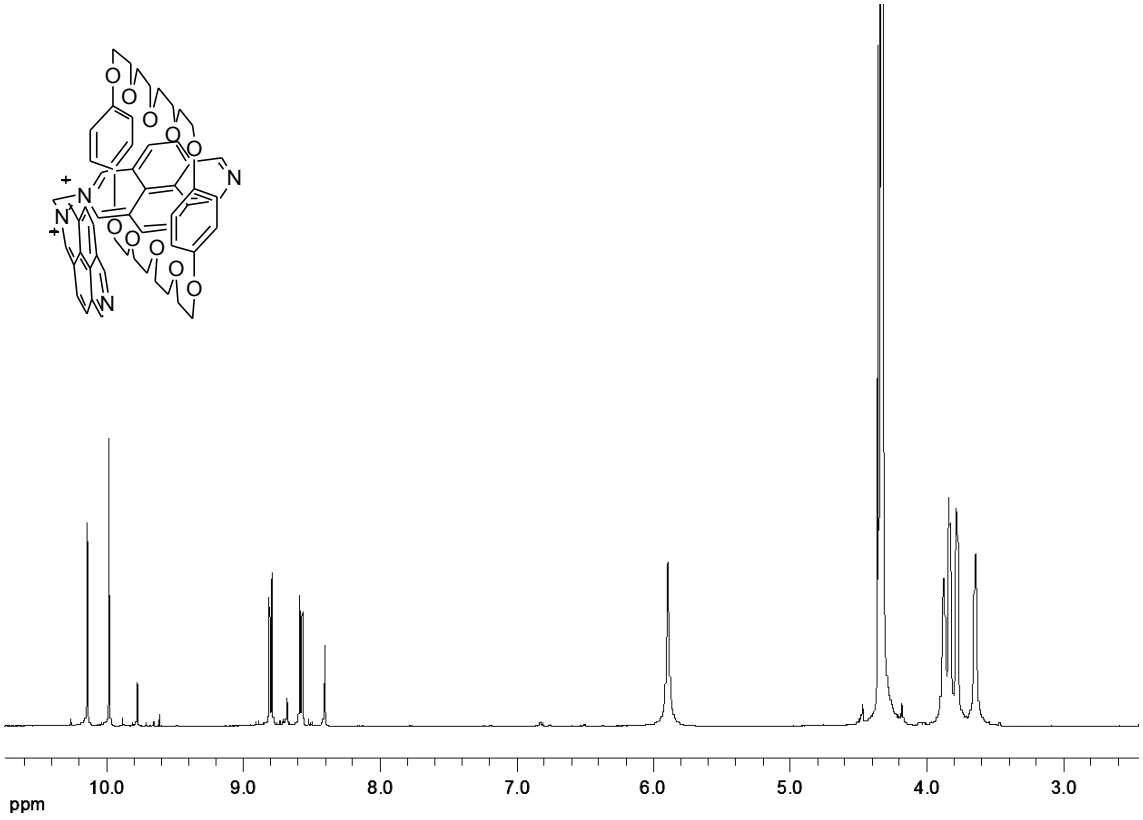

Figure S37: ^{1}H NMR (CD_3NO_2, 500 MHz) spectrum of $\mathbf{1} \cdot 2PF_6 \subset \mathbf{8}$.

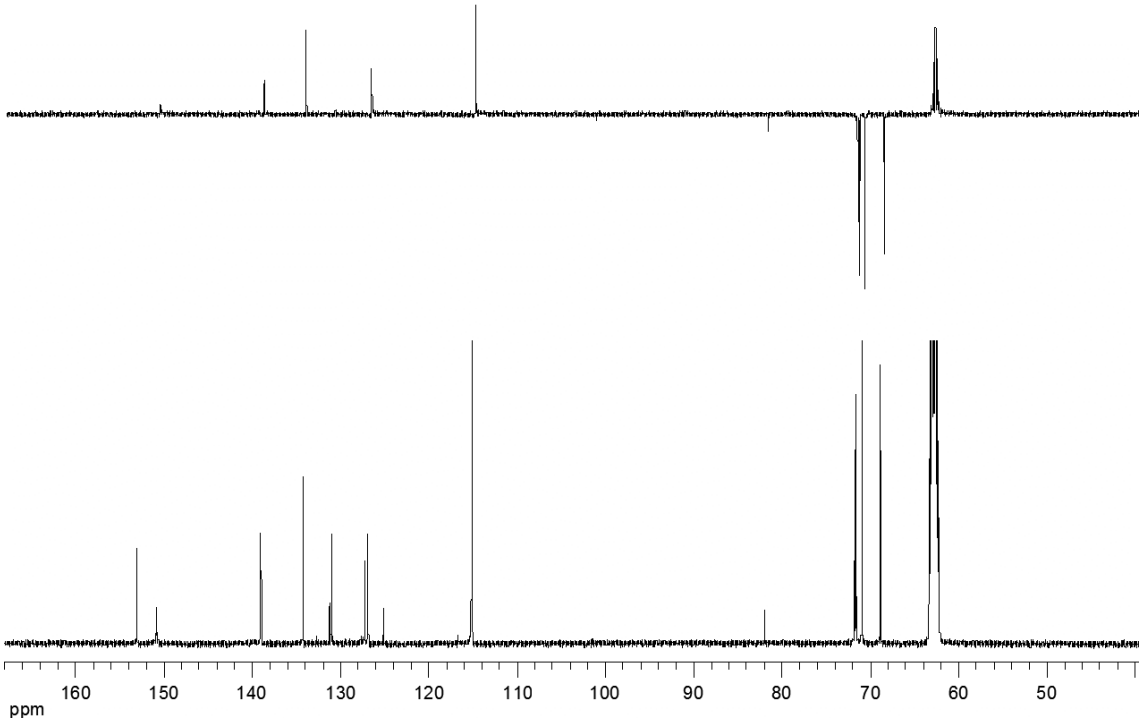

Figure S38: ^{13}C NMR (CD_3NO_2, 500 MHz) spectrum of $\mathbf{1} \cdot 2PF_6 \subset \mathbf{8}$.

Pseudorotaxane 1·2PF$_6$⊂9

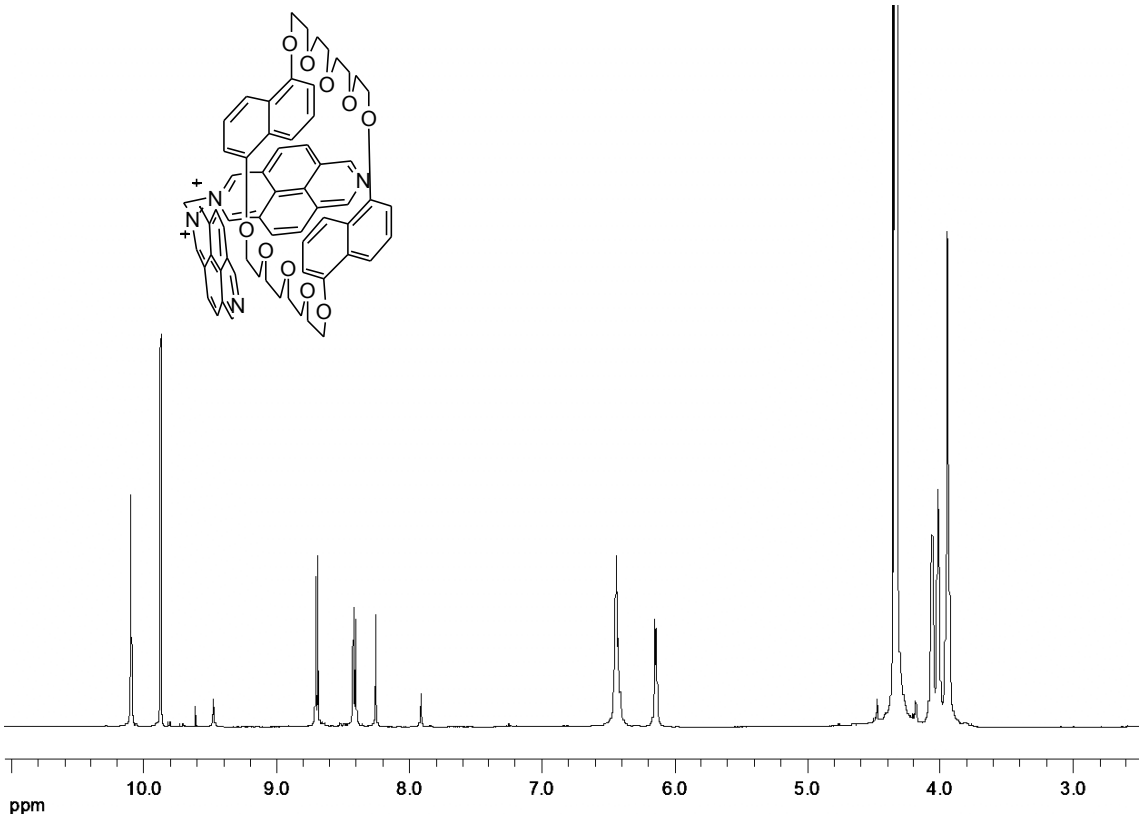

Figure S39: ^{1}H NMR (CD_3NO_2, 500 MHz) spectrum of **1**·2PF$_6$⊂**9**.

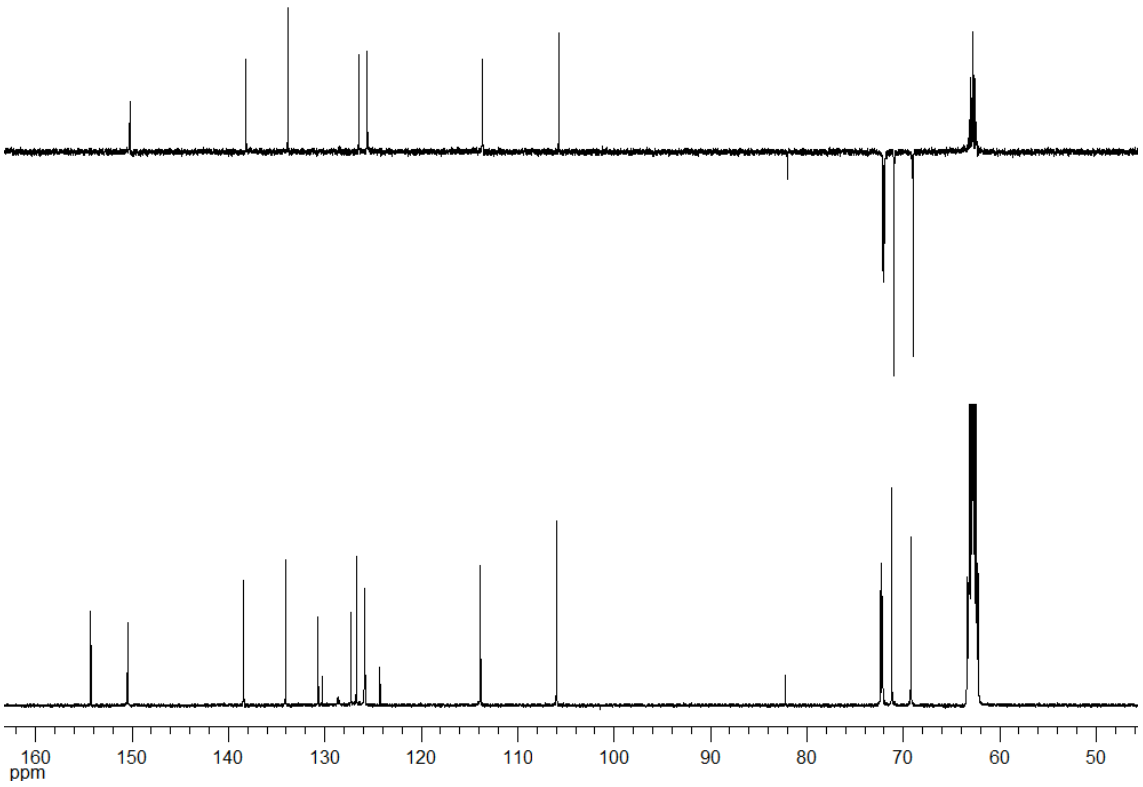

Figure S40: ^{13}C NMR (CD_3NO_2, 500 MHz) spectrum of **1**·2PF$_6$⊂**9**.

Catenane $3(8)_2 \cdot 4OTf \cdot 4PF_6$

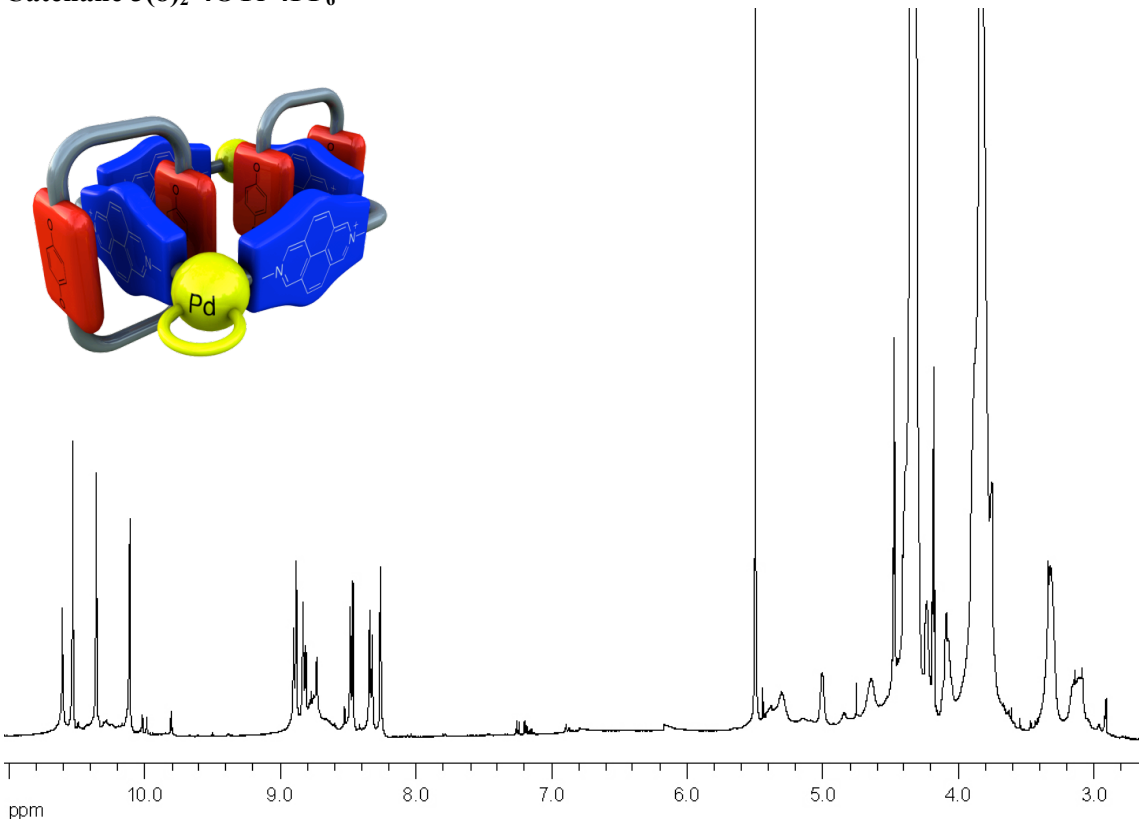

Figure S41: ^{1}H NMR (CD_3NO_2, 500 MHz) spectrum of **3**$(8)_2 \cdot 4OTf \cdot 4PF_6$.

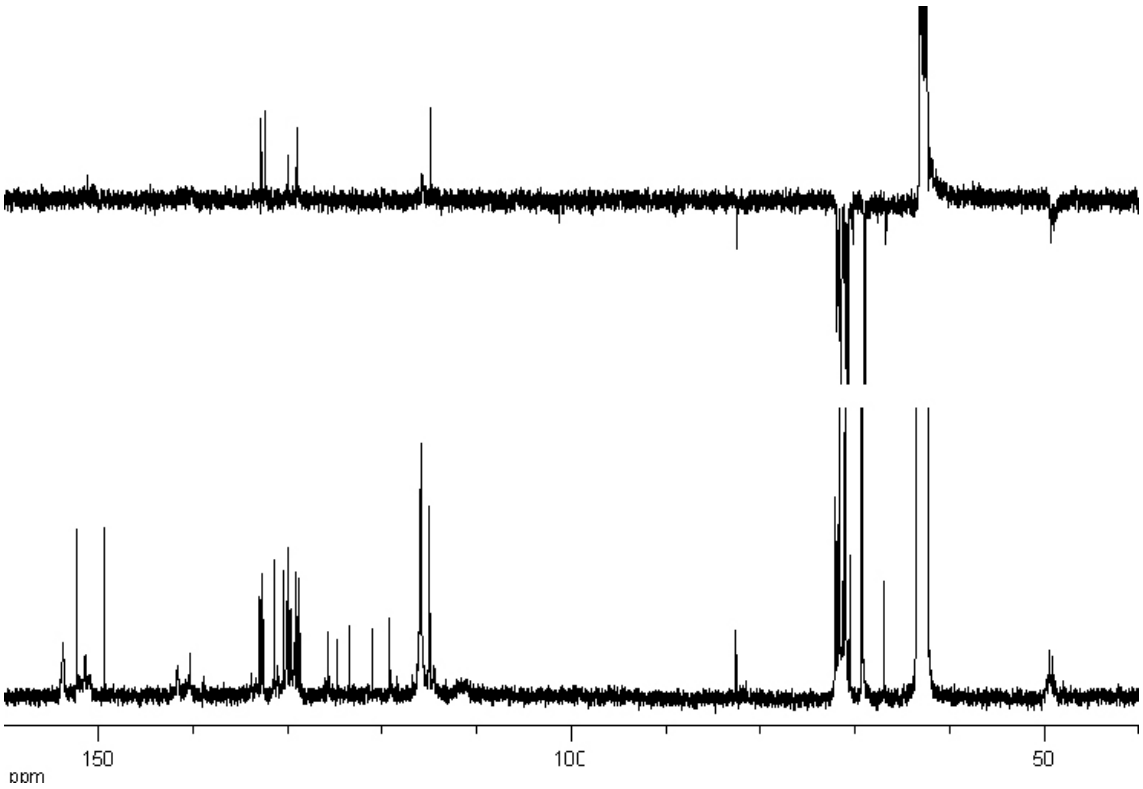

Figure S42: ^{13}C NMR (CD_3NO_2, 125 MHz) spectrum of **3**$(8)_2 \cdot 4OTf \cdot 4PF_6$.

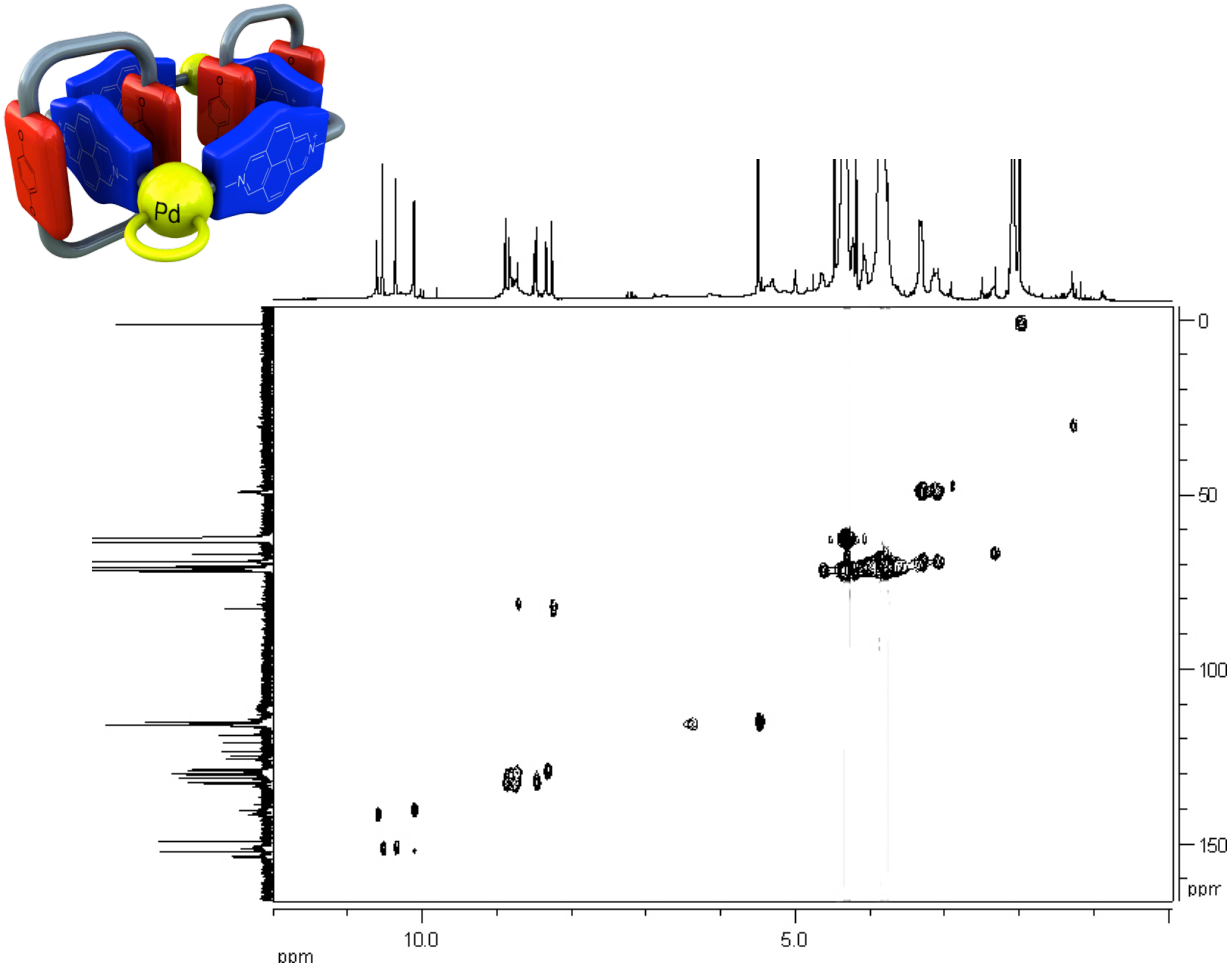

Figure S43: HSQC (CD_3NO_2, 500 and 125 MHz) spectrum of **3**(**8**)$_2$·4OTf·4PF$_6$.

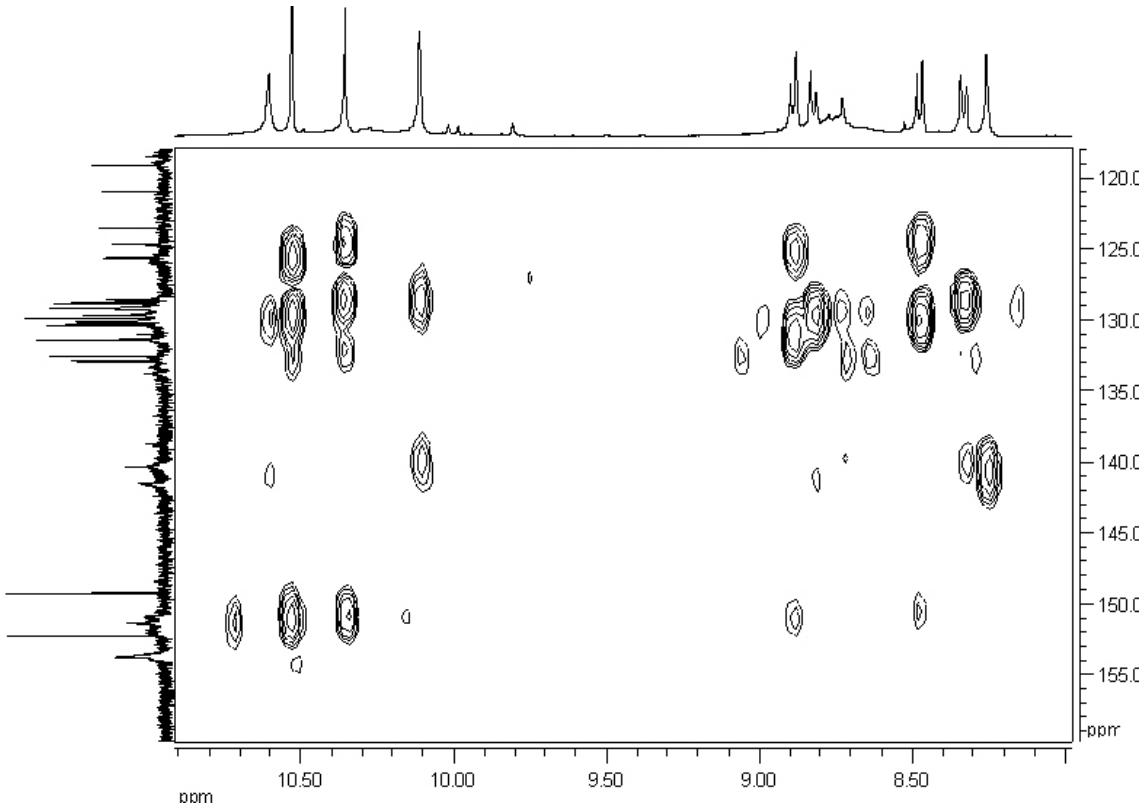

Figure S44: HMBC (CD_3NO_2, 500 and 125 MHz) spectrum of **3**(**8**)$_2$·4OTf·4PF$_6$.

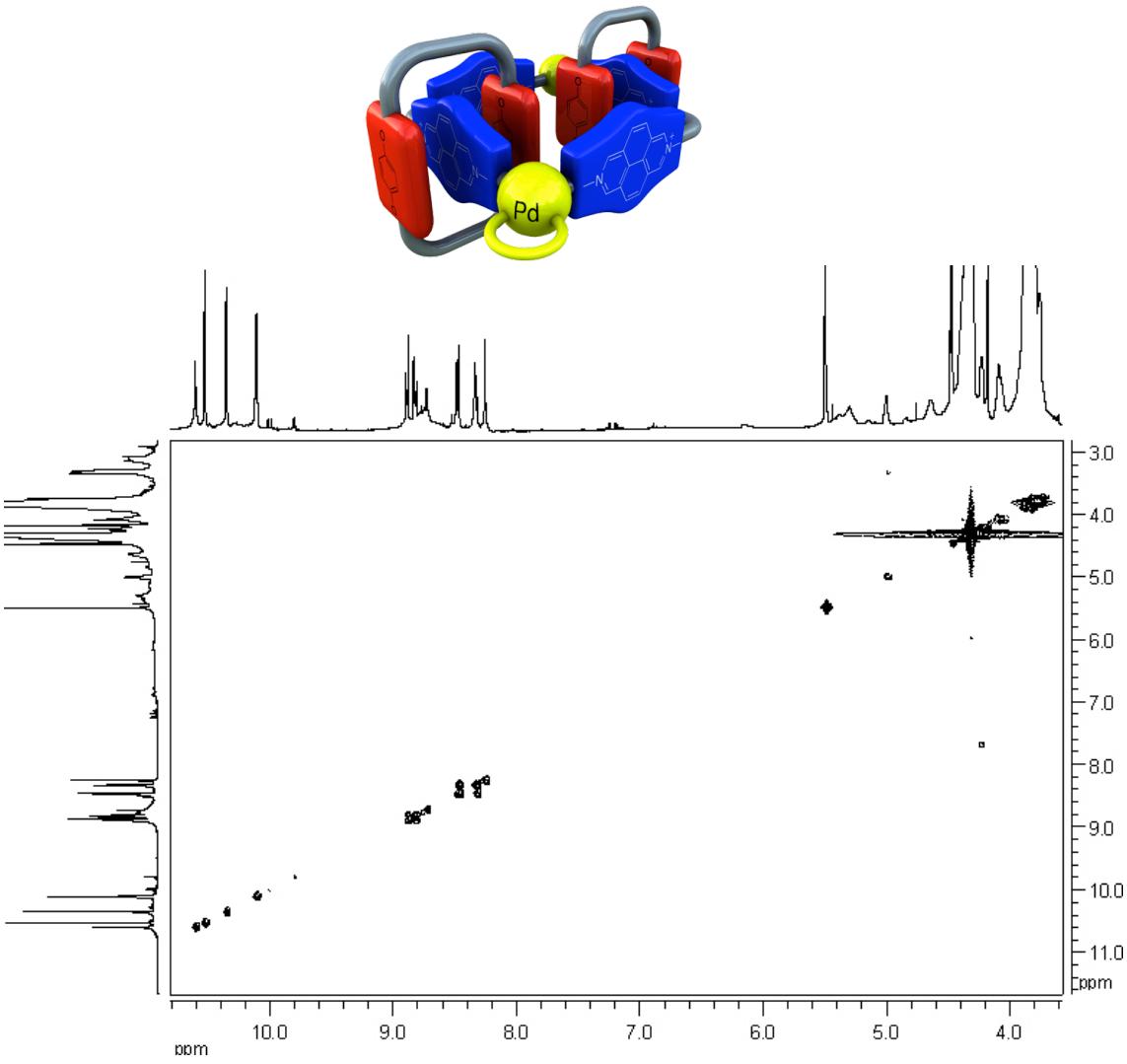

Figure S45: COSY (CD_3NO_2, 500 MHz) spectrum of **3**(**8**)$_2$·4OTf·4PF_6.

Catenane $3(9)_2 \cdot 4OTf \cdot 4PF_6$

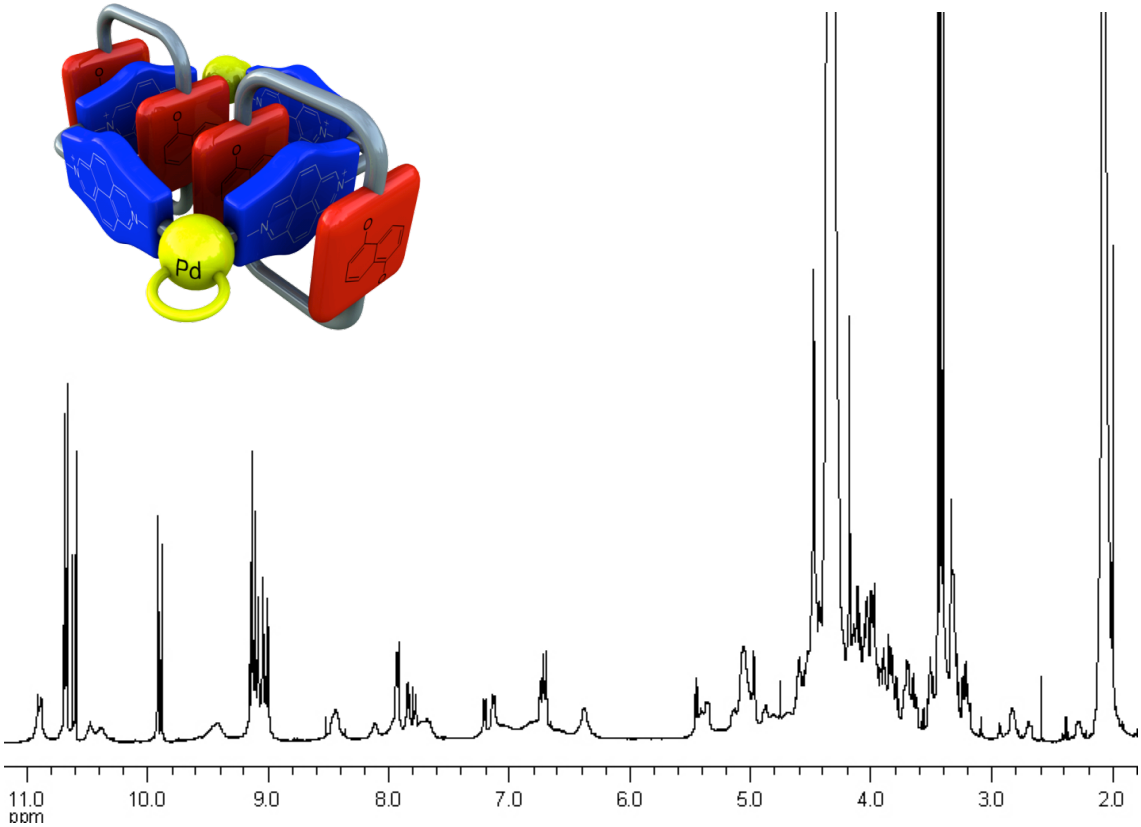

Figure S46: ^{1}H NMR (CD_3NO_2, 500 MHz, 298 K) spectrum of $\mathbf{3}(\mathbf{9})_2 \cdot 4OTf \cdot 4PF_6$.

Catenane 6a(8)$_2$·6PF$_6$

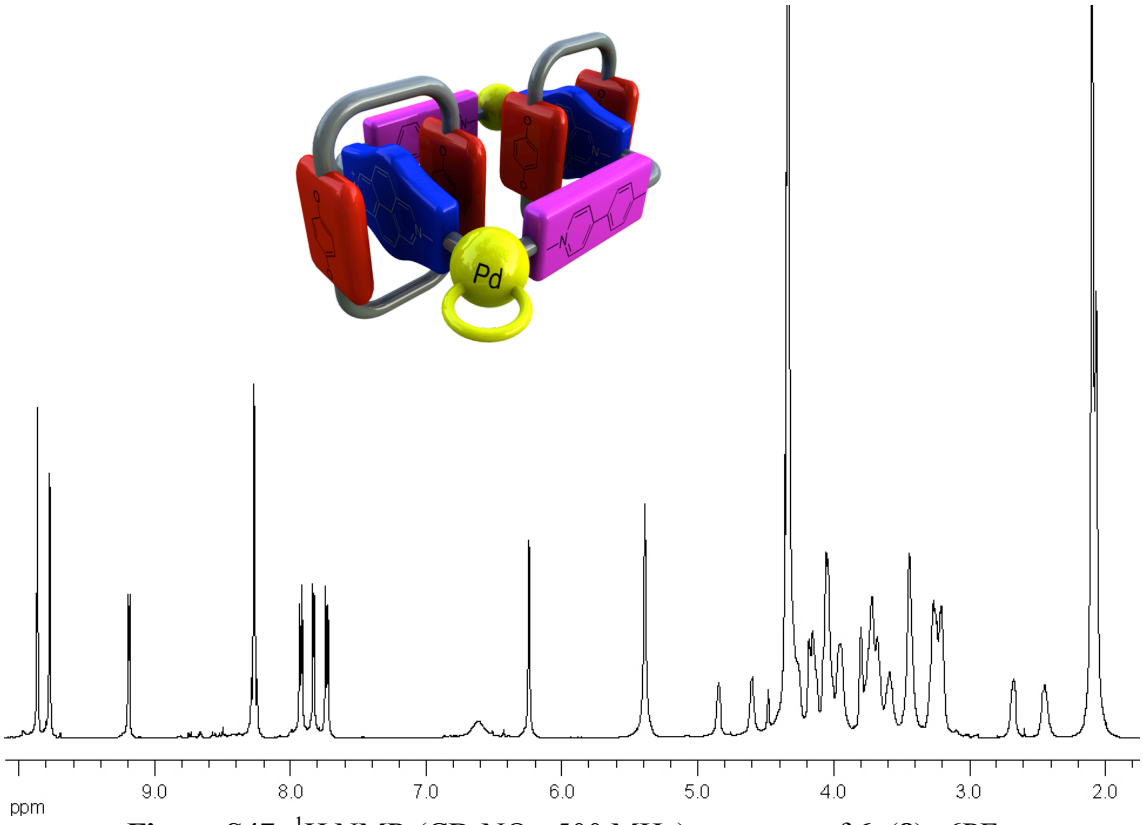

Figure S47: ^{1}H NMR (CD_3NO_2, 500 MHz) spectrum of **6a**(**8**)$_2$·6PF$_6$.

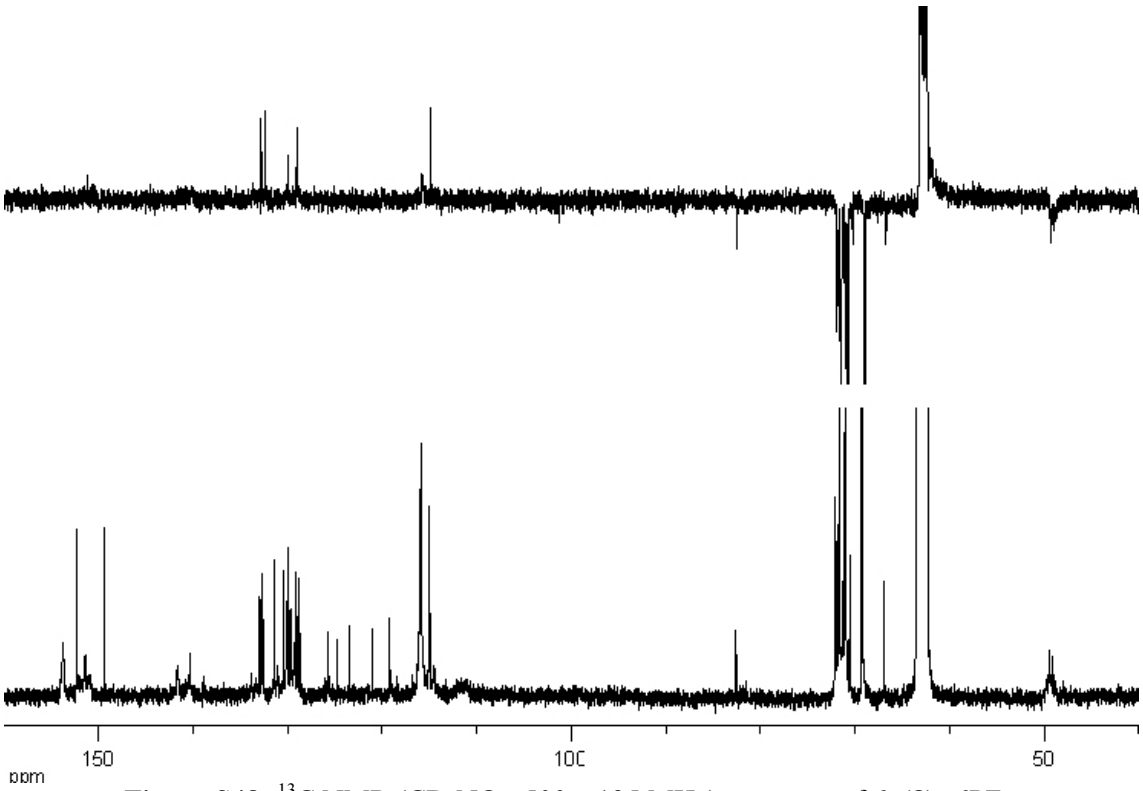

Figure S48: ^{13}C NMR (CD_3NO_2, 500 y 125 MHz) spectrum of **6a**(**8**)$_2$·6PF$_6$.

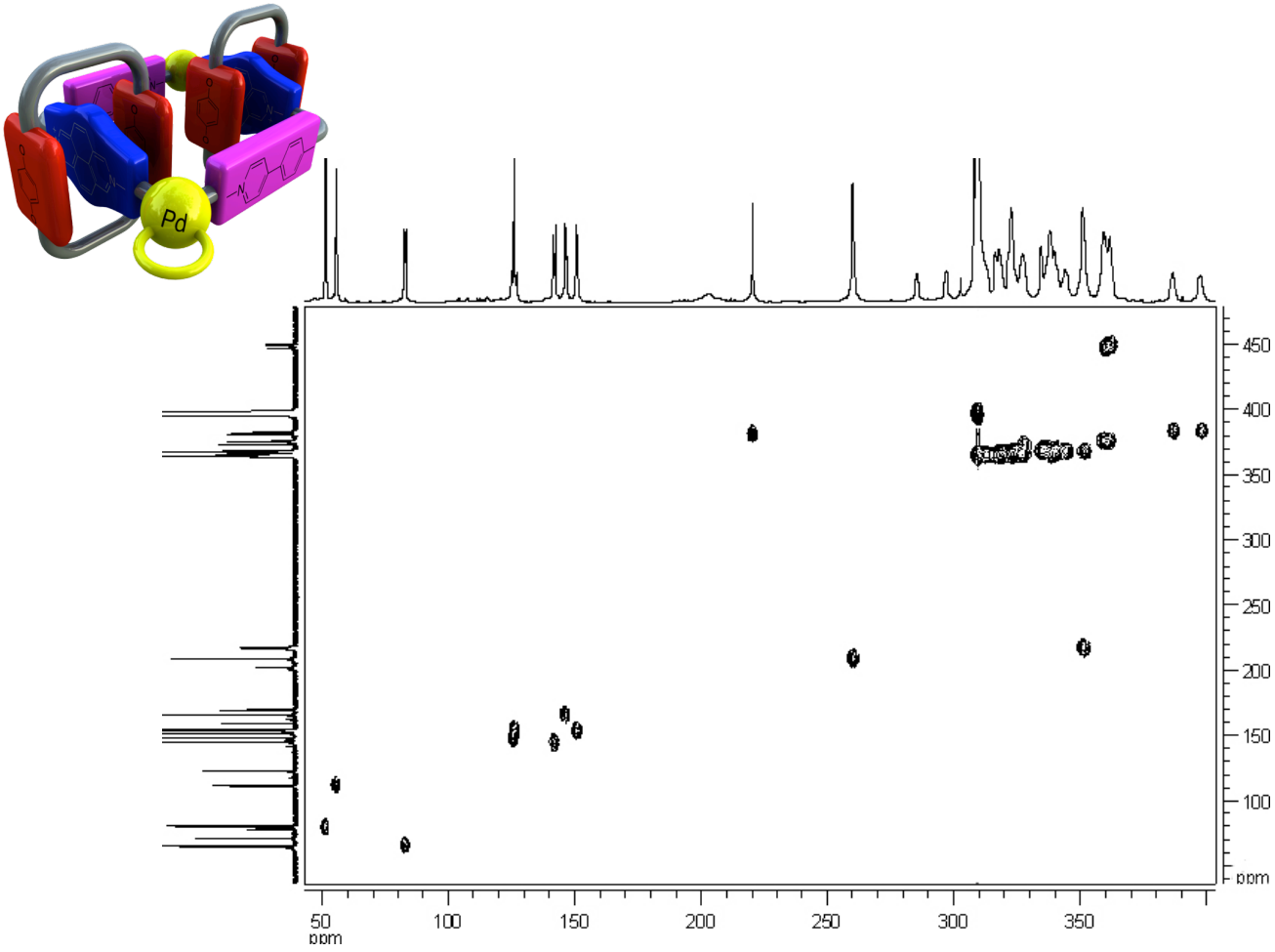

Figure S49: HSQC (CD_3NO_2, 500 and 125 MHz) spectrum of **6a**(**8**)$_2$·6PF_6.

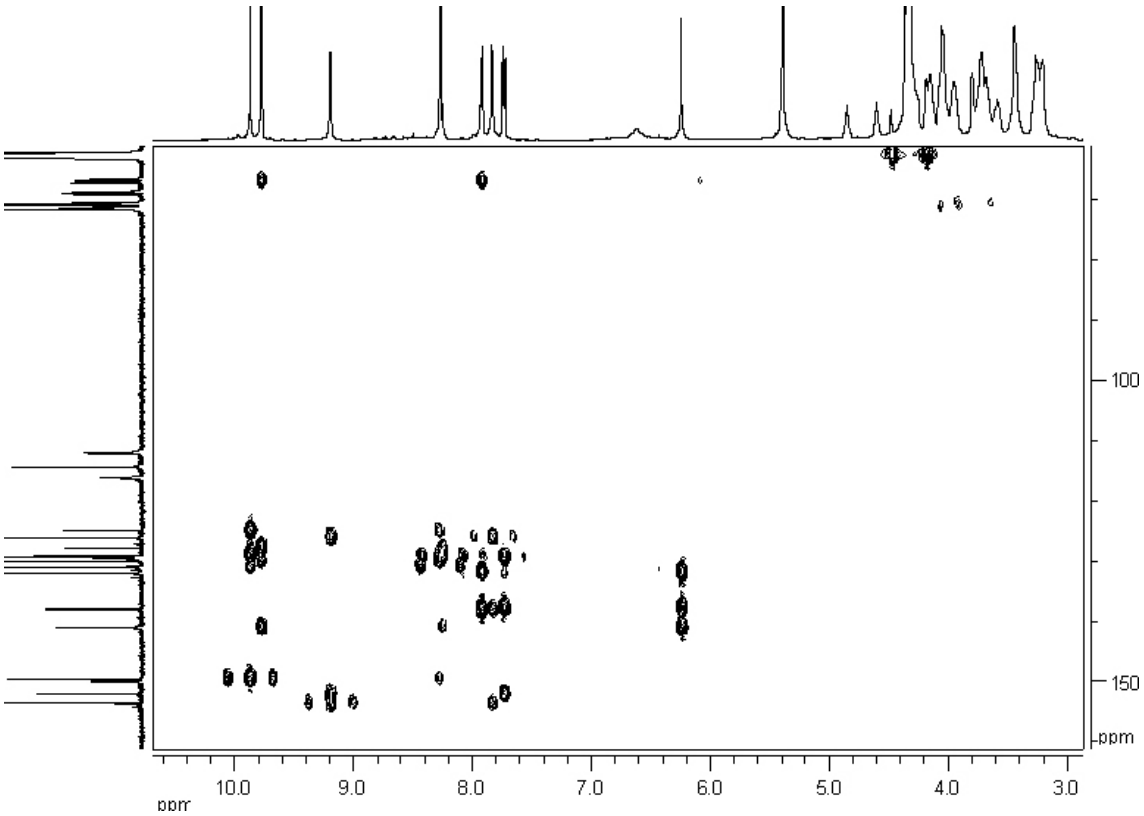

Figure S50: HMBC (CD_3NO_2, 500 and 125 MHz) spectrum of **6a**(**8**)$_2$·6PF_6.

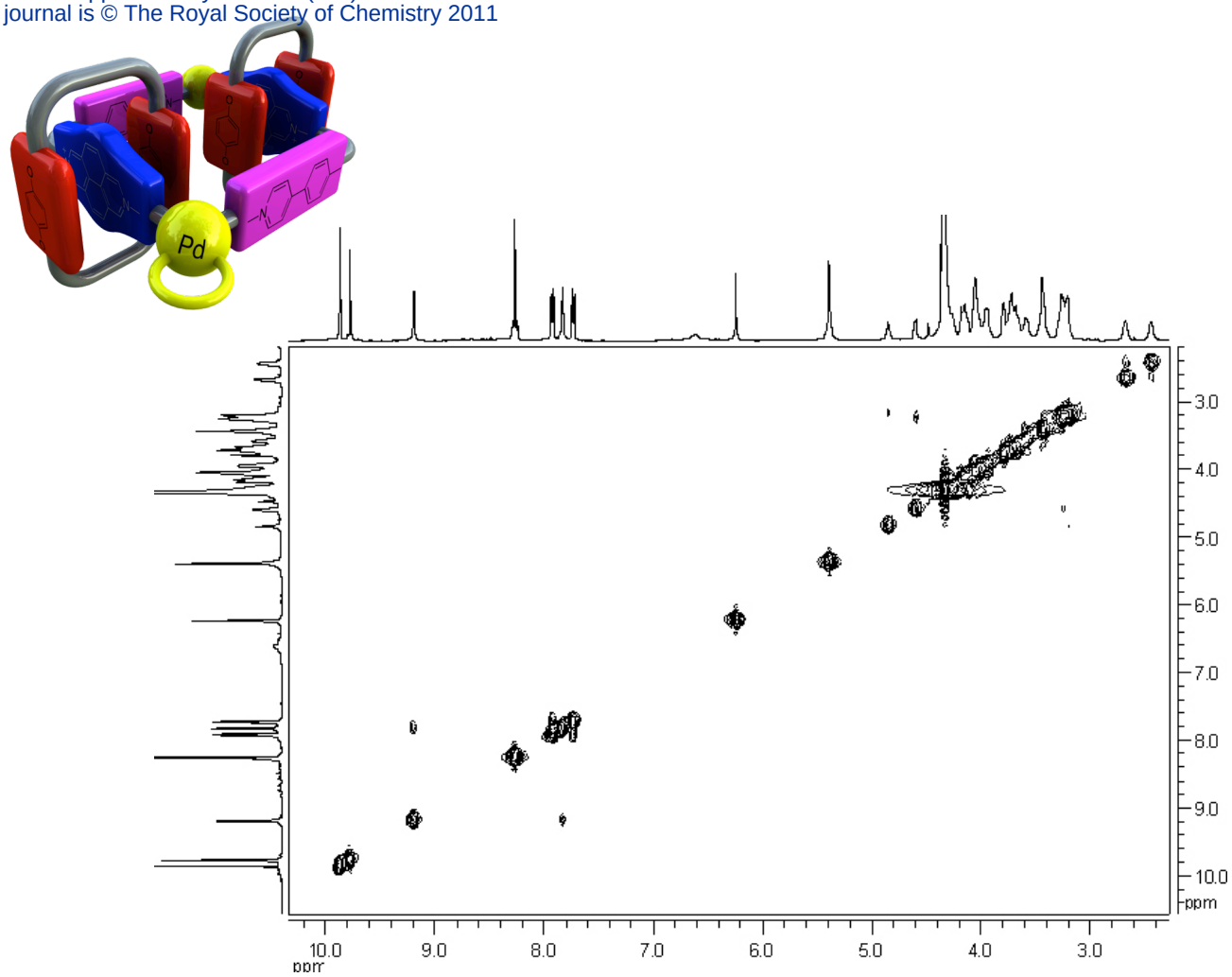

Figure S51: COSY (CD_3NO_2, 500 MHz) spectrum of **6a**(**8**)$_2$·6PF_6.

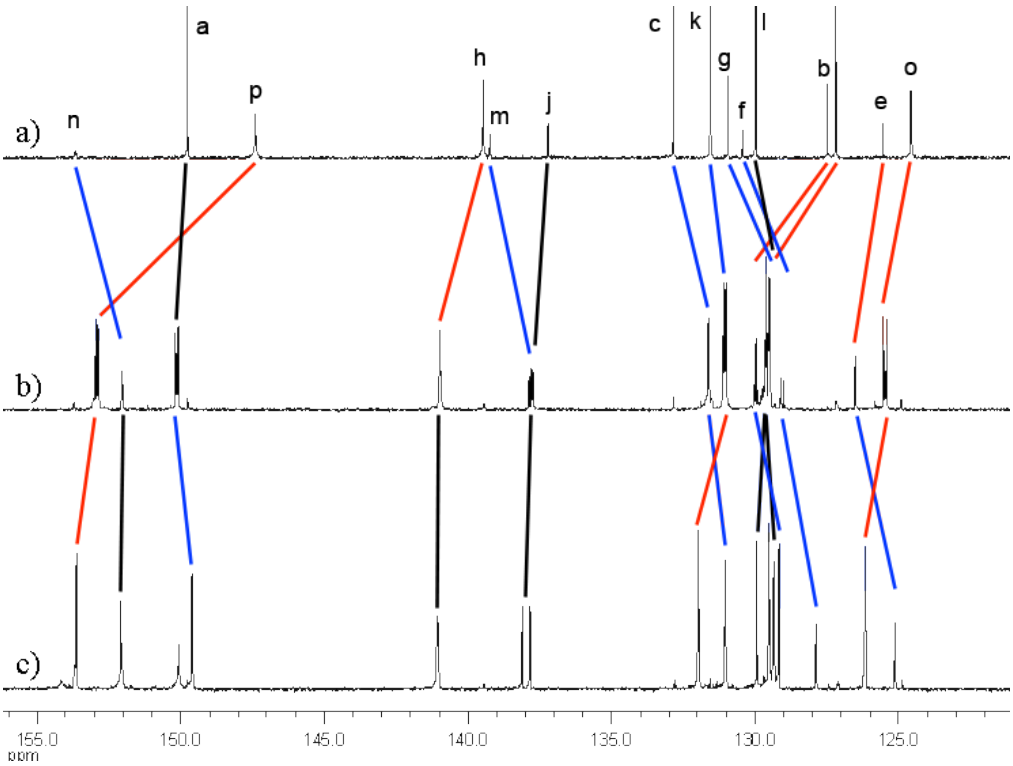

Figure S52: Partial ^{13}C NMR (CD_3NO_2, 125 MHz) spectra of: (a) ligand **4**·PF_6, (b) metallocycles **6a,b**·6PF_6, and (c) catenane **6a**(**8**)$_2$·6PF_6. Peak labels are defined in Scheme 1.

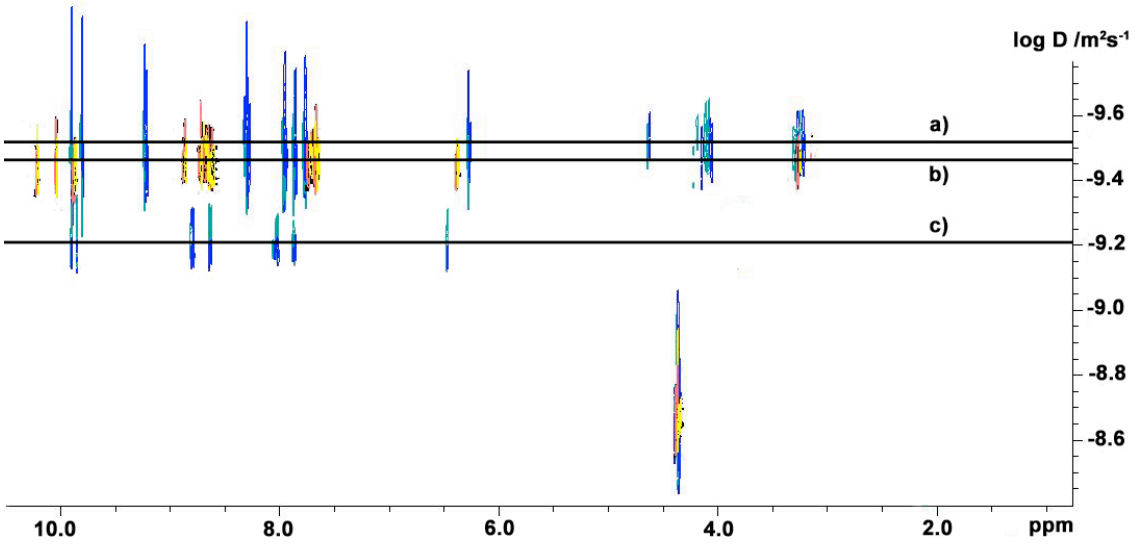

Figure S53: Superposed DOSY (CD_3NO_2, 500 MHz, 298 K) experiment of: a) 5 mM solution of **6a**(**8**)$_2$·6PF_6 (blue). b) 5 mM solution of **6a,b**·6PF_6 (yellow). c) 10 mM solution of ligand **4**·PF_6 (blue).

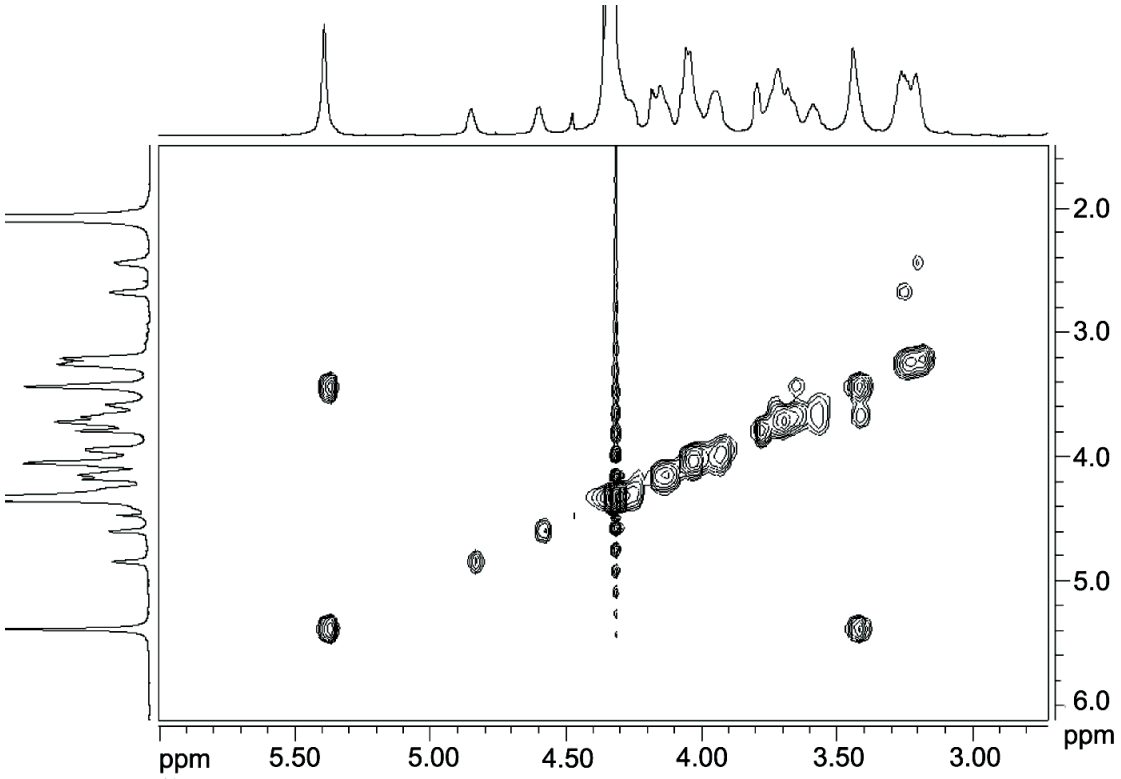

Figure S54: Partial EXSY (CD_3NO_2, 500 MHz, 298 K) spectrum showing the correlation between HQ_{out} and HQ_{in}

Catenane 6a(9)$_2$·6PF$_6$

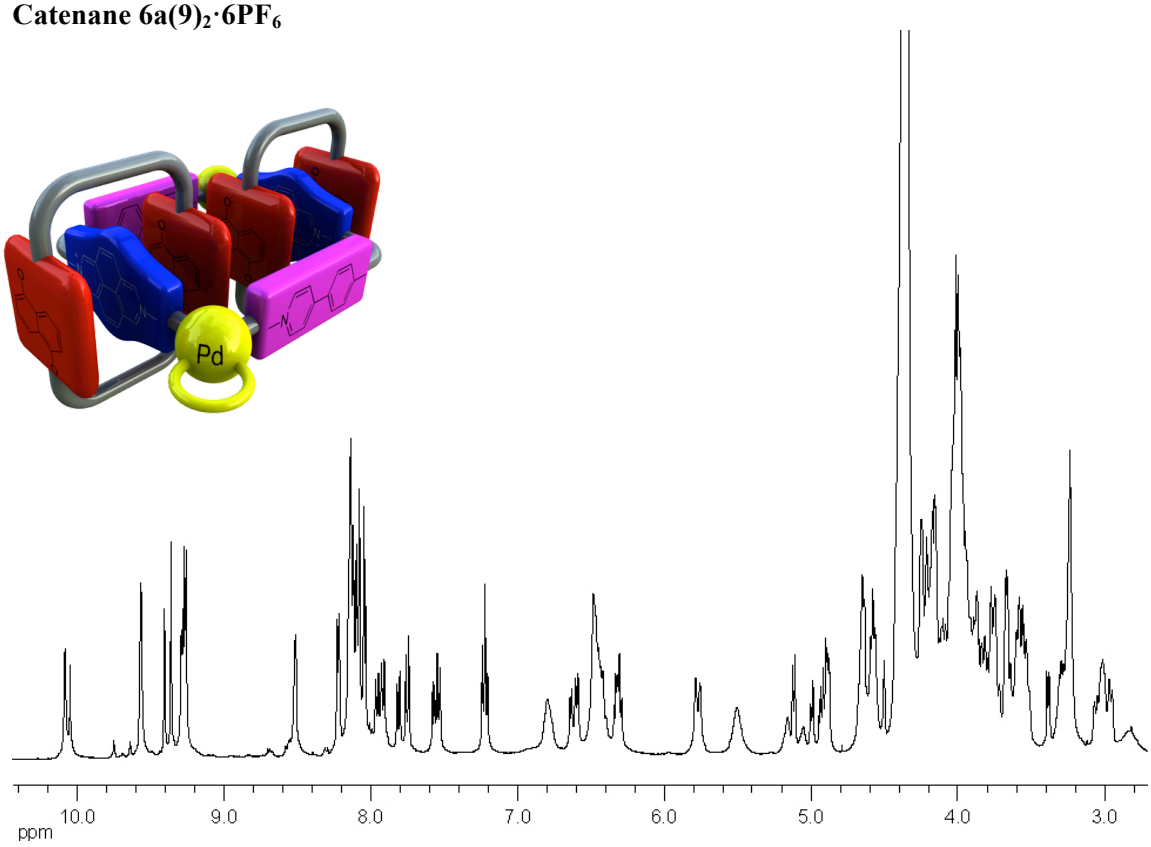

Figure S55: ^{1}H NMR (CD_3NO_2, 500 MHz, 298 K) spectrum of **6a**(**9**)$_2$·6PF$_6$.

Catenane 7a(8)$_2$·6PF$_6$

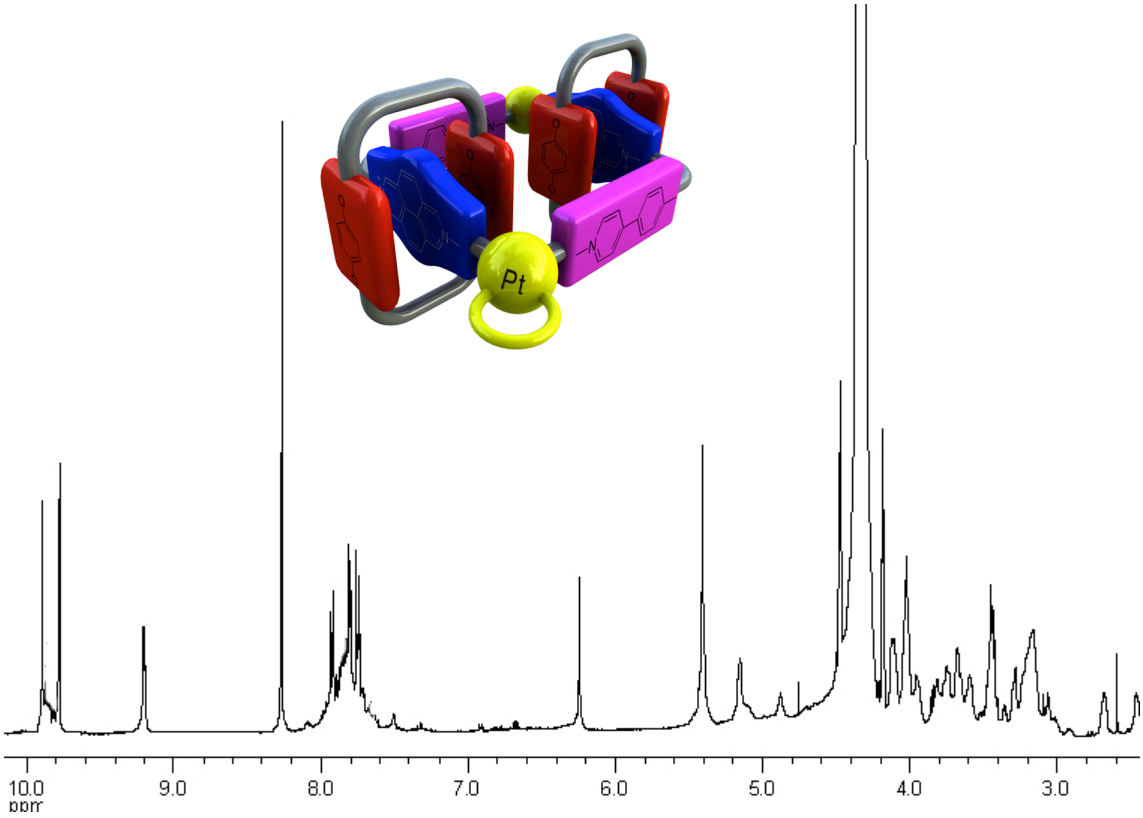

Figure S56: ^{1}H NMR (CD_3NO_2, 500 MHz) spectrum of **7a(8)**$_2$·6PF$_6$.

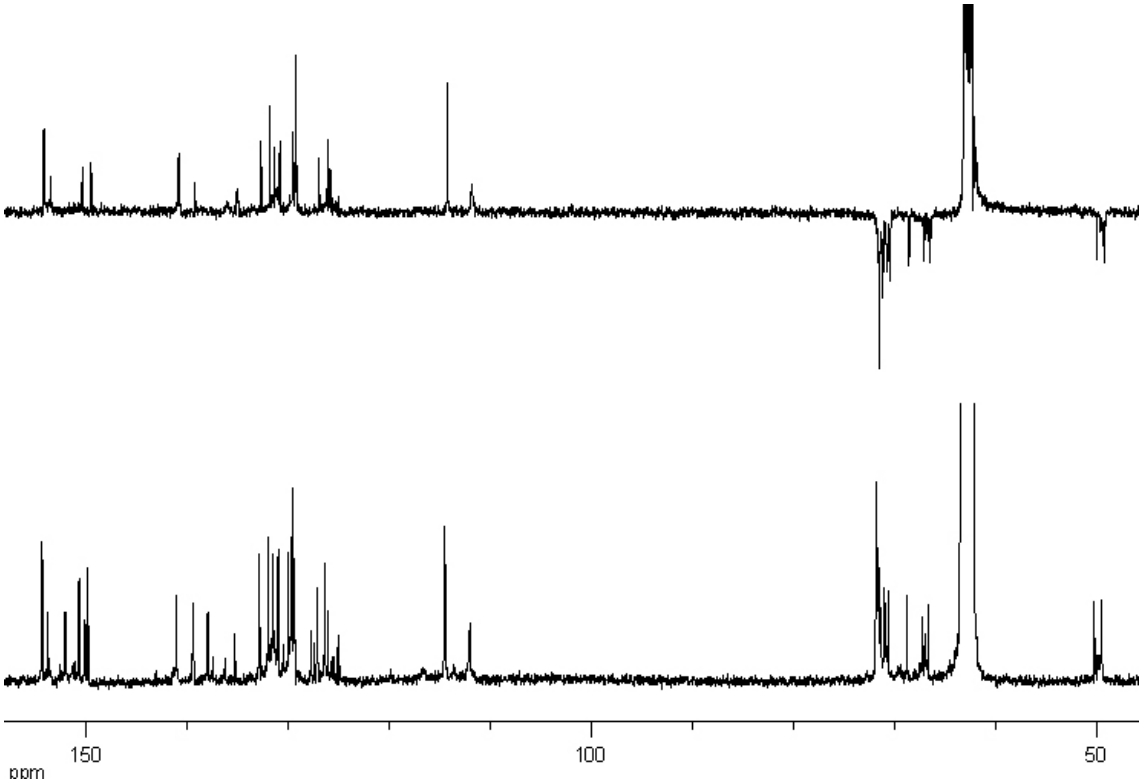

Figure S57: ^{13}C NMR (CD_3NO_2, 125 MHz) spectrum of **7a(8)**$_2$·6PF$_6$.

Catenane 7a(9)$_2$·6PF$_6$

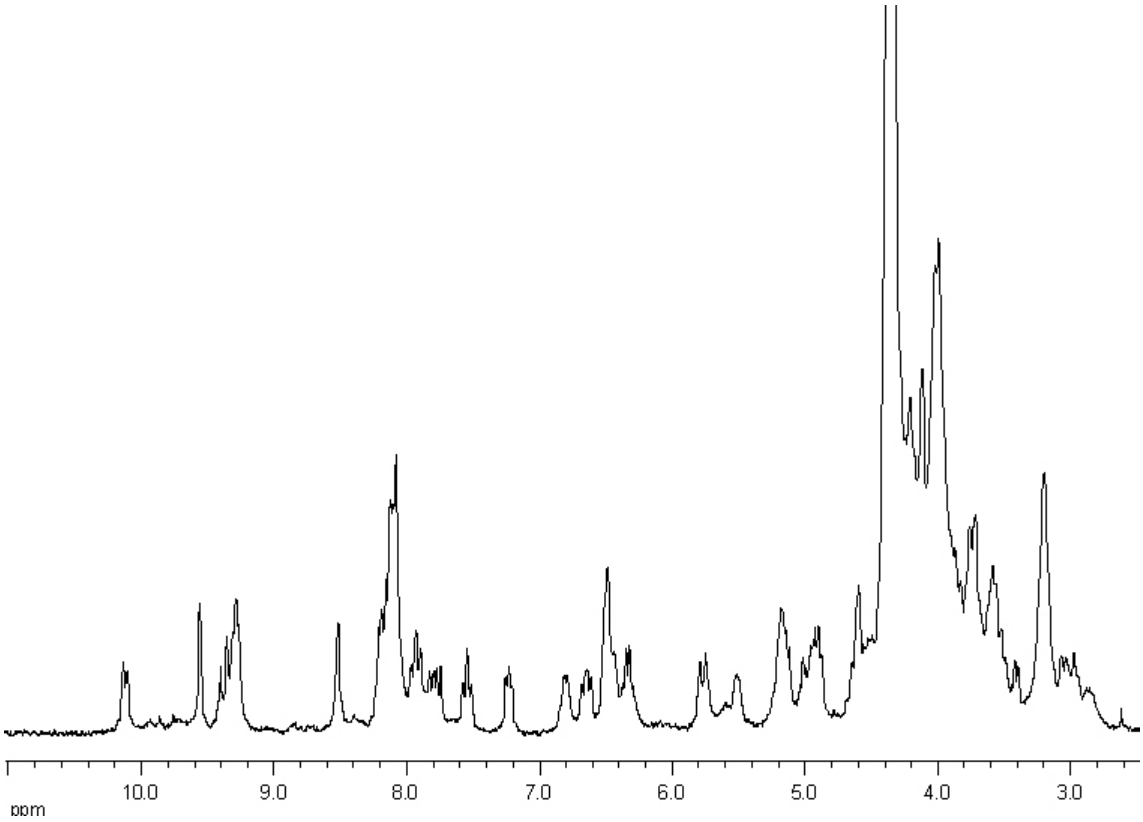

Figure S58: ^{1}H NMR (CD_3NO_2, 500 MHz) spectrum de **7a**(**9**)$_2$·6PF$_6$.

Inclusion complex $(10)_2 \subset 6a \cdot 6NO_3$

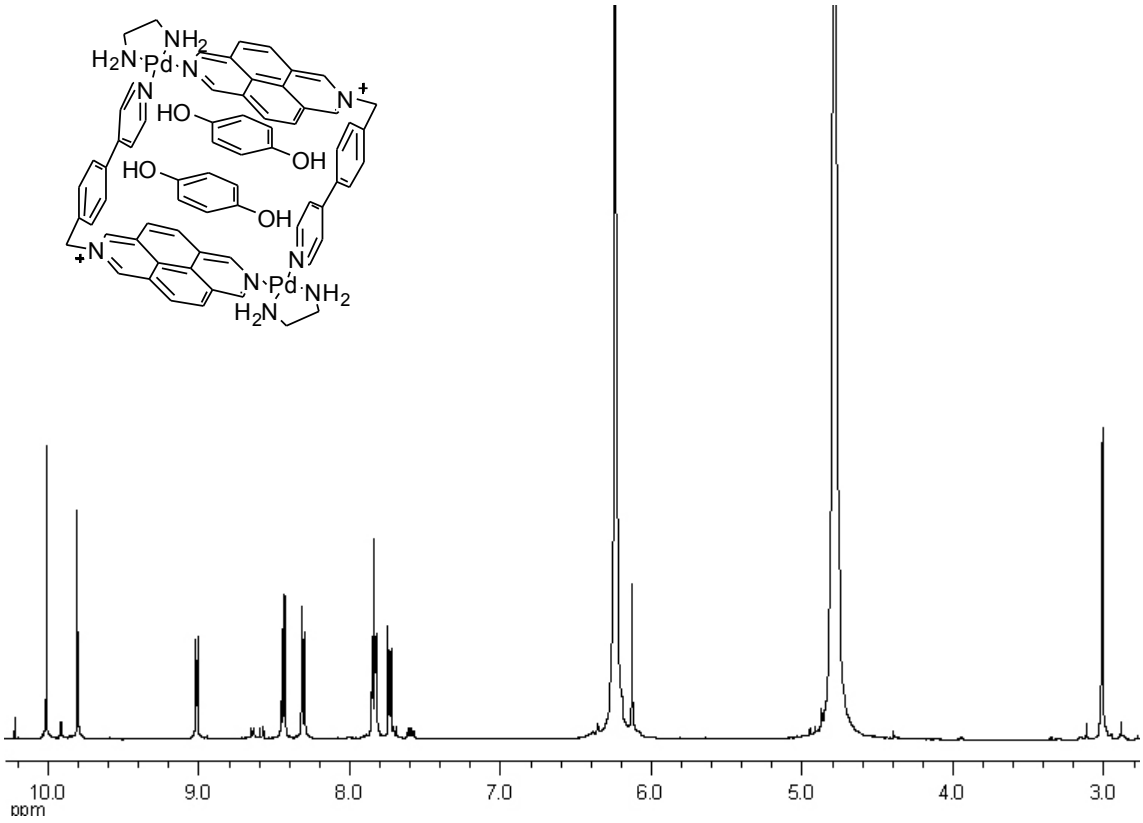

Figure S59: ^{1}H NMR (D_2O, 500 MHz) spectrum of $(\mathbf{10})_2 \subset \mathbf{6a} \cdot 6NO_3$

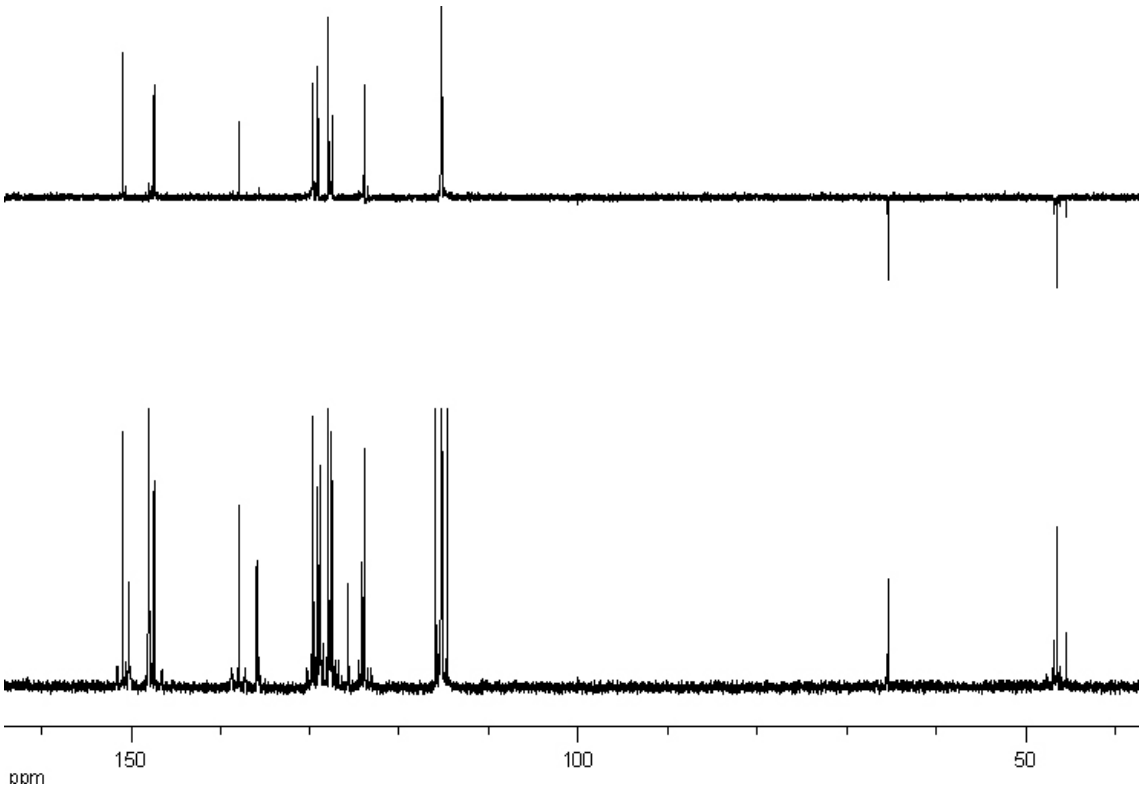

Figure S60: ^{13}C NMR (D_2O, 125 MHz) of $(\mathbf{10})_2 \subset \mathbf{6a} \cdot 6NO_3$.

Inclusion complex $(11)_2 \subset 6a \cdot 6NO_3$

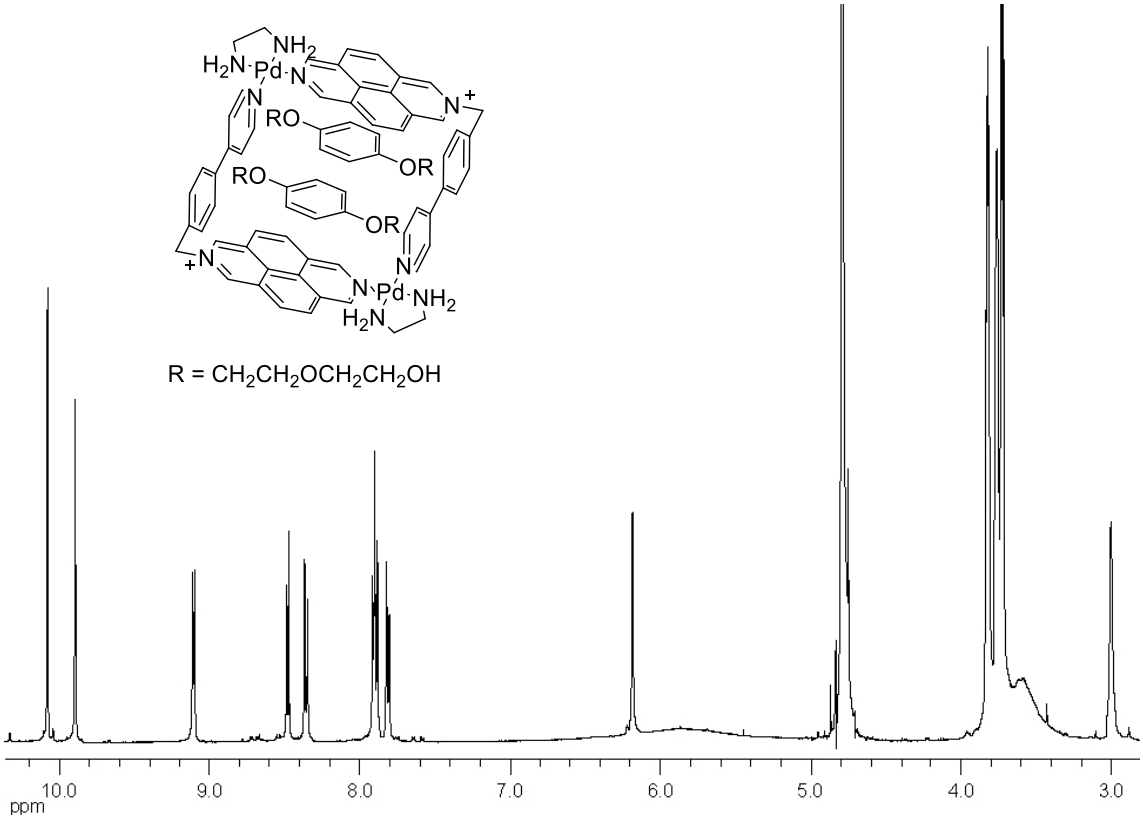

Figure S61: ^{1}H NMR (D_2O, 500 MHz) spectrum of $(11)_2 \subset 6a \cdot 6NO_3$.

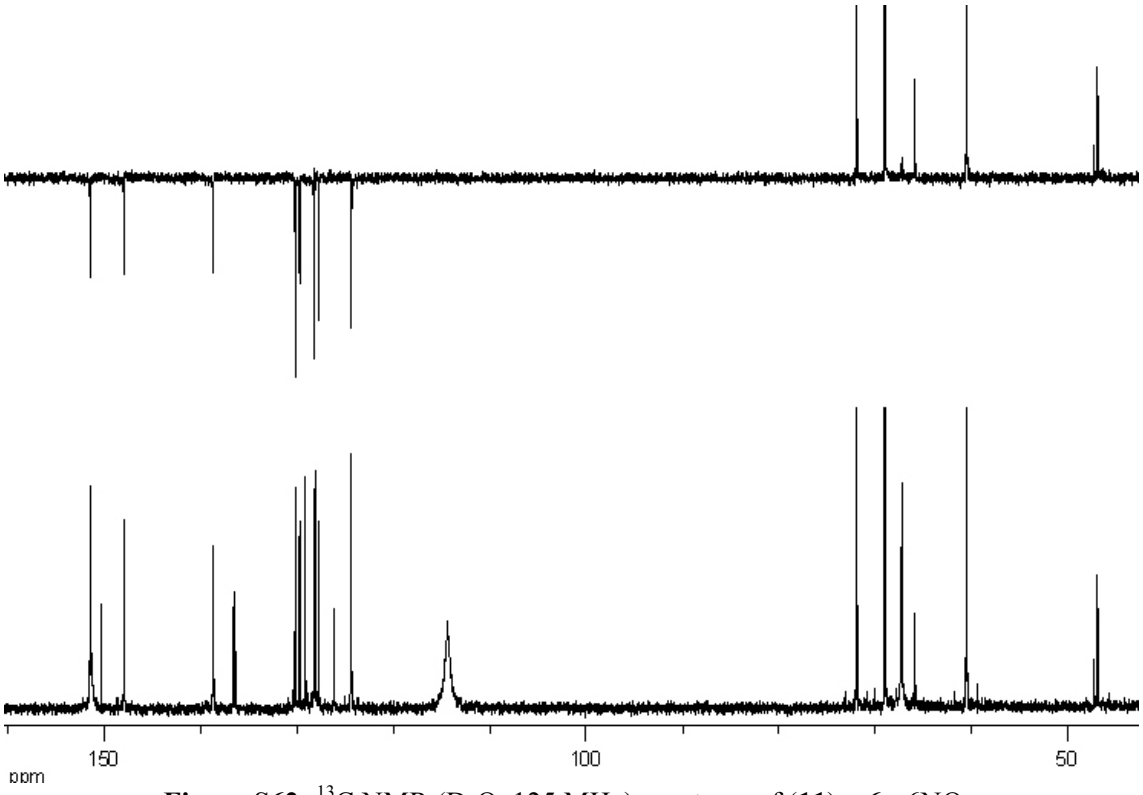

Figure S62: ^{13}C NMR (D_2O, 125 MHz) spectrum of $(11)_2 \subset 6a \cdot 6NO_3$.

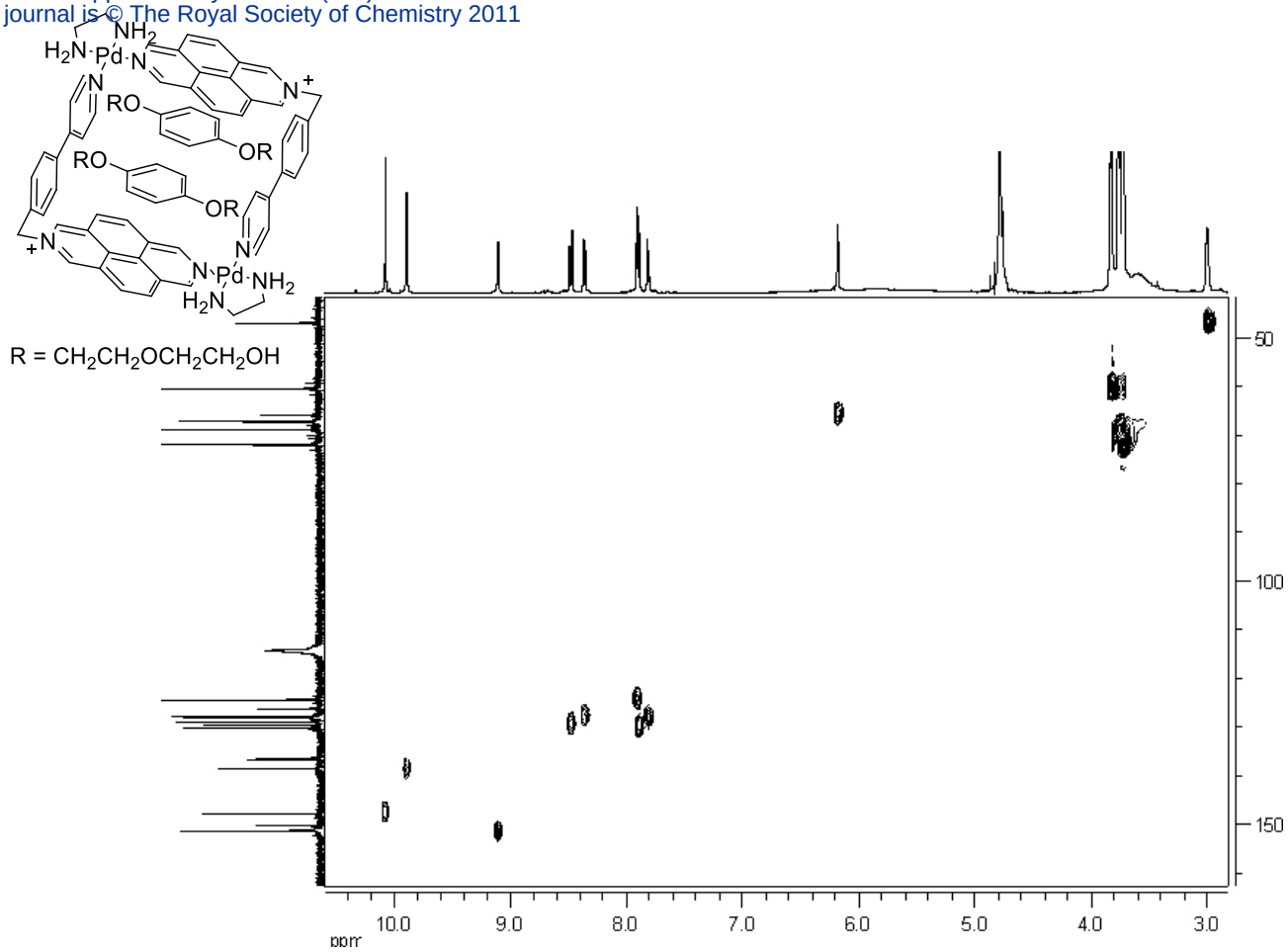

Figure S63: HSQC (D_2O, 500 and 125 MHz) spectrum of $(\mathbf{11})_2 \subset \mathbf{6a} \cdot 6NO_3$.

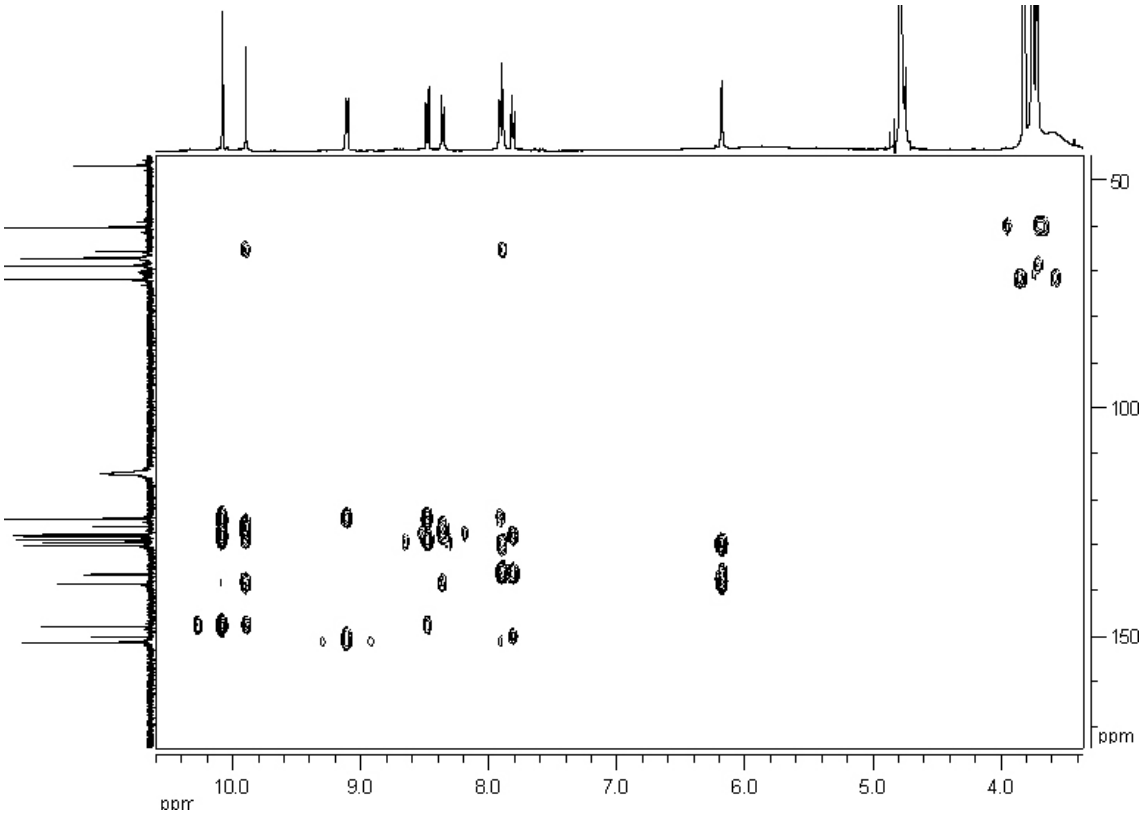

Figure S64: HMBC (D_2O, 500 and 125 MHz) spectrum of $(\mathbf{11})_2 \subset \mathbf{6a} \cdot 6NO_3$.

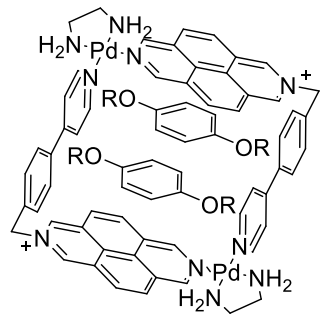

R = $CH_2CH_2OCH_2CH_2OH$

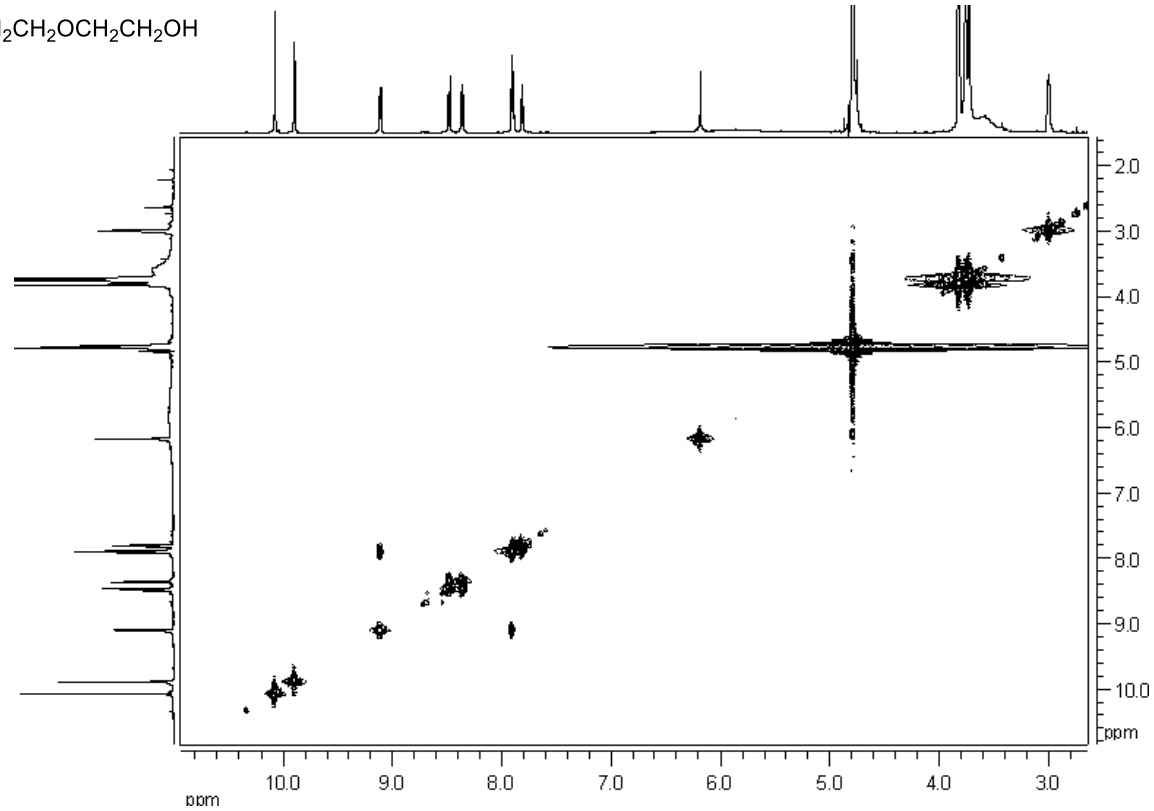

Figure S65: COSY (D_2O, 500 MHz) spectrum of $(\mathbf{11})_2 \subset \mathbf{6a} \cdot 6NO_3$.

Inclusion complex $(13)_2 \subset 6a \cdot 6NO_3$

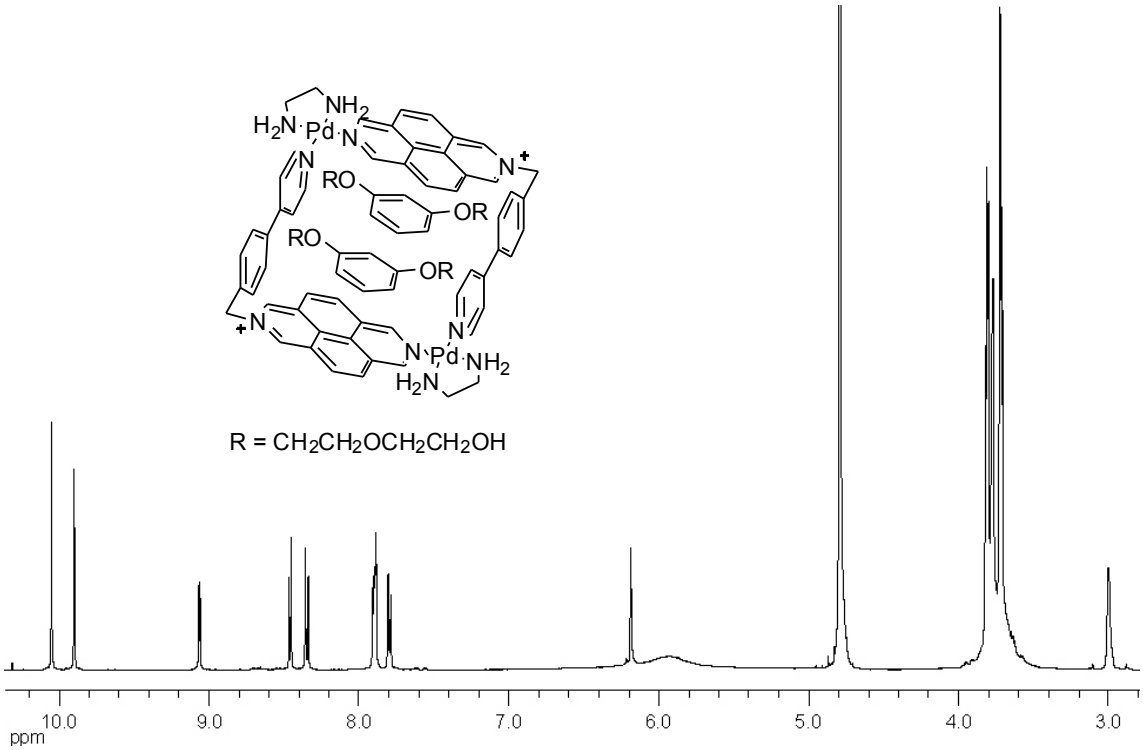

Figure S66: ^{1}H NMR (D_2O, 500 MHz) spectrum of $(13)_2 \subset 6a \cdot 6NO_3$

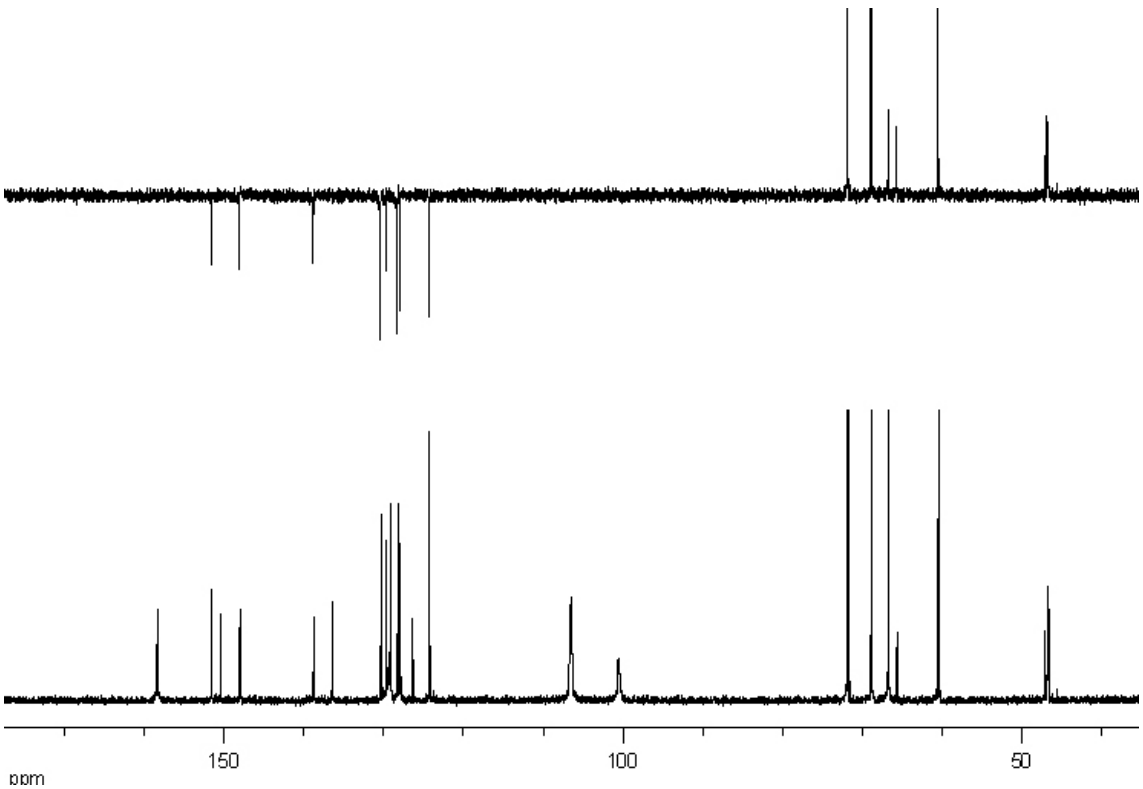

Figure S67: ^{13}C NMR (D_2O, 125 MHz) spectrum of $(13)_2 \subset 6a \cdot 6NO_3$

Inclusion complex $(14)_2 \subset 6a \cdot 6NO_3$

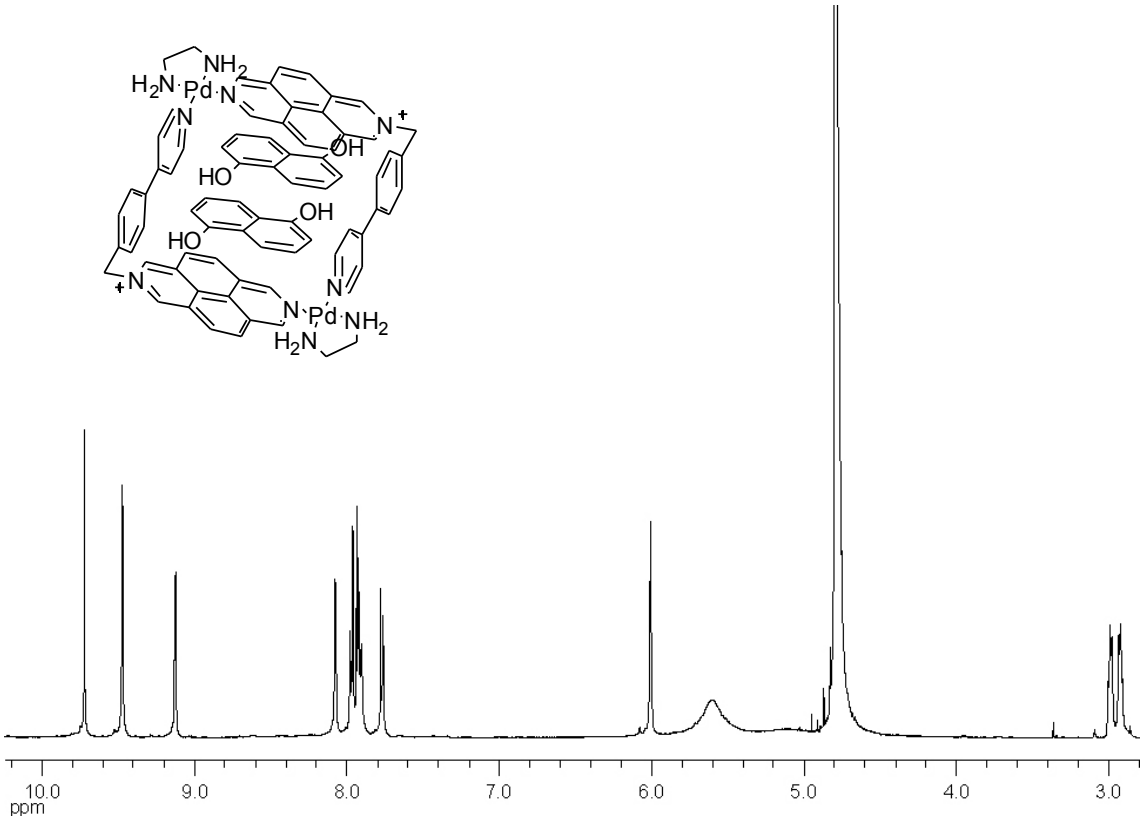

Figure S68: ^{1}H NMR (D_2O, 500 MHz) spectrum of $(\mathbf{14})_2 \subset \mathbf{6a} \cdot 6NO_3$.

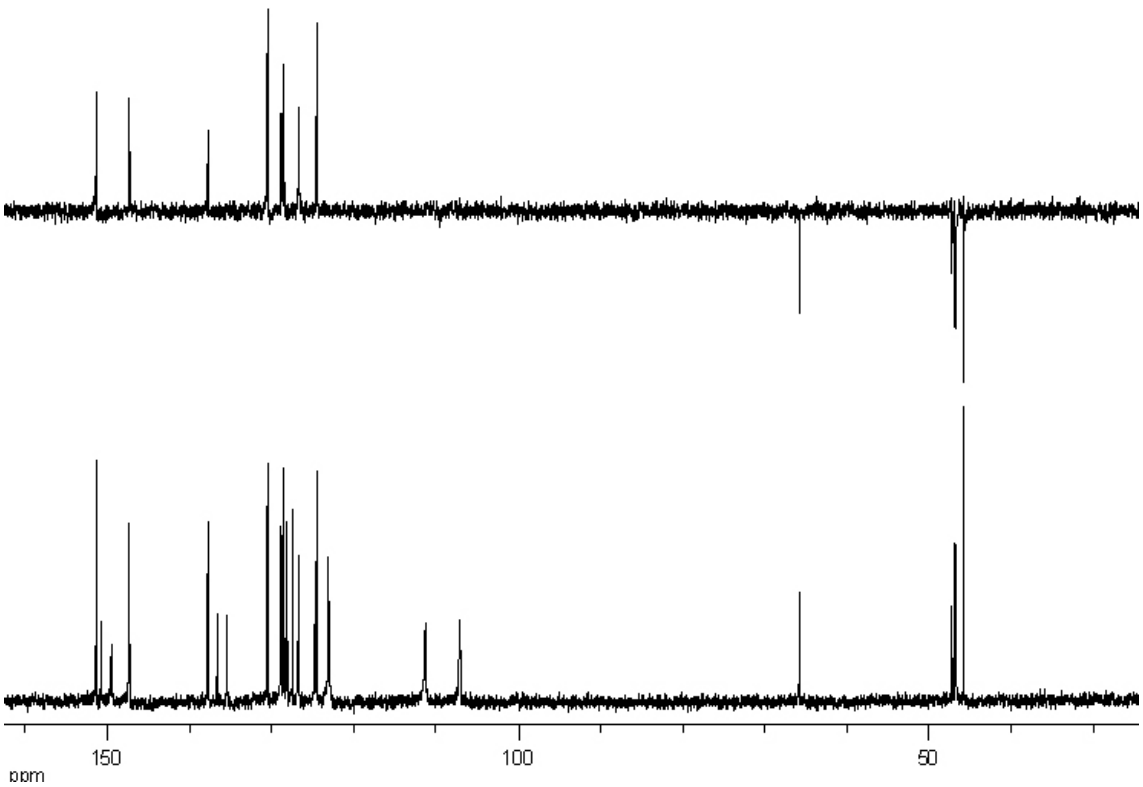

Figure S69: ^{13}C NMR (D_2O, 125 MHz) spectrum of $(\mathbf{14})_2 \subset \mathbf{6a} \cdot 6NO_3$.

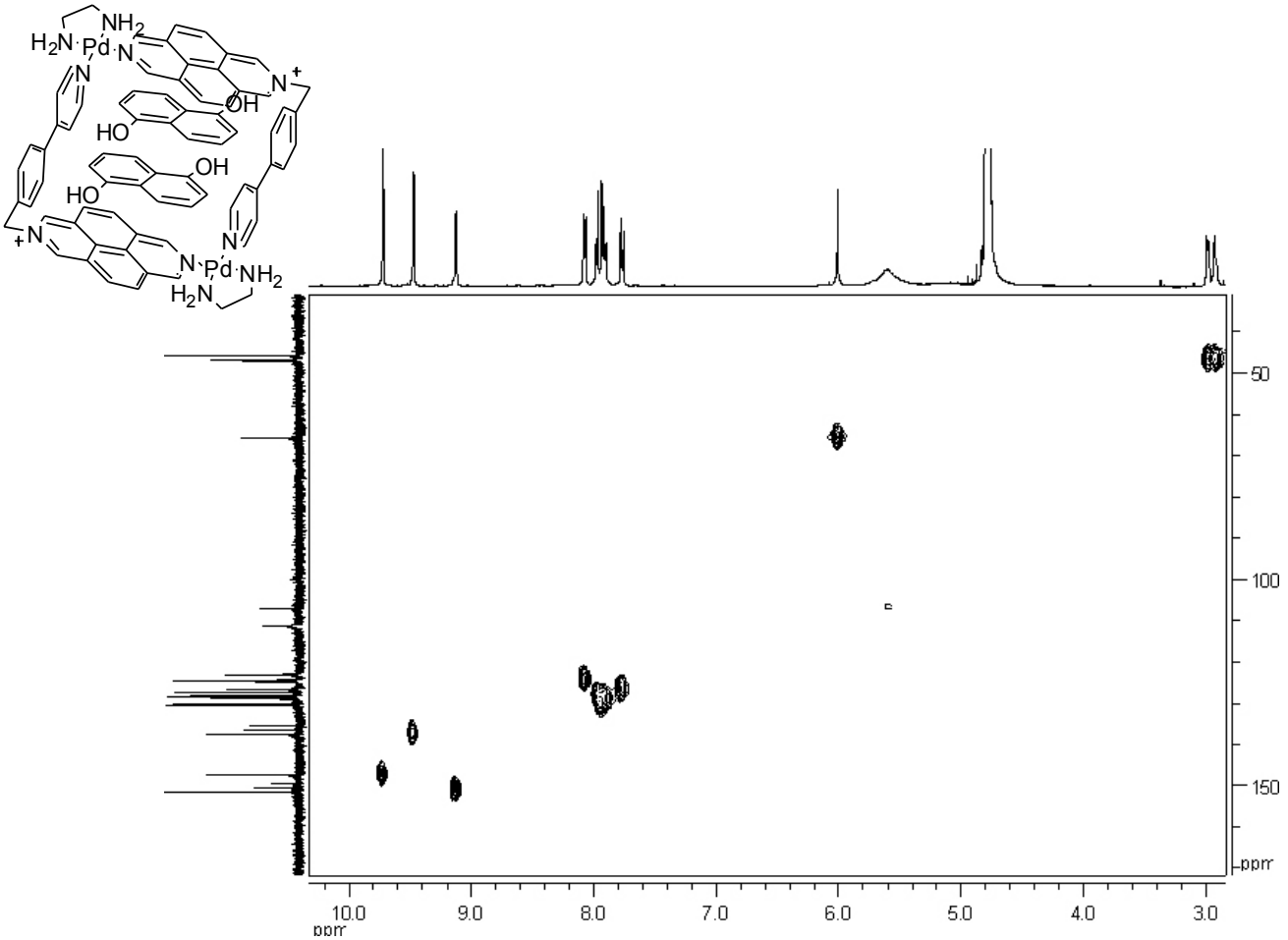

Figure S70: HSQC (D_2O, 500 and 125 MHz) spectrum of $(\mathbf{14})_2 \subset \mathbf{6a} \cdot 6NO_3$.

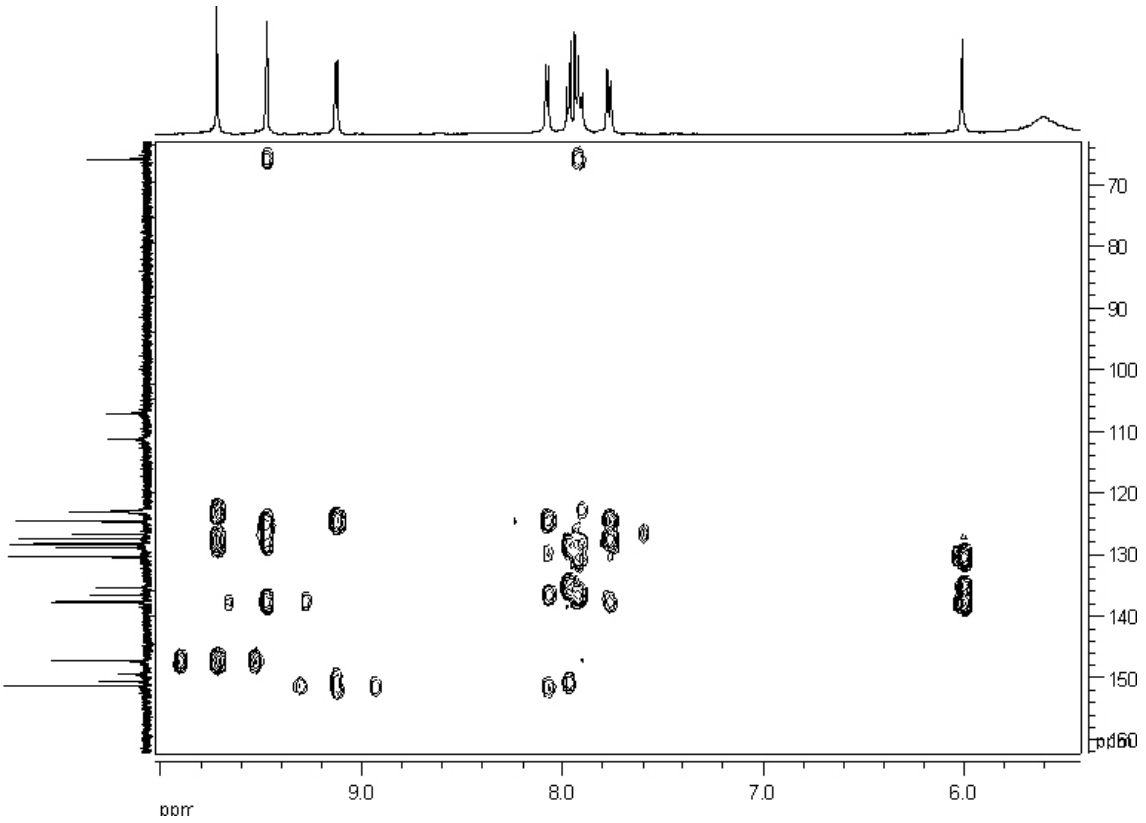

Figure S71: HMBC (D_2O, 500 and 125 MHz) spectrum of $(\mathbf{14})_2 \subset \mathbf{6a} \cdot 6NO_3$.

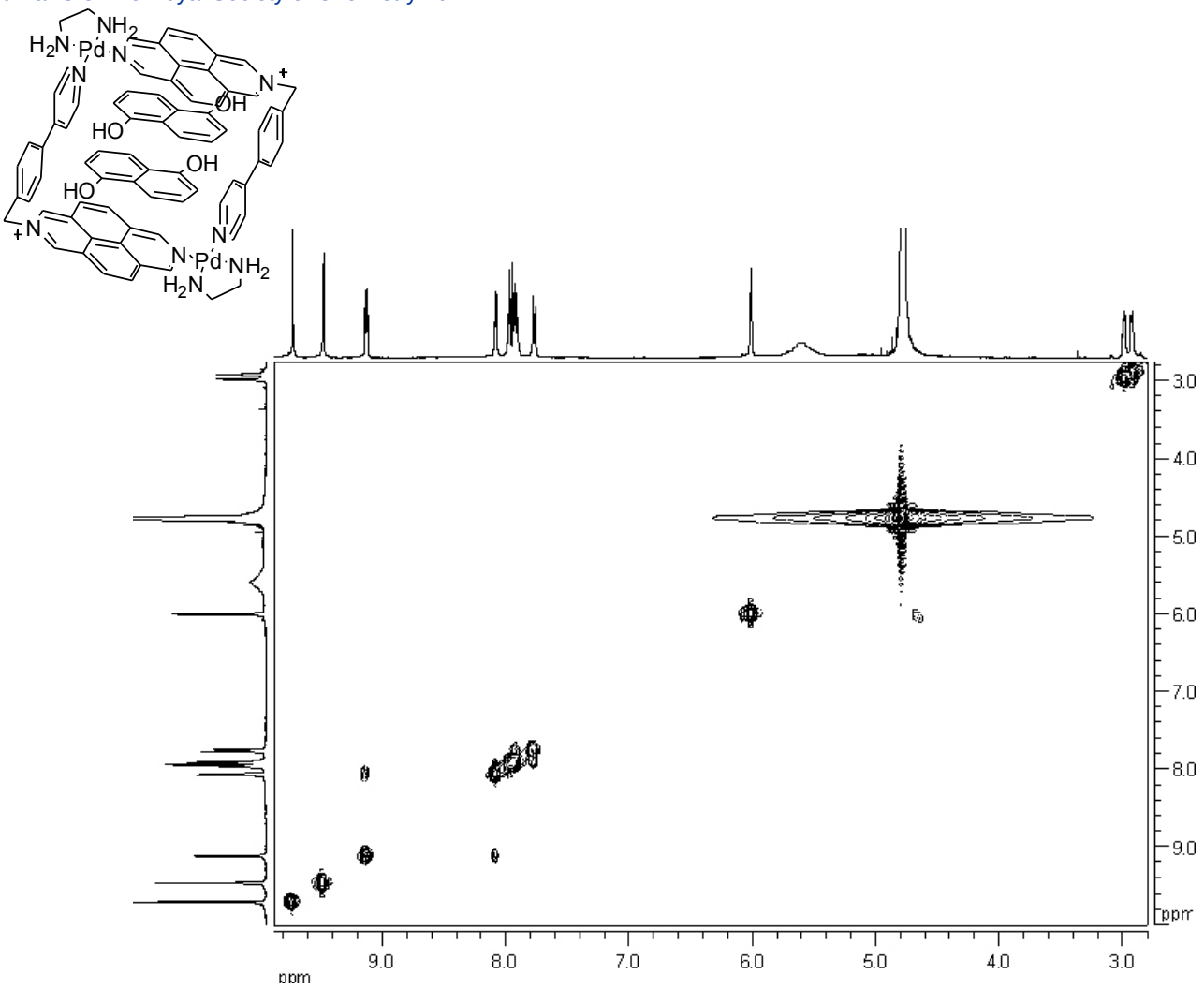

Figure S72: COSY (D_2O, 500 MHz) spectrum of $(\mathbf{14})_2 \subset \mathbf{6a} \cdot 6NO_3$.

Inclusion complex $(15)_2 \subset 6a \cdot 6NO_3$

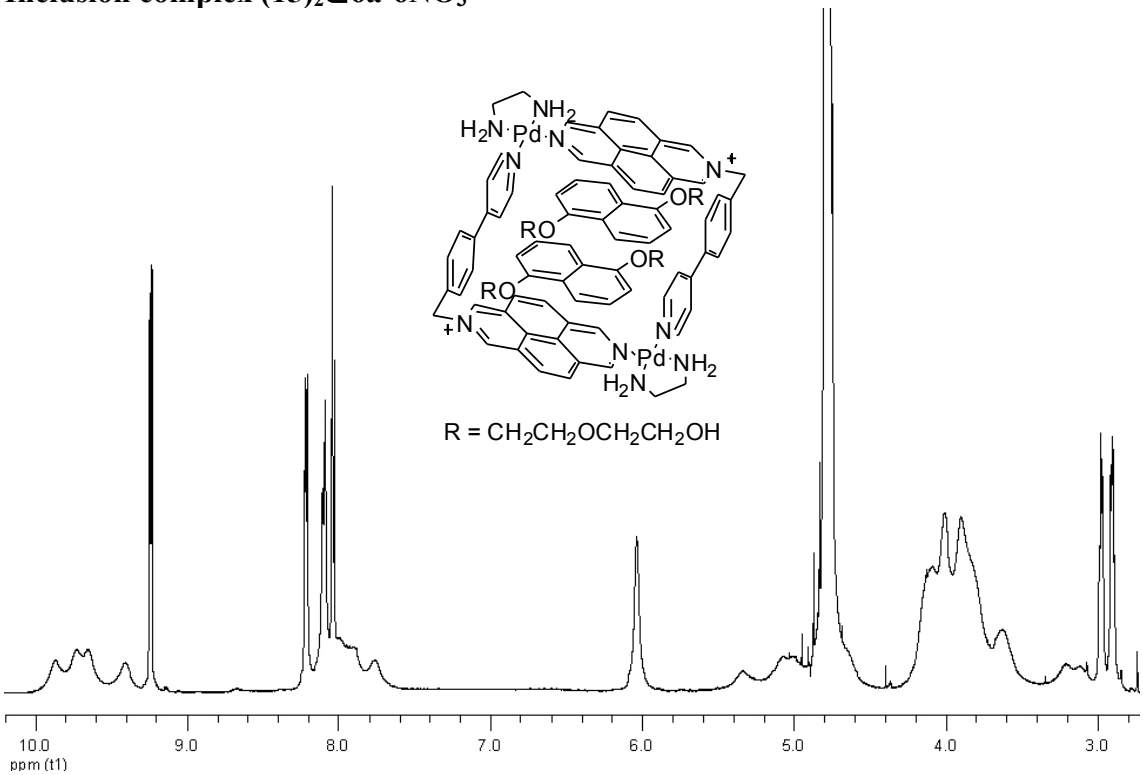

Figure S73: ^{1}H NMR (D_2O, 500 MHz, 298 K) spectrum of $(\mathbf{15})_2 \subset \mathbf{6a} \cdot 6NO_3$.

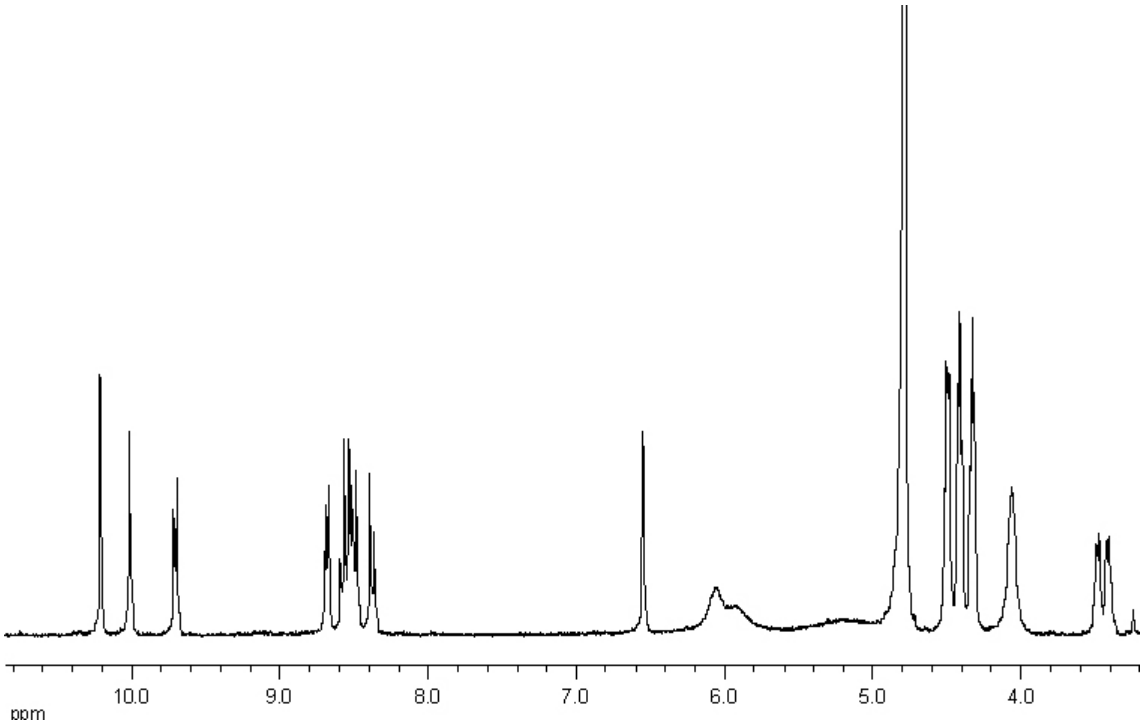

Figure S74: ^{1}H NMR (D_2O, 300 MHz, 353 K) spectrum of $(\mathbf{15})_2 \subset \mathbf{6a} \cdot 6NO_3$.

Inclusion complex $(16)_2 \subset 6a \cdot 6NO_3$

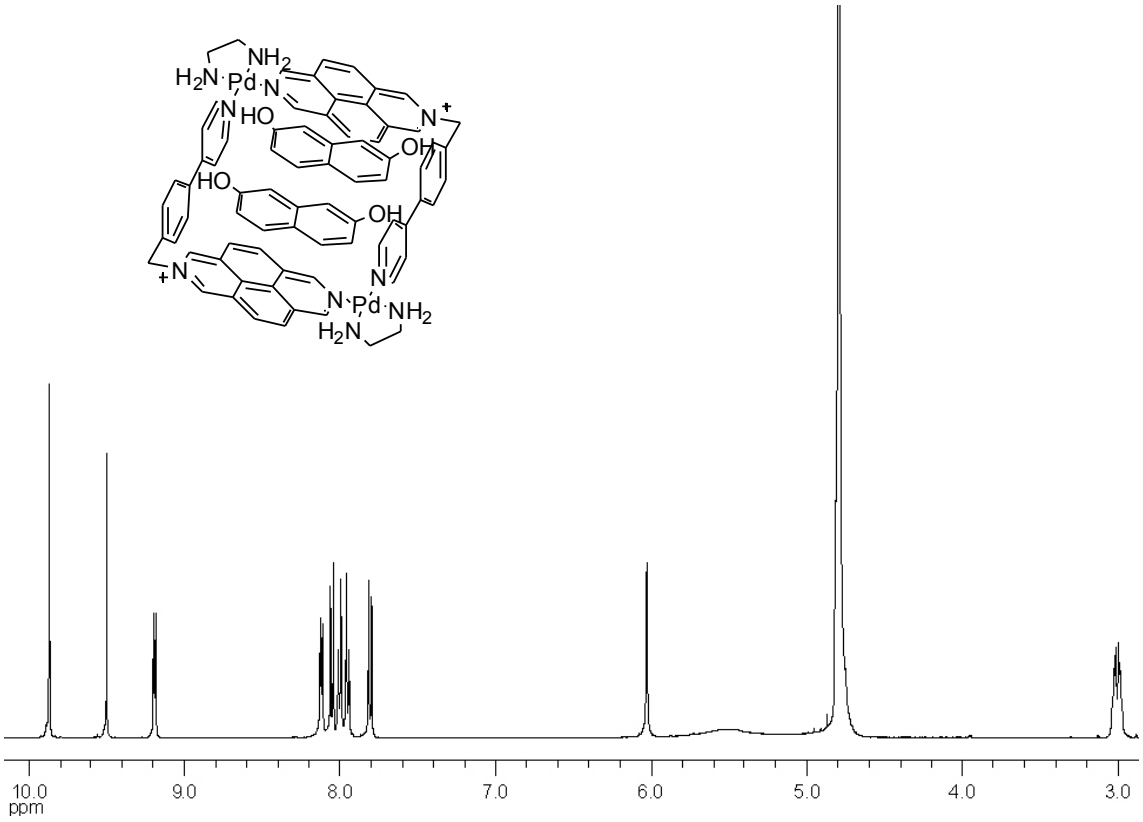

Figure S75: ^{1}H NMR (D_2O, 500 MHz) spectrum of $(\mathbf{16})_2 \subset \mathbf{6a} \cdot 6NO_3$.

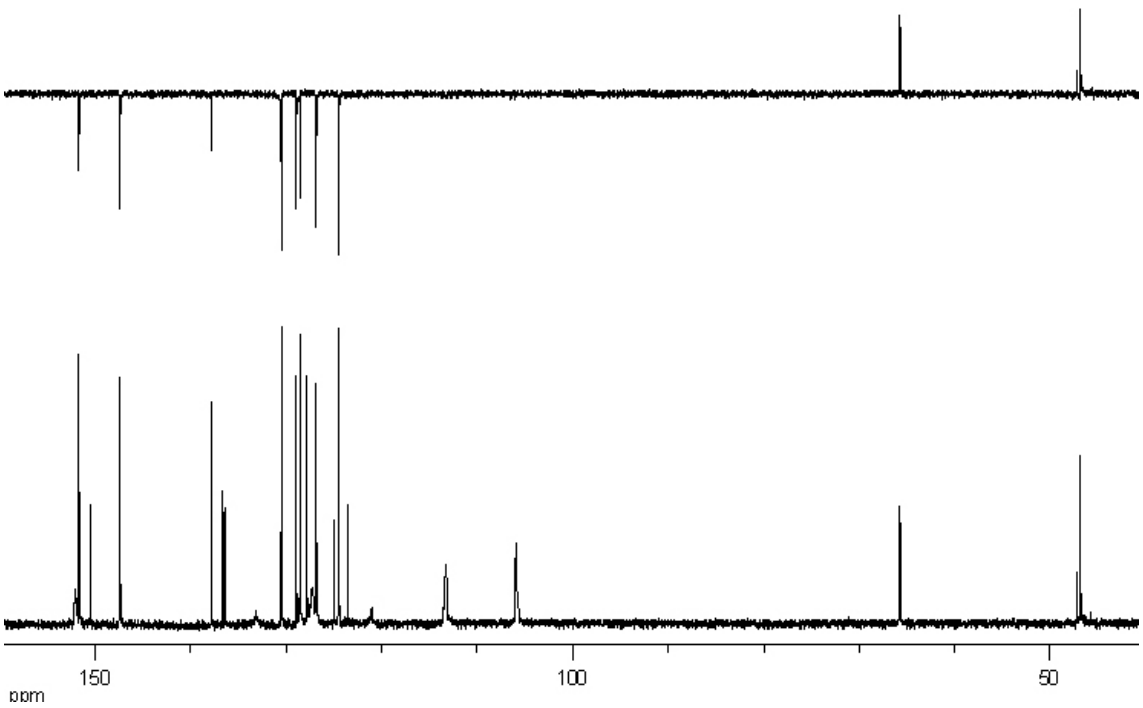

Figure S76: ^{13}C NMR (D_2O, 125 MHz) spectrum of $(\mathbf{16})_2 \subset \mathbf{6a} \cdot 6NO_3$.

Inclusion complex $(17)_2 \subset 6a \cdot 6NO_3$

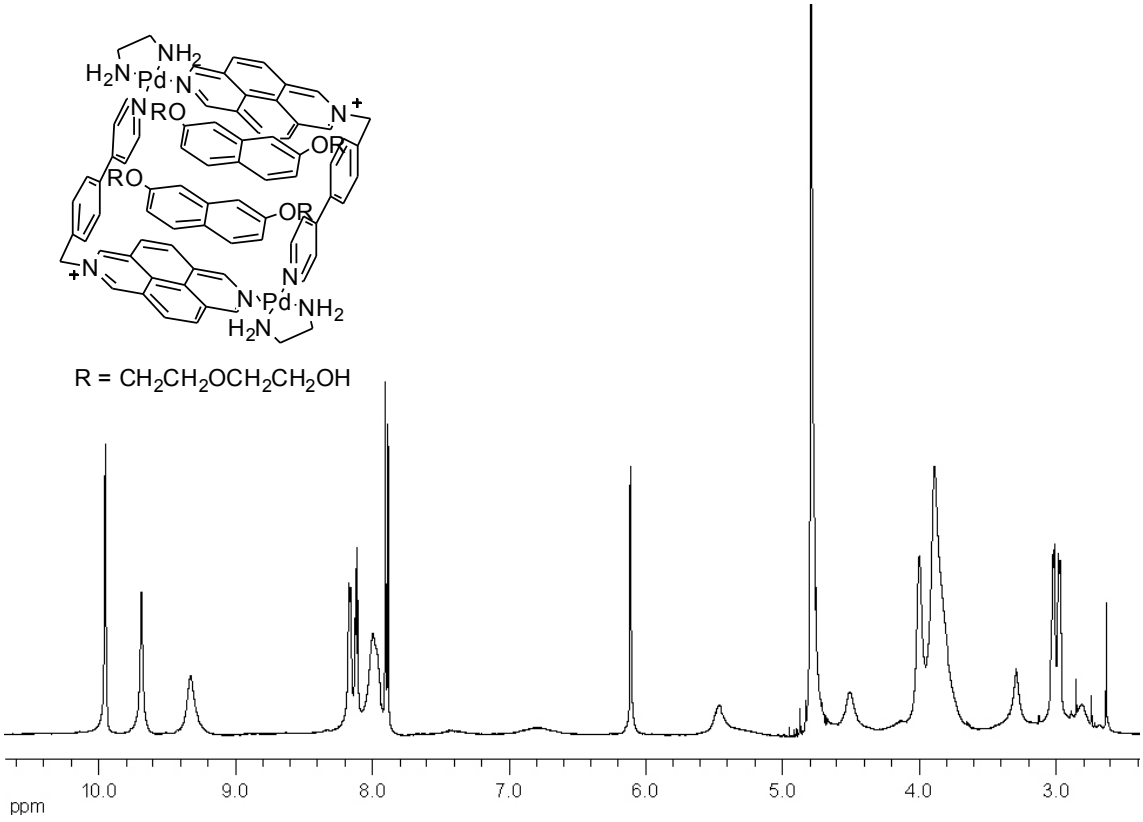

Figure S77: ^{1}H NMR (D_2O, 500 MHz) spectrum of de $(\mathbf{17})_2 \subset \mathbf{6a} \cdot 6NO_3$.

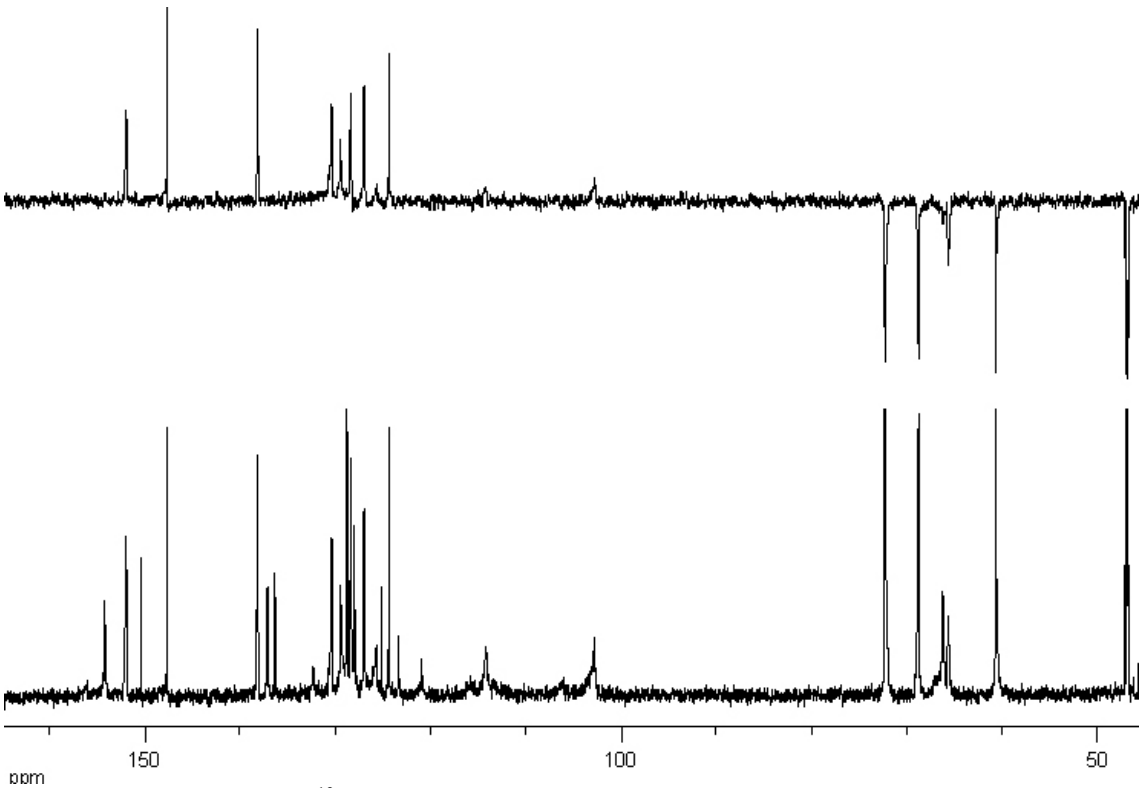

Figure S78: ^{13}C NMR (D_2O, 125 MHz) spectrum of $(\mathbf{17})_2 \subset \mathbf{6a} \cdot 6NO_3$.

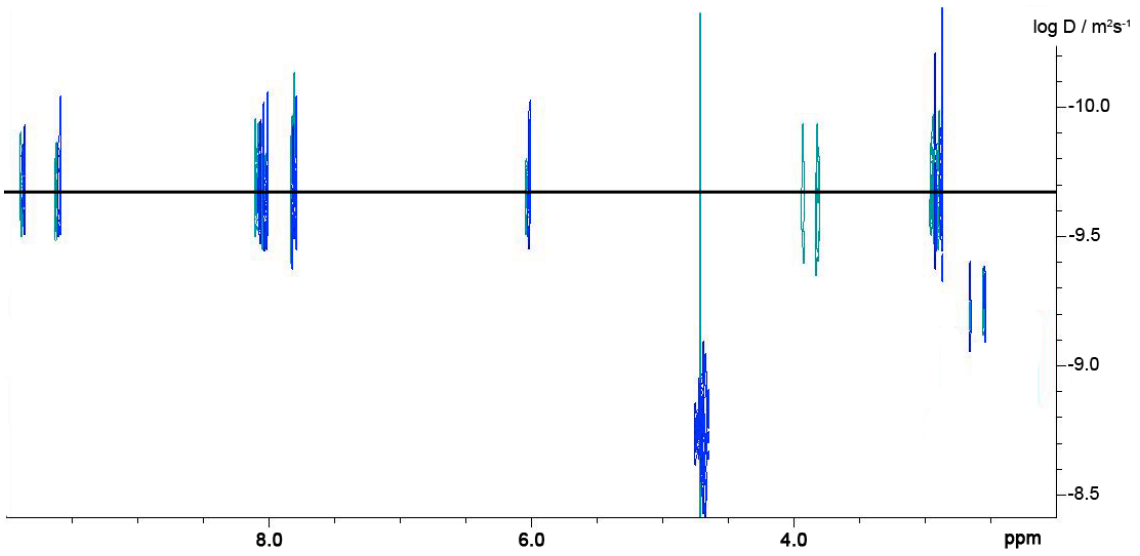

Figure S79: DOSY (D_2O, 500 MHz, 298 K) experiment of inclusion complex (**17**)$_2$⊂**6a**·6NO_3.

Inclusion complex $(18)_2 \subset 6a \cdot 6NO_3$

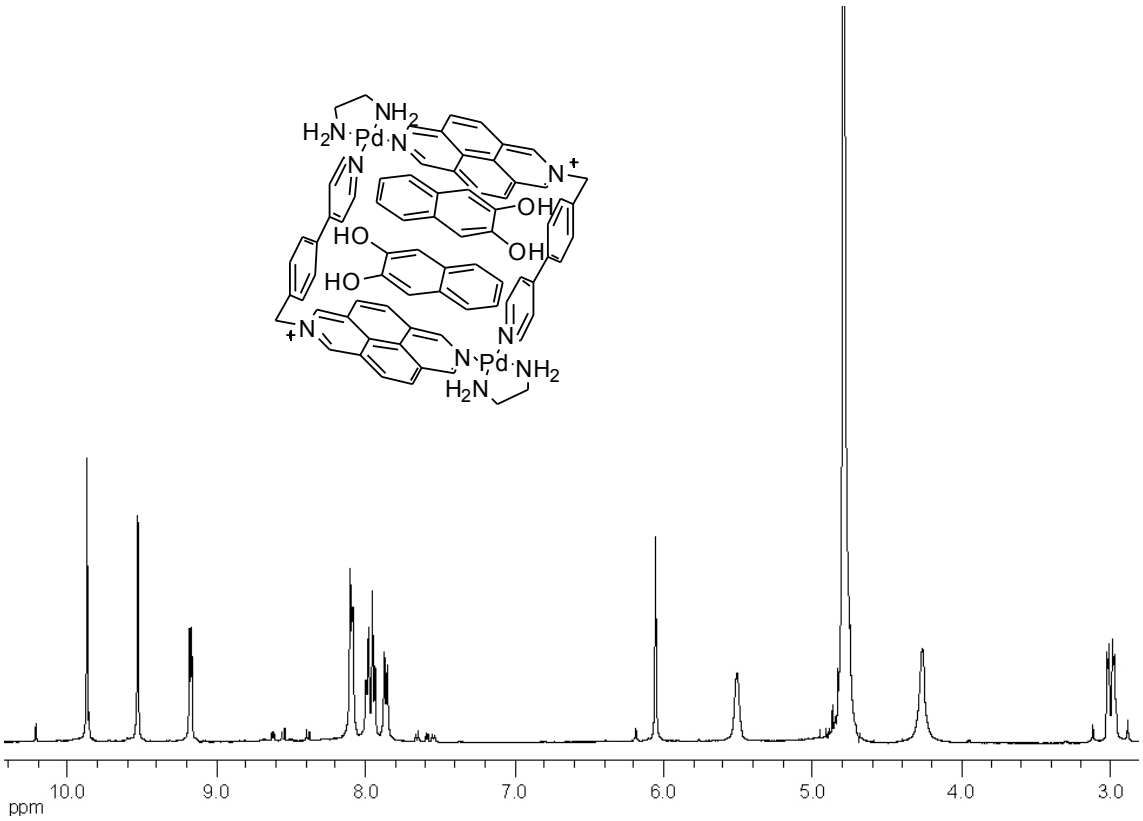

Figure S80: ^{1}H NMR (D_2O, 500 MHz) spectrum of $(\mathbf{18})_2 \subset \mathbf{6a} \cdot 6NO_3$.

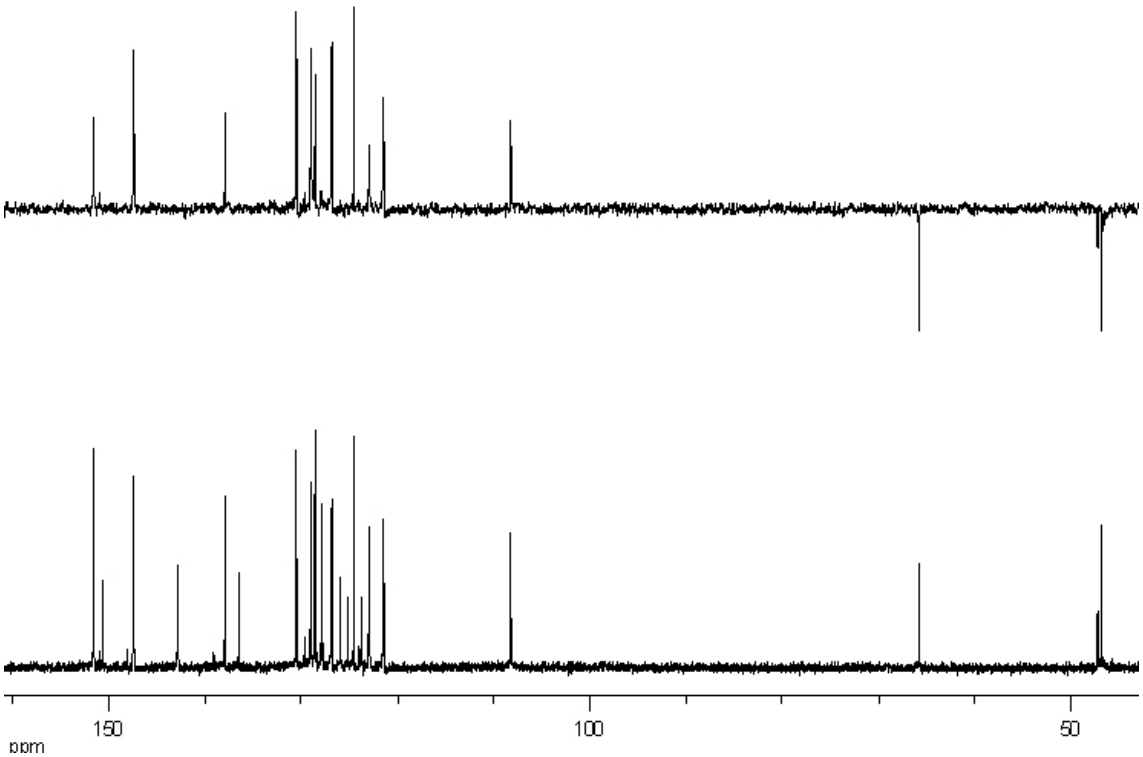

Figure S81: ^{13}C NMR (D_2O, 125 MHz) spectrum of $(\mathbf{18})_2 \subset \mathbf{6a} \cdot 6NO_3$.

Inclusion complex $(19)_2 \subset 6a \cdot 6NO_3$

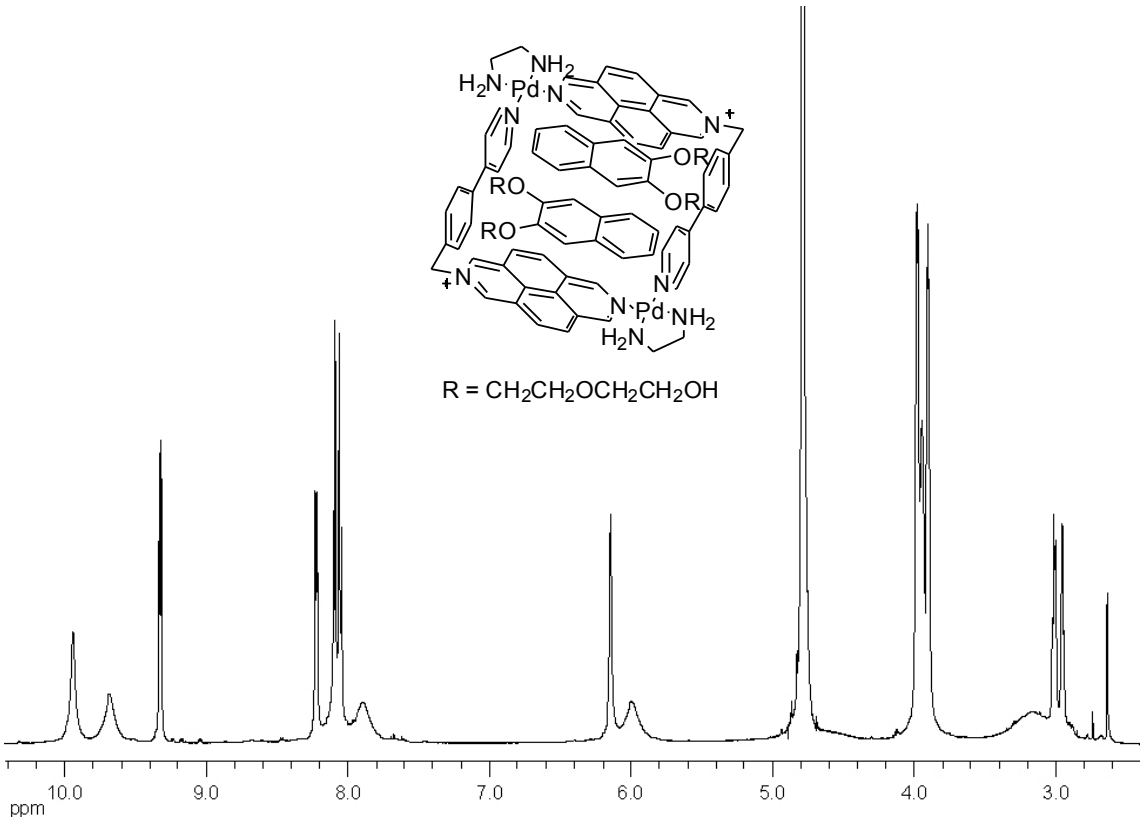

Figure S82: ^{1}H NMR (D_2O, 500 MHz) spectrum of $(\mathbf{19})_2 \subset \mathbf{6a} \cdot 6NO_3$.

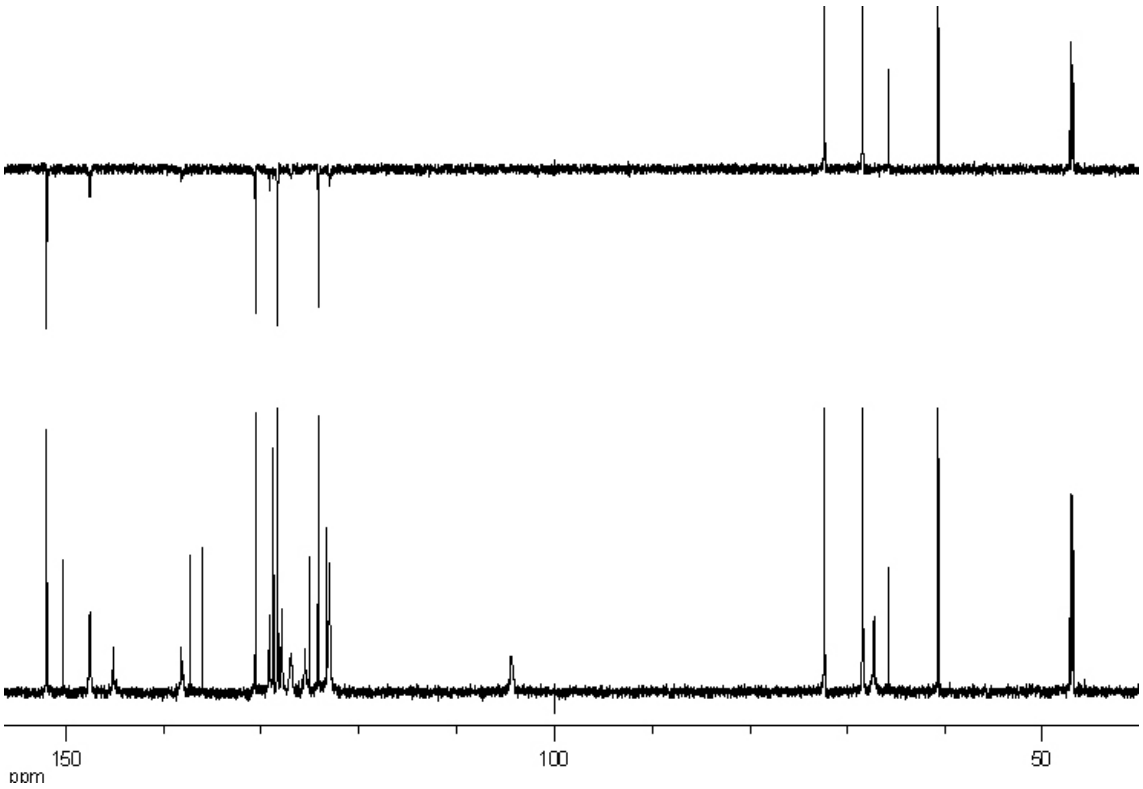

Figure S83: ^{13}C NMR (D_2O, 125 MHz) spectrum of $(\mathbf{19})_2 \subset \mathbf{6a} \cdot 6NO_3$.

Inclusion complex $(20)_2 \subset 6a \cdot 6NO_3$

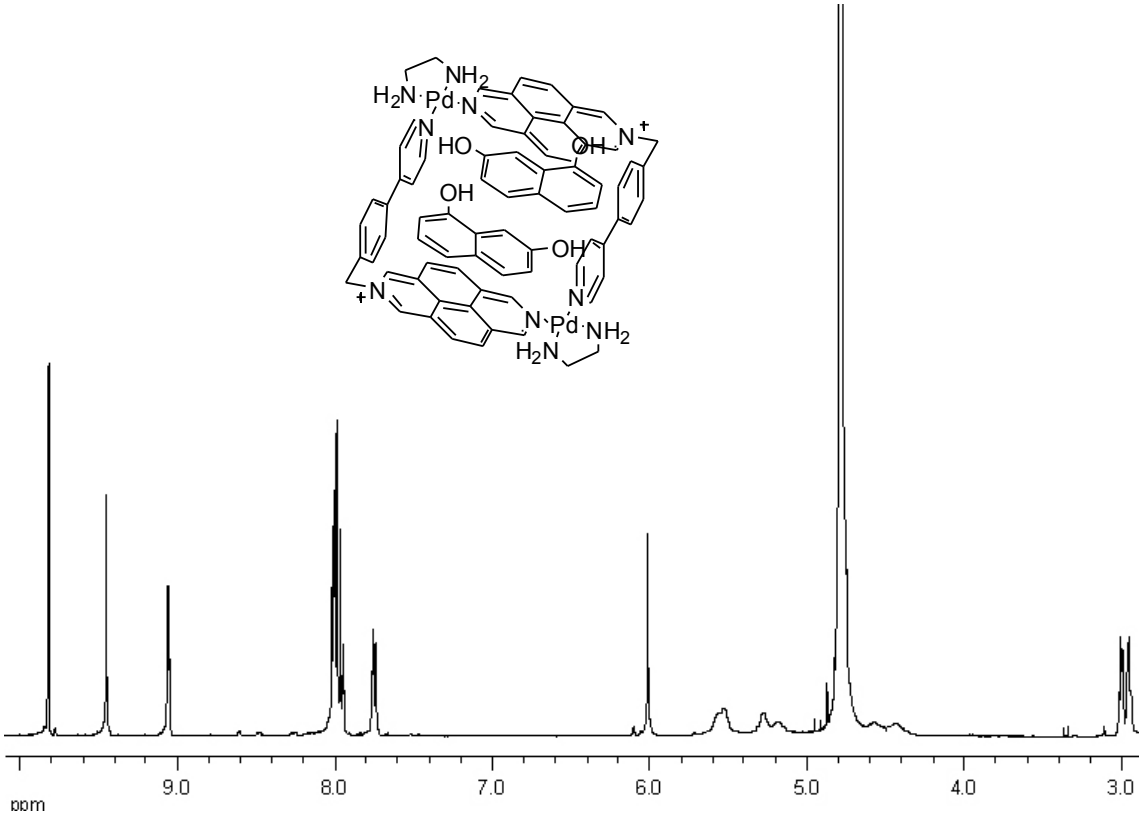

Figure S84: ^{1}H NMR (D_2O, 500 MHz) spectrum of $(\mathbf{20})_2 \subset \mathbf{6a} \cdot 6NO_3$.

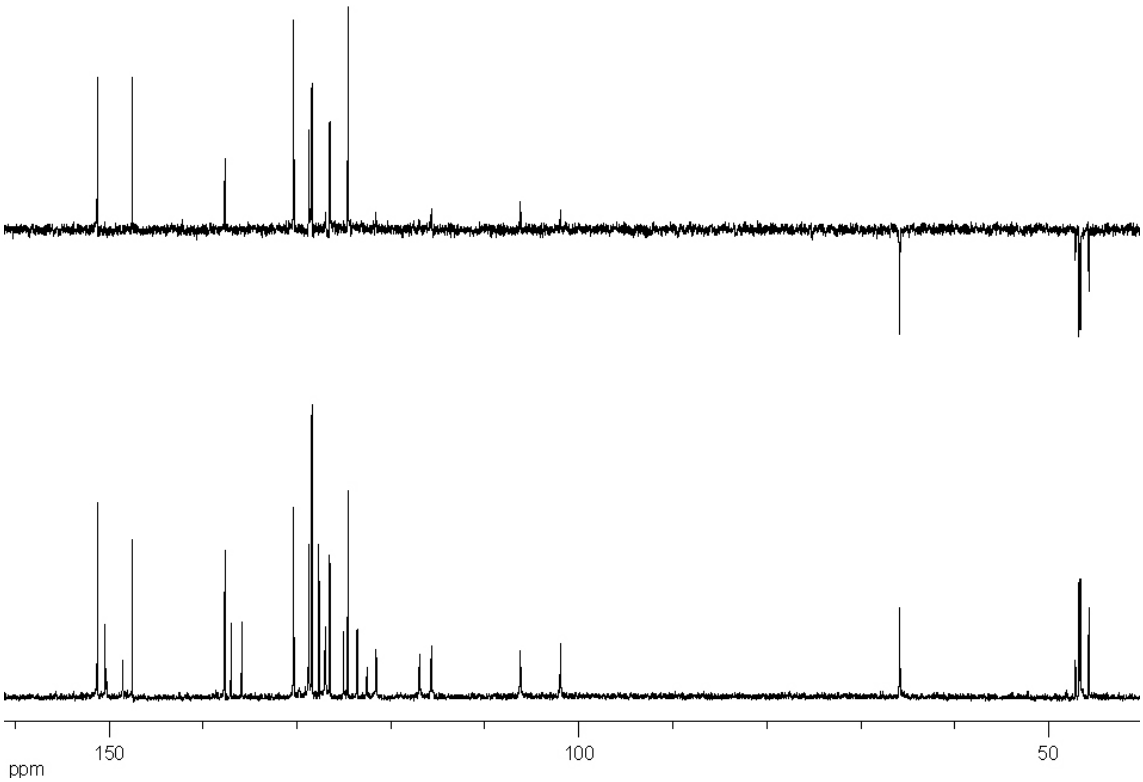

Figure S85: ^{13}C NMR (D_2O, 125 MHz) spectrum of $(\mathbf{20})_2 \subset \mathbf{6a} \cdot 6NO_3$.

Inclusion complex $(21)_2 \subset 6a \cdot 6NO_3$

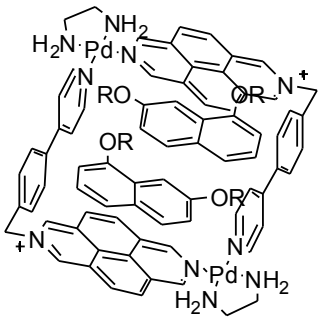

R = $OCH_2CH_2OCH_2CH_2OH$

Figure S86: ^{1}H NMR (D_2O, 300 MHz, 298 K) spectrum of $(21)_2 \subset 6a \cdot 6NO_3$.

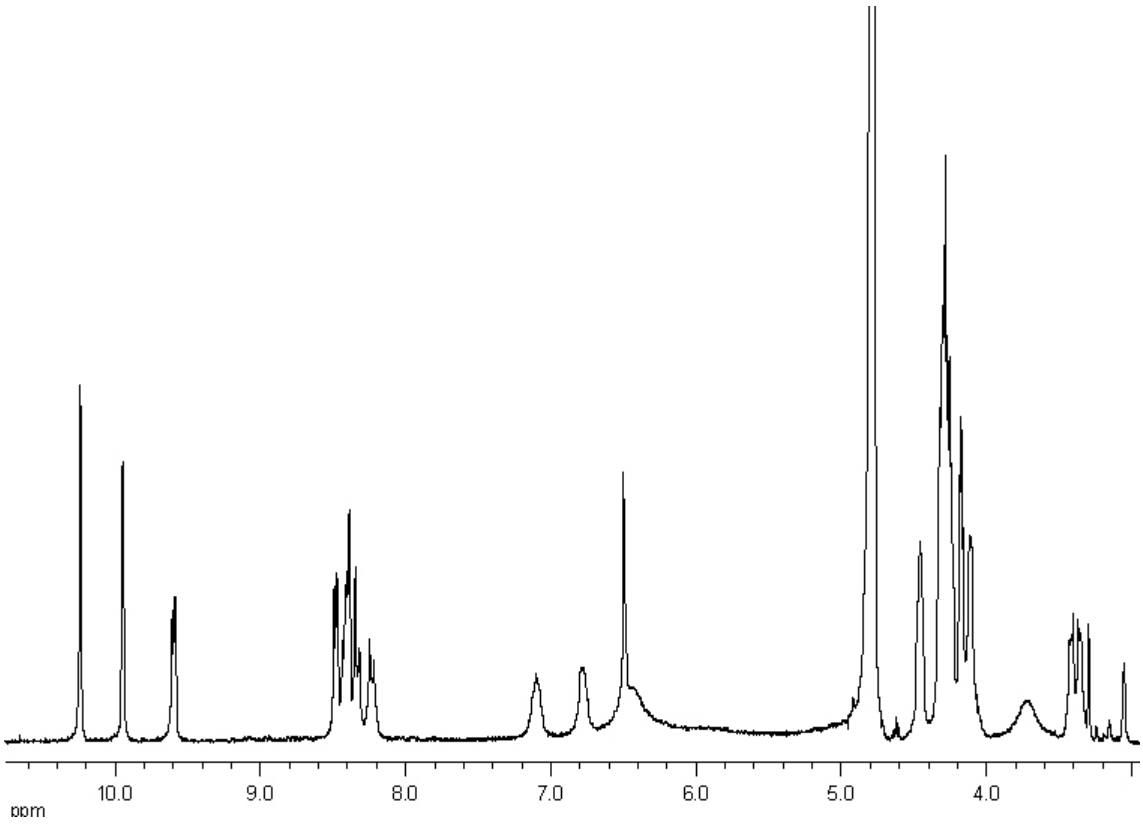

Figure S87: ^{1}H NMR (D_2O, 300 MHz, 338 K) spectrum of $(21)_2 \subset 6a \cdot 6NO_3$.

ORTEP X-ray structures

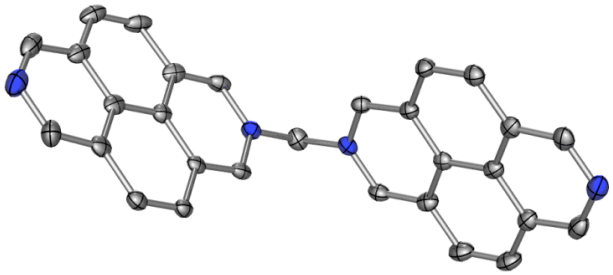

Figure S88: ORTEP drawing of the X-ray structure of ligand **1**·2PF_6. The displacement ellipsoids are drawn for 50% probability. H atoms, counterions and solvent molecules are omitted for clarity.

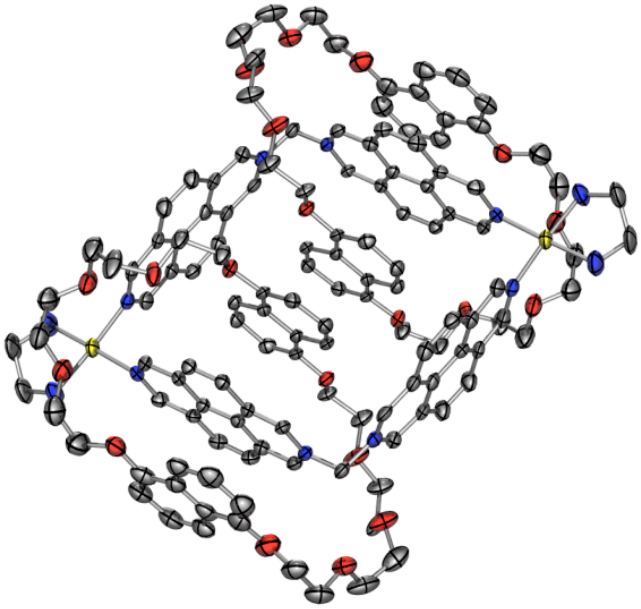

Figure S89: ORTEP representation of the X-ray structure of **3**(**9**)$_2$·4OTf·4PF_6 showing the 50% probability displacement ellipsoids. H atoms, counterions and solvent molecules are omitted for clarity.

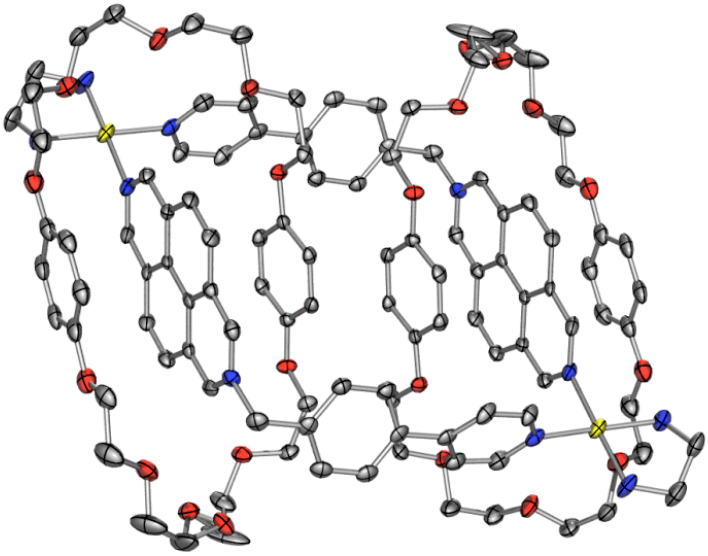

Figure S90: ORTEP drawing of the solid state structure of catenane **6a**(**8**)$_2$·6PF$_6$ showing the 50% probability displacement ellipsoids. H atoms, counterions and solvent molecules are omitted for clarity.

UV-Vis and fluorescence spectra

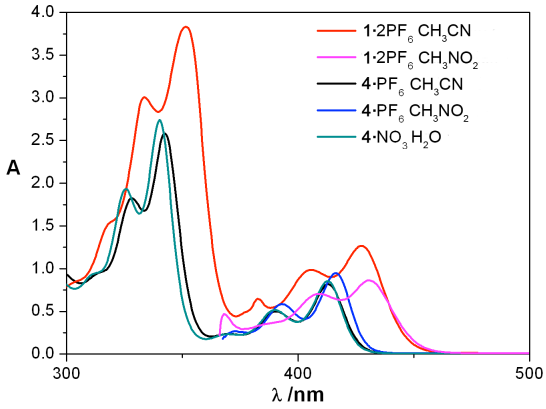

Figure S91: UV-Vis absorption spectra of ligands **1**·2PF$_6$ (1.0×10^{-4} mM), **4**·PF$_6$ (1.0×10^{-4} M) and **4**·NO$_3$ (1.0×10^{-4} mM).

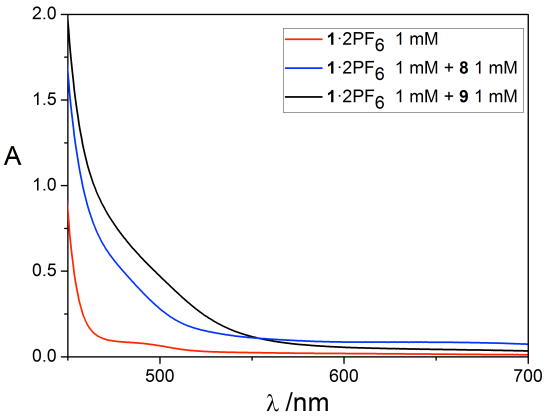

Figure S92: Charge transfer band region of the UV-Vis spectra (CH_3CN) of ligand **1**·2PF$_6$ and pseudorotaxanes **1**·2PF$_6$⊂**8** and **1**·2PF$_6$⊂**9.**

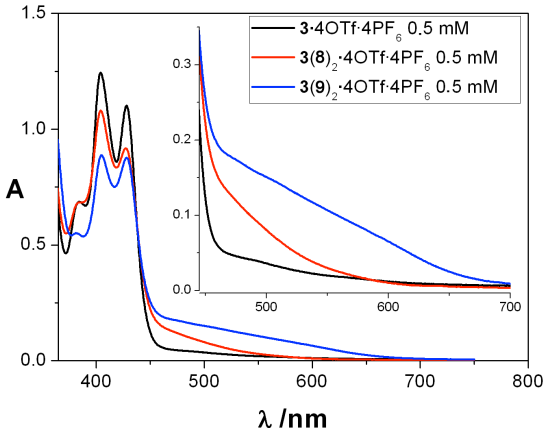

Figure S93: UV-Vis spectra (CH_3NO_2, optical path length 1.0 mm) of metallocycle **3**·4OTf·4PF$_6$ and catenanes **3**(**8**)$_2$·4OTf·4PF$_6$ and **3**(**9**)$_2$·4OTf·4PF$_6$. Inset: detail of the charge transfer band region (450-650 nm).

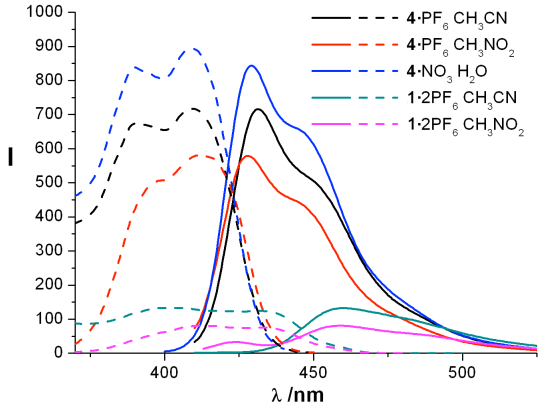

Figure S94: Fluorescence emission spectra (solid lines) and excitation spectra (dashed lines) (293 K) of ligands **1**·2PF$_6$ (1.0×10^{-4} mM), **4**·PF$_6$ (1.0×10^{-4} mM) and **4**·NO$_3$ (1.0×10^{-4} mM).

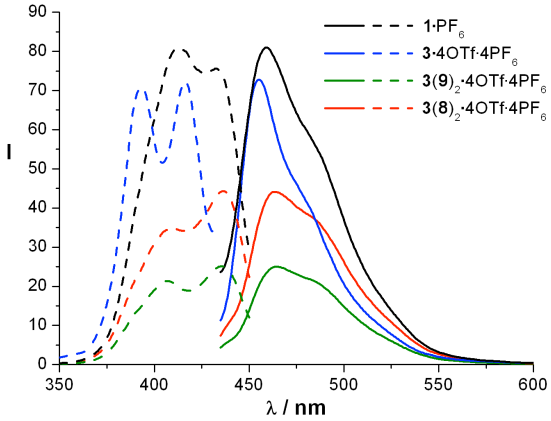

Figure S95: Fluorescence emission spectra (solid lines) and excitation spectra (dashed lines) (CH_3NO_2, 293 K) of ligand **1**·2PF$_6$ (1.0×10^{-4} M), metallocycle **3**·4OTf·4PF$_6$ (5.0×10^{-5} M) and catenanes **3**(**8**)$_2$·4OTf·4PF$_6$ (5.0×10^{-5} M) and **3**(**9**)$_2$·4OTf·4PF$_6$ (5.0×10^{-5} M).

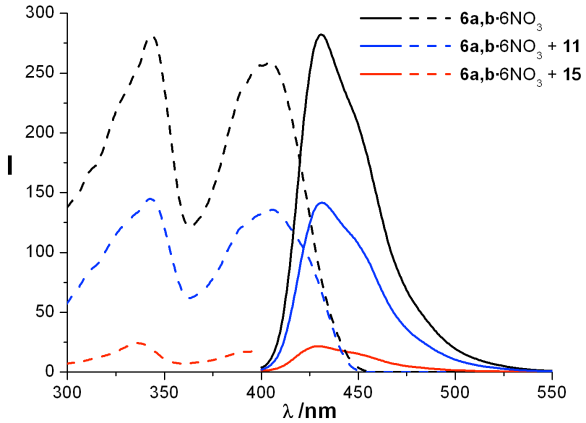

Figure S96: Fluorescence emission spectra (solid lines) and excitation spectra (dashed lines) (H_2O, 293 K) of metallocycles **6a,b**·NO$_3$ (5.0×10^{-5} M) and inclusion complexes (**11**)$_2$⊂**6a**·6NO$_3$ (5.0×10^{-5} mM) and (**15**)$_2$⊂**6a**·6NO$_3$ (5.0×10^{-5} M).

Determination of binding constant (K_a) between 1·2PF$_6$ and DN38C10 (9) by UV/Vis titration method.

A 0.5 mM solution of host **9** in acetonitrile and a solution of guest **1**·2PF$_6$ (6 mM) and host **9** (0.5 mM) in acetonitrile were separately prepared. Then, aliquots of the guest/host solution (initially 10 µL, then 20 µL; 50 µL and, finally 100 µL) were added to the host solution (2 mL), recording the spectrum of the mixture after each addition (overall 35 points). The association constants were determined by using the nonlinear least squares fitting of the titration curves plotting the corrected A ($\varepsilon_{1\cdot 2PF_6}$ = 101.7 L mol^{-1} at 470 nm) of the host-guest complex charge-transfer band against the concentration of the corresponding guest. The titration curve fits perfectly to the 1:1 binding isotherm (R^2 = 0.999).

Temperature: 298 K

λ_{max} = 470 nm

K_a = 4268 ± 124 M^{-1}

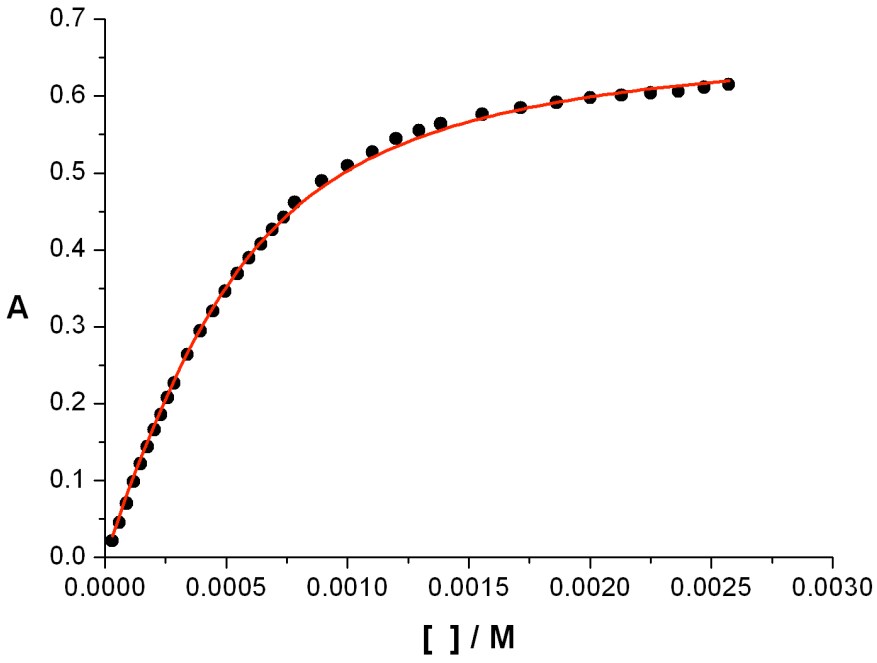

Absorbance	[**1**] /M	Total added volume (μL)	Absorbance	[**1**] /M	Total added volume (μL)
0.0213	0.000030	10	0.4421	0.000737	280
0.0448	0.000059	20	0.4616	0.000783	300
0.0700	0.000089	30	0.4892	0.000894	350
0.0983	0.000118	40	0.5095	0.001000	400
0.1216	0.000146	50	0.5268	0.001102	450
0.1437	0.000175	60	0.5445	0.001200	500
0.1657	0.000203	70	0.5554	0.001385	550
0.1854	0.000231	80	0.5638	0.001556	600
0.2077	0.000258	90	0.5760	0.001714	700
0.2265	0.000286	100	0.5848	0.001862	800
0.2635	0.000340	120	0.5919	0.002000	900
0.2945	0.000393	140	0.5978	0.002129	1000
0.3202	0.000444	160	0.6010	0.002250	1100
0.3460	0.000495	180	0.6041	0.002364	1200
0.3691	0.000545	200	0.6059	0.002471	1300
0.3892	0.000595	220	0.6115	0.002571	1400
0.4073	0.000643	240	0.6150	0.002667	1500
0.4261	0.000690	260			

[1] (*a*) P. R. Ashton, S. E. Boyd, A. Brindle, S. J. Langford, L. Pérez-García, J. A. Preece, F. M. Raymo, N. Spencer, J. F. Stoddart, A. J. P. White, D. J. Williams, *New J. Chem*. 1999, **23**, 587; (*b*) J. A. Blake, G. Baum, N. R. Champness, S. S. M. Chung, P. A. Cooke, D. Fenske, A. N. Khlobystov, D. A. Lemenovskii, W.-S. Li, M. Schröder, *J. Chem. Soc., Dalton Trans*. **2000**, 4285.

[2] C. Peinador, V. Blanco, J. M. Quintela, *J. Am. Chem. Soc.* 2009, **131**, 920.

[3] **2**: *(a)* C. Diver, G. A. Lawrance *J. Chem. Soc., Dalton Trans.* **1988**, 931. *(b)* P. de Wolf, S. L. Heath; J. M. Thomas, *Inorg. Chim. Acta* **2003**, 280. **5a:** *(c)* H. D. K. Drew, F. W. Pinkard, G. H. Preston, W. J. Wardlaw. *Chem. Soc.* **1932**, 1895. **5b**: *(d) L. V.* Popov; N. N. Zheligovskaya, A. M. Grevtsev, E. A. Kharina, V. I. Spitsyn. *Seriya Khimicheskaya* 1977, **7**, 1677. *(e)* M. Fujita, J. Yazaki, K. Ogura, *Chem. Lett.* **1991**, 1031.

[4] V. Blanco, D. Abella, E. Pía, C. Platas-Iglesias, C. Peinador, J. M. Quintela, *Inorg. Chem.* 2009, **48**, 4098.

[5] D. B. Amabilino, P. L. Anelli, P. R. Ashton, G. R. Brown, E. Córdova, L. A. Godínez, W. Hayes, A. E. Kaifer, D. Philp, A. M. Z. Slawin, N. Spencer, J. F. Stoddart, M. S. Tolley, D. J. Williams, *J. Am. Chem. Soc.* 1995, **117**, 11142.

[6] D. B. Amabilino, P. R. Ashton, V. Balzani, S. E. Boyd, A. Credi, J. Y. Lee, S. Menzer, J. F. Stoddart, M. Venturi, D. J. Williams, *J. Am. Chem. Soc.* 1998, **120**, 4295.

[7] P. R. Anelli, P. R. Ashton, R. Ballardini, V. Balzani, M. Delgado, M. T. Gandolfi, T. T. Goodnow, A. E. Kaifer, D. Philp, M. Pietraszkiewicz, L. Prodi, M. V. Reddington, A. M. Z. Slawin, N. Spencer, J. F. Stoddart, C. Vicent, D. J. Williams, *J. Am.Chem. Soc.* 1992, **114**, 193.

[8]

[9] M. Asakawa, P. R. Ashton, S. E. Boyd, C. L. Brown, R. E. Gillard, O. Kocian, F. M. Raymo, J. F. Stoddart, M. S. Tolley, A. J. P. White, D. J. Williams, *J. Org. Chem.* 1997, **62**, 26.

[10] B. Czech, A. Czech, R. A. Bartsch, *J. Heterocycl. Chem.* 1984, **21**, 341.

[11] V. Blanco, A. Gutiérrez, C. Platas-Iglesias, C. Peinador, J. M. Quintela, *J. Org. Chem*. 2009, **74**, 6577.

[12] L. G. Longsworth, *J. Phys. Chem.* 1960, **64**, 1914.

[13] T. Megyes, H. Jude, T. Grósz, I. Bakó, R. Radnai, G. Tárkányi, G.Pálinkás, P. J. Stang, *J. Am. Chem. Soc*. 2005, **127**, 10731.

[14] *SHELX-97*, Release 97-2; G. M. Sheldrick, University of Göttingen, Germany, 1997.